DIVERSIFICATION OF THE FERN GENUS *CRYPTOGRAMMA* ACROSS TIME AND SPACE

By

Jordan S. Metzgar

RECOMMENDED:

Dr. Kathleen Pryer
Advisory Committee Member

Dr. Naoki Takebayashi
Advisory Committee Member

Dr. Michael Windham
Advisory Committee Member

Dr. Diana Wolf
Advisory Committee Member

Dr. Stefanie Ickert-Bond
Advisory Committee Chair

Dr. Diane Wagner
Chair, Department of Biology and Wildlife

APPROVED:

Dr. Paul Layer
Dean, College of Natural Science and Mathematics

Dr. John Eichelberger
Dean of the Graduate School

12 April 2016
Date

DIVERSIFICATION OF THE FERN GENUS *CRYPTOGRAMMA* ACROSS TIME AND SPACE

A

DISSERTATION

Presented to the Faculty

of the University of Alaska Fairbanks

in Partial Fulfillment of the Requirements

for the Degree of

DOCTOR OF PHILOSOPHY

By

Jordan S. Metzgar, B.S.

Fairbanks, Alaska

May 2016

Abstract

I examined diversification, biogeographic history and polyploidy within the parsley ferns (*Cryptogramma*) across multiple time scales. *Cryptogramma* is a small circumboreal genus of rock ferns in the large, diverse family Pteridaceae and is most closely related to the Asian genus *Coniogramme* and the monotypic Central American genus *Llavea*. I generated a combined six locus plastid sequence alignment (*rbcL*, *rbcL-accD*, *rbcL-atpB*, *rps4-trnS*, *trnG-trnR*, and *trnP-petG*) and a low-copy nuclear marker (*gapCp*) alignment for 40 accessions. Phylogenetic analysis of these datasets using maximum parsimony, maximum likelihood, and Bayesian inference demonstrate that all three genera are reciprocally monophyletic, with *Cryptogramma* and *Coniogramme* most closely related to one another. This analysis also recovered the monotypic *Cryptogramma* section *Homopteris* and sect. *Cryptogramma* as reciprocally monophyletic. Within sect. *Cryptogramma*, the unambiguously supported phylogeny supported recognizing most described species as reciprocally monophyletic clades that are mostly allopatric and can be delineated by a few morphological characters. The nuclear DNA phylogeny supported the hypothesis that the allotetraploid *Cr. sitchensis* originated from a hybridization event between the Asian *Cr. raddeana* and the Beringian *Cr. acrostichoides*, and the plastid DNA phylogeny revealed that *Cr. acrostichoides* was the maternal parent. In contrast, the tetraploid *Cr. crispa* appears to have originated as an autopolyploid from an undiscovered or extinct ancestor. Further phylogenetic investigation of European *Cryptogramma* species using DNA sequence data from 15 accessions from Europe and southwest Asia revealed that Pleistocene glacial cycles have created genetic partitioning of *Cr. crispa* into eastern and western clades and have also led to the formation of the Turkish auto-octoploid *Cr. bithynica* with *Cr. crispa* as the parental taxon. Divergence time estimates for key nodes were inferred using Bayesian analysis of the plastid data set coupled with secondary time constraints to reveal that crown group *Cryptogramma* began diversifying in the Oligocene, with most present-day species originating in the Pliocene and Pleistocene. The genus was inferred by likelihood-based ancestral area reconstruction of the chronogram and geographic distribution data to have originated in east Asia, with four colonization events reconstructed by vicariance or dispersal to the New World. My Bayesian Analysis of Macroevolutionary Mixtures (BAMM) showed no significant difference in speciation rates across time or among clades. The morphological stasis

of *Cryptogramma* and its stable speciation rates in response to climate cycles during the Pleistocene suggest it will survive future range shifts caused by anthropogenically induced climate change.

Table of Contents

Page

List of Figures

Page

List of Tables

Page

Acknowledgements

I am greatly indebted to my major advisor Stefanie Ickert-Bond for the assistance, training, and mentoring she provided me while completing my dissertation. I am also thankful to Kathleen Pryer, Naoki Takebayashi, Michael Windham, and Diana Wolf for their encouragement, advice, and assistance as members of my graduate committee. I was greatly aided in publishing this research by my co-authors Edward Alverson, Sinian Chen, Mackenzie Stamey, and Alexey Vaganov, who provided hypotheses, unpublished data and assisted in preparing manuscripts. I am also grateful for the many collectors who supplied tissue or voucher material, including Ellen Anderson, Polly Bass, David Boufford, Walter Bujnoch, David Gernandt, Stefan Jessen, Li-Yaung Kuo, Juan Larraín, Anders Larsson, Manuel González Ledesma, Phan Ke Loc, Alicia Marticorena, Emily Metzgar, Yulia Mikhaylova, Santiago Pajarón, Emilia Pangua, Georg Pflugbeil, Kathleen Pryer, Richard Ree, Carl Rothfels, Erin Sigel, A. Shmakov, Mary Stensvold, Stacy Studebaker, Andreas Tribsch, Mike Windham, Valentin Yakubov, and Peter Zika. I also thank Mac Campbell, Katie Everson, Tzu-Tong Kao, Itay Mayrose, Zach Meyers, Margaret Oliver, Link Olson, Kathleen Pryer, Carl Rothfels, Eric Schuettpelz, Lisa Strecker, Gabrielle Vance, and Stina Weststrand for helpful discussion or assistance with technical obstacles. Most of all, I would like to thank my wonderful wife, Emily Metzgar, and our children, Jedediah, and Nathanael, for their ceaseless support, love, and encouragement during this long process. My research was funded internally by the Alaska Experimental Program to Stimulate Competitive Research Landscape Genetics Student Research Award, Alaska Quaternary Center David and Rachel Hopkins Fellowship, Center for Global Change Student Research Grant, Graduate School Travel Grant, and Ted McHenry Biology Field Research Scholarship. External funding sources included the American Fern Society, the American Society of Plant Taxonomists, The Explorers Club, iDigBio, and the National Science Foundation Doctoral Dissertation Improvement Grant (DEB-1311685).

Chapter 1. Introduction

1.1. The Importance of the Leptosporangiate Ferns

Vascular plants arose in the Paleozoic and have since transformed the earth, spurring the evolution of many lineages such as animals and fungi (Kenrick and Crane, 1997). The leptosporangiate ferns are the second-largest group of vascular plants on earth, trailing only the angiosperms with approximately 12,000 extant species of ferns (Pryer et al. 2004). Along with the horsetails, whisk ferns, and eusporangiate ferns, this group is most closely related to the seed plants (Pryer et al. 2001). This lineage has ancient roots, with ferns first appearing in the early Carboniferous (Galtier and Phillips, 1996) and dominating the late Palaeozoic and early Mesozoic (Schneider et al., 2004). Their key innovation is the leptosporangium, which develops from a single cell to produce spores and then disperse them via a violent catapult-like motion (Gifford and Foster, 1989). Ferns have a pronounced alternation of generations, with free-living, independent gametophytes that can persist for years. Fertilization occurs when a sperm cell can swim across the gametophyte to reach an egg in an archegonium (Gifford and Foster, 1989).

Ferns are remarkably diverse, with body forms ranging from the small, single-cell thick filmy ferns to large arborescent tree ferns (Smith et al., 2006). They are geographically widespread and occur globally, with Antarctica and marine environments the only exceptions (Kramer and Green, 1990). That water is needed for fertilization has led to a false reputation that ferns are only present in lush environments such as rainforests. Ferns are ecologically quite variable and can be found in environments as diverse as tropical rain forests, deserts and the Arctic (Kramer and Green, 1990).

Extant ferns are often assumed to be ancient because of the antiquity of the entire group. Some living taxa certainly qualify as ancient, such as the genus *Osmunda* L. originating in the Permian (Tidwell and Ash, 1994) and persisting to the present day. However, most species are of much more recent origin. Combined analysis of molecular data and fossil data has shown that most fern genera originated in the Cenozoic and most extant species being comparatively young (Schuettpelz and Pryer, 2009). The Cenozoic radiation exploited the appearance of many novel niches in multi-stratal rainforests and most present-fern species are entire-leaved epiphytes in tropical rain forests (Kawai et al., 2003; Rothwell, 1987; Schneider et al., 2004; Schuettpelz and Pryer, 2009).

1.2. Importance of Polyploidy in Fern Diversification

Polyploidy is a widespread phenomenon with far-ranging effects on lineages (Otto 2007). Polyploidy has had a large historical impact on plant diversity, as many extant plant clades result from ancient polyploidization events (Adams and Wendel, 2005; Li et al., 2015). In more recent timeframes, the formation of polyploids has been a common speciation method and adds adaptability to a lineage (Otto and Whitton, 2000). The origin and genomic composition of polyploid taxa is further complicated by the frequent recurrent origins of many polyploid taxa (Soltis and Soltis, 1999). Polyploidization has dramatic effects on the genome of the new lineage including rapid genome downsizing (Leitch and Bennett, 2004), often accomplished by reciprocal silencing of homeologous alleles, dosage changes or subfunctionalization (Adams, 2007).

Ferns are renowned for their numerous polyploid taxa, with the highest rates of polyploid speciation of vascular plants (Wood et al., 2009) and the highest chromosome count ever recorded for any seed plant (*Ophioglossum* L., 2 n = >1200; Löve et al., 1977). Many taxa were first discovered to be polyploid during the pioneering cytological research of Irene Manton (Manton, 1950). Manton also explained the unusual asexual propagation of apogamous fern lineages through Dopp-Manton sporogenesis (Manton, 1950). Further groundbreaking research on polyploid ferns included early work on reticulate evolution and polyploid complexes (Wagner, 1954), chromosome evolution (Haufler and Soltis, 1986), gene expression (Soltis, 1986; Haufler, 1987), heterozygosity (Klekowski and Baker, 1966), recurrent formation (Werth et al., 1985), and speciation rates (Mayrose et al., 2010).

1.3. Influence of Environments Impacted by Glacial Cycles on Diversification

In addition to the aforementioned effects on polyploid formation, high altitude environments subject to glacial climate fluctuations also increase the number of recurrent origins and rates of fixed heterozygosity of polyploid taxa (Brochmann et al., 2004). These climate fluctuations have also been shown to lead to pre-adaption in taxa to utilize habitat exposed by changes in glacial extent (Crawford and Abbott, 1994), possibly by providing higher genetic variability across a species range (Aitken et al., 2008). They have also led to speciation events (Fan et al., 2013). Range contractions and expansions caused by glacial fluctuations have generated strong patterns of genetic diversity within fern lineages (Shepherd et al., 2007;

Trewick et al., 2002; Vogel et al., 1999). The role of morphological stasis in ensuring the continued use of similar niches worldwide during changing climate regimes has been demonstrated for plant taxa previously (McDaniel and Shaw, 2003), leaving the possibility that this is an adaptive strategy for a high-altitude or high-latitude lineage.

Wide-ranging high-latitude ranges also frequently have a complicated biogeographic history due to chance dispersal, shifting glaciers and land bridges (e.g., Sessa et al., 2012). Interchange between east Asia and North America has been common (Wen, 1999) and frequently led to subsequent speciation (Huttunen et al., 2015). Land bridges have been of particular importance for colonization between continents, such as Beringia facilitating Asian-North American connections (Ickert-Bond and Wen, 2006) and the North American Land Bridge connecting North America and Asia (Tiffney, 1985).

1.4. Historical Understanding of the Fern Genus *Cryptogramma*

Cryptogramma R.Br. is a small genus of epipetric, cold-tolerant ferns in the cryptogrammoid clade that is the sister taxon of the diverse Pteridaceae E.D.M. Kirchn. (Tryon and Tryon, 1990). Earlier authors segregated the genus in the Crytogrammaceae Pic.Serm. with *Llavea* Lag. and *Onychium* Kaulf. (Pichi-Sermolli, 1963), but later research has shown that the preferred monophyletic option is including it in a more inclusive Pteridaceae (Smith et al., 2006). The Pteridaceae are the largest leptosporangiate fern family with a high degree of morphological, ecological and geographic variation (Schuettpelz et al., 2007). *Cryptogramma* has since been found to be most closely related to the central American *Llavea* and southeast Asian *Coniogramme* Fée, and not closely related to *Onychium* based on molecular phylogenetic relationships (Prado et al., 2007; Schuettpelz et al., 2007; Zhang et al., 2005). This morphologically surprising grouping is known as the cryptogrammoid fern clade and is the sister lineage to the rest of the Pteridaceae (Gastony and Rollo, 1995; Prado et al., 2007; Schuettpelz and Pryer, 2007; Schuettpelz et al., 2007). *Cryptogramma* is found throughout boreal regions as well as one disjunct taxon occurring in Chile and Argentina (Tryon and Tryon, 1990).

Traditionally, two sections are recognized within *Cryptogramma* (Alverson, 1989; Tryon and Tryon, 1990). Section *Homopteris* (Rupr.) C. Chr. has always been considered to contain only *C. stelleri* (S.G. Gmel.) Prantl, while sect. *Cryptogramma* has been variously considered to consist of one species or up to ten (Alverson, 1989; Tryon and Tryon, 1990). Both sections are

epipetric and have dimorphic leaves, with fertile leaves taller and less dissected than sterile leaves (Lellinger, 1985). *Cryptogramma stelleri* has weakly dimorphic leaves, creeping rhizomes, thin lamina and a preference for limestone habitats (Alverson, 1993; Hultén, 1968). Section *Cryptogramma* uniformly has strongly dimorphic leaves, erect rhizomes, coriaceous lamina and a preference for acidic habitats (Alverson, 1993; Lellinger, 1985). The composition of sect. *Cryptogramma* has long been a matter of dispute. The traditional view suggests a single species that is broadly distributed and morphologically variable (e.g., Hultén, 1968; Tryon and Tryon, 1990). Other researchers have argued for recognizing 8-10 species that are more narrowly distributed and less morphologically variable (Alverson, 1989; Jessen et al., 2012; Lellinger, 1985; Vaganov et al., 2010).

Morphological revision of the Asian members of sect. *Cryptogramma* synonymized the two Chinese microspecies *Cryptogramma emiensis* Ching & K.H. Shing and *C. shensiensis* Ching with the widespread east Asian *C. brunoniana* Hook. & Grev. (Zhang and Zhang, 2003). Recent treatments have also supported recognizing the east Asian *C. raddeana* Fomin as a distinct taxon (Vaganov et al., 2010; Zhang and Zhang, 2003), but this conclusion is not unanimous (Fraser-Jenkins, 2008). The taxonomy of sect. *Cryptogramma* is also complicated by the presence of multiple polyploid species, including the octoploid *C. bithynica* S. Jess, L. Lehm. & Bujnoch in Turkey, tetraploid *C. crispa* (L.) R.Br. in Europe, and tetraploid *C. sitchensis* (Rupr.) Moore in Beringia (Alverson, 1989; Jessen et al., 2012). Cytological data and morphological traits suggest *C. crispa* as the progenitor of *C. bithynica,* but other species cannot be ruled out (Jessen et al., 2012). The genome of *Cryptogramma crispa* has been characterized as diploidized using breeding system data, but its progenitors are unknown (Pajarón et al., 1999). The Beringian tetraploid *C. sitchensis* is an autotetraploid based on allozyme and morphological data (Alverson, 1989). The widespread diploid *C. acrostichoides* R.Br. is one of the progenitors and morphological data suggest the other progenitor is *C. raddeana* (Alverson, 1989).

1.5. Suitability of *Cryptogramma* as a Model System

I have elected to use *Cryptogramma* as a model system for examining questions of taxonomy, polyploidy, and high latitude diversification. This genus is well-suited for examining taxonomy in a phylogenetic perspective due to the long-standing controversy over its species-level diversity across its circumboreal distribution. The cryptic polyploid taxa in the genus

provide an excellent opportunity to understand the roles of auto- and allo-polyploidy in the lineage, as well as the climatic and biogeographic factors involved in their formation. The presence of *Cryptogramma* on four continents also raises many questions of the biogeographic processes involved in the formation of its present-day range. Specifically, the broad high latitude distribution of *Cryptogramma* in boreal regions and a small austral disjunct region also permits us to examine the unique processes that occur at high latitudes and determine what effect they have had on polyploid formation, speciation rate, and morphological stasis.

1.6. Research Goals

This dissertation will add to our understanding of leptosporangiate ferns and enhance our knowledge of taxonomy, polyploidy and climate responses by clarifying taxonomic confusion within *Cryptogramma*, recovering effects of glacial cycles on species-level and genetic diversity, and providing a temporal and geographic perspective on the lineage. First, I will use DNA sequence data to determine if *Cryptogramma* and its two described sections are monophyletic. I will then use these data to resolve the debate over species-level diversity in sect. *Cryptogramma* and reconstruct the formation of polyploid taxa. I will use more intensive sampling of European populations to determine any potential effects of Pleistocene glacial cycles on genetic diversity today within the Eurasian *C. crispa* complex. I will also construct a temporal framework for diversification and estimating ages of key nodes for the genus-wide phylogeny in BEAST v.1.7.5 (Drummond and Rambaut, 2007; Drummond et al., 2012). These temporal estimates will also be used to reconstruct the biogeographic history of *Cryptogramma* using the dispersal-extinction-cladogenesis (DEC) approach implemented in Lagrange (Ree et al., 2005; Ree and Smith, 2008). The roles of climate and morphological stasis on speciation will also be examined in a Bayesian Analysis of Macroevolutionary Mixtures (BAMM; Rabosky et al., 2013; Rabosky et al., 2014).

Chapter 2. Diversification and reticulation in the circumboreal fern genus *Cryptogramma*[1]

2.1 Abstract

We investigated the evolutionary complexity that resulted from cryptic diversification and polyploidy in parsley ferns (*Cryptogramma*). A total of 14 species were included in our data set, with six outgroup species and eight *Cryptogramma* species. DNA sequence data from six plastid loci (*rbcL*, *rbcL-accD*, *rbcL-atpB*, *rps4-trnS*, *trnG-trnR* and *trnP-petG*) were analyzed using maximum likelihood and Bayesian methods to provide the first rigorous assessment of diversification in the genus, including testing the monophyly of the genus and sections. *Cryptogramma* and *Coniogramme* are recovered as reciprocally monophyletic sister genera. We established the monophyly of both sections within *Cryptogramma*. Furthermore, our sequence data reveal that described species reflect mostly allopatric reciprocally monophyletic lineages that are independent evolutionary trajectories. Using sequence data from the nuclear locus (*gapCp*) we find that the European *C. crispa* is an autotetraploid with a partially diploidized genome, while the North American tetraploid *Cryptogramma sitchensis* is an allopolyploid derived from *C. acrostichoides* and *C. raddeana*. Subsequent backcrossing between *C. sitchensis* and *C. acrostichoides* has allowed the introgression of *C. raddeana* alleles into northern populations of *C. acrostichoides*.

2.2 Introduction

The leptosporangiate fern genus *Cryptogramma* R.Br. is comprised of nine species in two sections. Referred to as parsley ferns for the resemblance of their foliage to that of parsley, they combine to have a circumboreal distribution with a bipolar disjunction as one taxon is present in southern South America (Alverson, 1989a; Raven, 1963). All members of the genus possess dimorphic leaves, with erect fertile leaves and shorter more finely divided sterile leaves. Fertile leaves possess false indusia and the chromosome base number for the genus is 30 (Tryon and Tryon, 1990).

Cryptogramma stelleri (S.G. Gmel.) Prantl is the only representative of section *Homopteris* (Rupr.) C. Chr. Found in the northern regions of North America, Asia and extreme

[1] Metzgar, J.S., E.R. Alverson, S. Chen, A.V. Vaganov, and S.M. Ickert-Bond. 2013. Diversification and reticulation in the circumboreal fern genus *Cryptogramma*. *Molecular Phylogenetics and Evolution* 67: 589-599.

northeastern Europe, it has a creeping rhizome, leaves with a membraneous texture and is often a calciphile (Alverson, 1993; Hultén and Fries, 1986). Authors have been in wide agreement on the taxonomy of this section (Alverson, 1993; Hultén, 1968; Lellinger, 1985; Tryon and Tryon, 1990; Vaganov et al., 2010), while previous treatments of sect. *Cryptogramma* Prantl have ranged from including one species (Hultén, 1968; Tryon and Tryon, 1990) to ten (Alverson, 1989a; Lellinger, 1985; Vaganov et al., 2010). Found across temperate and boreal regions of North America, Asia and Europe, one taxon is also found in southern South America (Tryon and Tryon, 1990). Species in sect. *Cryptogramma* have erect rhizomes, leaves with a more coriaceous texture and generally prefer acidic, rocky habitats (Alverson, 1989a).

Previous research has shown *Cryptogramma* to be closely related to *Coniogramme* Fée, a genus of approximately 30 species in the Old World tropics, and the monotypic Mexican genus *Llavea* Lag. (Prado et al., 2007; Schuettpelz et al., 2007; Zhang et al., 2005). These cryptogrammoid ferns occupy an important phylogenetic position as the sister lineage to the remainder of the Pteridaceae (Gastony and Rollo, 1995; Prado et al., 2007; Schuettpelz and Pryer, 2007; Schuettpelz et al., 2007), comprising the subfamily Cryptogrammoideae (*sensu* Smith et al., 2006). This family is closely related to the large eupolypod clade (Schuettpelz and Pryer, 2007). With many active research inquiries into other subfamilies of the Pteridaceae, particularly the cheilanthoid ferns (e.g., Beck et al., 2011; Grusz et al., 2009; Kirkpatrick, 2007; Rothfels et al., 2008; Schuettpelz et al., 2008; Sigel et al., 2011) and the emerging model system *Ceratopteris* (e.g., McGrath and Hickok, 1999; Nakazato et al., 2007; Scott et al., 2007), there is an urgent need for a better understanding of the relationships and characteristics of the cryptogrammoid clade.

No study has previously analyzed the evolution or taxonomy of the genus as a whole, with studies that are regional in scope predominating. Recent studies of the Chinese taxa reduced *Cryptogramma emiensis* Ching & K.H. Shing and *Cr. shensiensis* Ching to synonymy with *Cr. brunoniana* Hook. & Grev. (Zhang and Zhang, 2003). Disagreement regarding the specific status of the Asian *Cr. raddeana* Fomin has emerged, with some authors treating it as a variety (Zhang and Zhang, 2003) or subspecies (Fraser-Jenkins, 2008) of *Cr. brunoniana,* while others maintain *Cr. raddeana* at the species level (Zhang et al., 2013). Although it was unknown if it was of allopolyploid or autoployploid origin, the European tetraploid *Cr. crispa* (L.) R.Br. has been studied more extensively using breeding system evidence that suggests that its genome

has been effectively diploidized (Pajarón et al., 1999). The North American members of sect. *Cryptogramma* were studied using a biosystematic approach (Alverson, 1989a; Alverson, 1989b), which yielded the description of a new diploid species (*Cr. cascadensis* E.R. Alverson; Alverson, 1989b). Allozyme and morphological evidence established that *Cr. sitchensis* (Rupr.) Moore is an allotetraploid (Alverson, 1988; Alverson, 1989a) with *Cr. acrostichoides* R.Br. serving as one parent and the other hypothesized to be the Asian *Cr. raddeana*. In addition, these studies discovered that triploid hybrids between *Cr. acrostichoides* and *Cr. sitchensis* are common and caused much of the taxonomic confusion regarding these species (Alverson, 1988). However, a comprehensive molecular study of the group is wholly lacking, with no previous molecular evidence supporting the monophyly of the genus, sections or species.

Cryptogramma represents an excellent system to further our understanding of fern evolution, polyploidy, introgression and chromosome number evolution. Our study will be the first comprehensive examination of the genus, using multiple molecular data sets to test generic and subgeneric circumscriptions and evaluating correspondence between described species and molecular differentiation. Subtle morphological variation between putative species in sect. *Cryptogramma* has led some authors to recognize only one species (Hultén, 1968; Tryon and Tryon, 1990) and others to recognizing up to ten (Alverson, 1989a; Lellinger, 1985; Vaganov et al., 2010). We will test these species circumscriptions using molecular data to determine if it supports the existence of one nearly worldwide species or a series of partially geographically isolated species that are in reciprocally monophyletic lineages with slight but consistent distinguishing morphological traits. Chromosome number evolution will also be reconstructed using an explicit likelihood framework to determine the number and location of polyploidization events. The combination of an explicit chromosome evolution hypothesis in combination with the molecular data sets will permit a detailed examination of both the tetraploid *Cr. crispa* and the North American allotetraploid *Cr. sitchensis*. We will deduce origins of both tetraploid species and examine introgression of *gapCp* alleles into *Cr. acrostichoides* following the formation of *Cr. sitchensis*.

2.3 Materials and Methods

2.3.1 Taxon sampling

A total of 14 species were included in our data set, with *Llavea cordifolia*, five *Coniogramme* species and eight *Cryptogramma* species. Many species were represented by samples from multiple populations in an attempt to encompass potential geographic variation, with a total of 40 samples included in the data set (Table 2.1). An extensive effort was made to include material for as many species and populations as possible; however, no sequence data could be obtained for the recently described *Cr. gorovoii* A. Vaganov and Schmakov from the Russian Far East and Japan (sensu *Cr. crispa* var. *japonica*; Vaganov and Shmakov, 2007) or for the newly described *Cr. bithynica* S. Jess, L. Lehm. & Bujnoch (Jessen et al., 2012) from northwestern Turkey. *Llavea* accessions were used as the outgroup based on previously established relationships (Prado et al., 2007; Schuettpelz et al., 2007; Zhang et al., 2005).

2.3.2 DNA extraction, PCR amplification and sequencing

Genomic DNA was extracted from 15-20 mg of silica-dried leaf tissue per sample using the Qiagen DNeasy Plant Mini Kit (Qiagen, Valencia, California, USA). Six plastid loci (*rbcL*, *rbcL-accD*, *rbcL-atpB*, *rps4-trnS*, *trnG-trnR* and *trnP-petG*) were amplified and sequenced according to existing protocols (Table 2.1; Grusz et al., 2009; Korall et al., 2007).

For seven species of *Cryptogramma*, one exemplar accession was amplified and sequenced for the nuclear locus (*gapCp*) and three specimens of *Cr. acrostichoides* were amplified and sequenced to characterize potential introgression. Amplification protocols for this marker followed Schuettpelz et al. (2008) and PCR products were cloned using the Invitrogen TOPO TA Cloning kit (Invitrogen, Carlsbad, California, USA). Clones were amplified using Invitrogen's M13 primer pair and the same *gapCp* thermalcycler conditions as mentioned earlier. Alleles corresponding to the "short" copy and "long" copy of the *gapCp* locus were recovered (Schuettpelz et al., 2008).

All plastid and nuclear sequencing chromatograms were corrected by eye using Sequencher version 4.10.1 (Gene Codes Corporation, Ann Arbor, Michigan, USA). For *gapCp* sequences, separate projects were used containing all of the sequences for a given individual. Mutations and indels were then charted through the length of the consensus sequence, allowing for the identification of separate alleles. PCR artifacts such as chimeric sequences were detected

and removed during this step (Mason-Gamer et al., 2008). This study generated a combined total of 240 plastid and nuclear sequences and all were deposited in GenBank (Table 2.2).

2.3.3 Sequence alignments

For each locus, sequences were aligned using ClustalX 2.1 (Larkin et al., 2007) and the resulting alignments were then refined by eye. The aligned data matrix for the protein-coding *rbcL* locus lacked any insertions or deletions (indels). All of the alignments for the remaining loci included indels. Ambiguously aligned regions and indels were excluded from the final analyses, with excluded bases totaling 122 bp in *rbcL-accD,* 68 bp in *rbcL-atpB*, 324 bp in *rps4-trnS*, 219 bp in *trnG-trnR*, 249 bp in *trnP-petG*, 85 bp in the *gapCp* "short" copy and 53 bp in the *gapCp* "long" copy. Much of the non-coding portion of the *rps4-trnS* matrix was excluded, as the alignment in this region was extremely ambiguous between the different sections of *Cryptogramma* and between *Cryptogramma* and the other genera. We did not use any gap-coding method.

2.3.4 Plastid data set combinability

Bayesian Markov chain Monte Carlo (B/MCMC) analyses were implemented in MrBayes version 3.2 (Huelsenbeck and Ronquist, 2001; Ronquist and Huelsenbeck, 2003; Ronquist et al., 2012) for each single locus data set following the protocol used for the combined data matrix analysis (see section 2.5). Majority-rule consensus topologies were calculated for each locus. These topologies were manually inspected for topological conflicts (Mason-Gamer and Kellogg, 1996) using a minimum threshold of 0.95 posterior probability. No topological conflict among data sets was observed so all six plastid loci data sets were combined into a single data set. The combined plastid locus matrix had a length of 7,143 base pairs.

2.3.5 Phylogenetic analyses

MrModeltest 2.3 (Nylander et al., 2004) was used to determine the optimal model of sequence evolution for each ML and B/MCMC analysis based on Akaike Information Criterion scores (Table 2.3).

Analyses for both the combined plastid data set and the nuclear data sets used the same procedures. Maximum parsimony (MP) searches were implemented in PAUP* 4.0b10

(Swofford, 2002), with heuristic searches of 1,000 random addition sequence (RAS) replicates using tree-bisection-reconnection (TBR) branch swapping to determine the most parsimonious tree(s). Subsequent MP bootstrap analyses used 500 replicates, with 10 random-addition-sequence replicates each, TBR branch swapping and the nchuck option set to 100 trees to allow the bootstrap replicates to run to completion.

Maximum likelihood (ML) analyses and ML bootstrap analyses were run using Garli 2.0 (Zwickl, 2006) and implemented on the CIPRES Science Gateway computational portal (Miller et al., 2010). To avoid introducing potential biases in sequence evolution parameter values by combining loci (Winkworth et al., 2008), we instead partitioned the data set by locus and assigned each locus its own model of sequence evolution, with parameters determined by the optimal Akaike Information Criterion scores in MrModeltest 2.3 (Table 2.3). Each ML analysis was performed twice, once using random starting trees and once using stepwise addition starting trees. All ML analyses used eight replicates. ML bootstrap analyses included 100 bootstrap replicates each.

The combined plastid dataset and nuclear datasets were analysed separately using a B/MCMC approach in MrBayes version 3.2 with each of the plastid loci and each of the nuclear loci receiving its own model of sequence evolution as determined using the Akaike Information Criterion scores in MrModeltest 2.3 (Table 2.3). Each analysis used four runs, with four chains each, for 10 million generations. Default priors were used with a sampling frequency of 1,000 generations. Likelihood and generation scores were plotted to check for stationarity using Tracer v1.5 (Rambaut and Drummond, 2007). We conservatively discarded the first 2.5 million generations as the burn-in period. The remaining 30,000 trees were pooled to calculate the majority-rule consensus tree with average branch lengths and posterior probabilities.

2.3.6 chromEvol analysis

We also reconstructed genome evolution in the cryptogrammoid clade to test for ancient genome duplication events that could complicate interpretation of the nuclear gene results. The evolution of chromosome numbers in *Cryptogramma* was evaluated using the program chromEvol (Mayrose et al., 2010), which infers polyploidization events, chromosome gain/loss events and demi-polyploidization at ancestral nodes using a series of likelihood models. In order to detect any possible biases introduced by the analytical method or process used to generate the

input reference tree topology required by chromEvol, four separate topologies were used (Mayrose, pers. comm.). Two of the topologies were generated by pruning accessions from our combined plastid data matrix until each taxon was represented by a single specimen. This data set was then analyzed using the ML and B/MCMC analytical procedures outlined in section 2.5. The two resulting topologies were used as reference trees for the chromsome number evolution reconstruction. The other two topologies were obtained by modifying the optimal ML and B/MCMC topologies inferred for the full, 40-accession combined plastid data matrix in section 2.5. These topologies had the same excess accessions pruned so that only one sample per species remained. Branch lengths for the ML and B/MCMC topolgies were then re-estimated for that data set in PAUP* 4.0b10 (Swofford, 2002) and MrBayes version 3.2 (Huelsenbeck and Ronquist, 2001; Ronquist and Huelsenbeck, 2003; Ronquist et al., 2012), respectively.

Chromosome number counts were compiled from the literature and species with unknown counts were coded as missing data (Table 2.4). *Coniogramme intermedia* Hieron. and *Co. fraxinea* (D. Don) Fée each have published counts of both $n = 30$ and $n = 60$, so they were coded as polymorphic with both counts having a 50 % occurrence rate.

Chromosome number reconstruction analyses were then run in chromEvol v1.3 (Mayrose et al., 2010; http://www.zoology.ubc.ca/~mayrose/cp/chromEvol/) on the University of Alaska Fairbanks Life Science Informatics Computational Portal for all four topologies. All eight models of chromosome transition properties were evaluated for each run. Default parameters were used.

2.4 Results

2.4.1 Phylogenetic analyses of the combined plastid data set

The MP, ML and B/MCMC analyses all returned well-resolved, robust and congruent topologies (Fig. 2.1) . The MP analysis found a single island of 300 most parsimonious trees (length=1307 steps) on all heuristic replicates. ML analyses using random and stepwise starting trees in GARLi (Zwickl, 2006) returned identical topologies and likelihood scores. After achieving stationarity, the remaining 7.5 million generations of B/MCMC topologies all achieved convergence.

Coniogramme and *Cryptogramma* were retrieved as reciprocally monophyletic sister taxa, as were both sections within *Cryptogramma* (Fig. 2.1). All intergeneric and interspecific

relationships were well -supported (MPBS ≥ 91 %; MLBS ≥ 95 %; B/MCMC PP = 1.00). Accessions of the allotetraploid *Cr. sitchensis* formed a moderately supported monophyletic group (MPBS = 61 %; MLBS = 95 %; B/MCMC PP = 0.97) within the *Cr. acrostichoides* clade, while all other species were strongly supported as monophyletic lineages (Fig. 2.1). Two intraspecific relationships were significantly supported by MPBS, MLBS and B/MCMC, with two *Cr. acrostichoides* accessions (277 and 359) consistently supported as sister taxa and the two mainland Chinese *Cr. brunoniana* accessions retrieved as sister taxa (accessions 457 and 458).

2.4.2 Phylogenetic analyses of the gapCp data sets

The *gapCp* "short" copy data set yielded MP, ML and B/MCMC topologies that were mostly congruent with one another and with the combined plastid loci data set analyses (Fig. 2.2). Alleles from most species formed supported, reciprocally monophyletic clades (MPBS ≥ 70 %; MLBS ≥ 100 %; B/MCMC PP = 0.99). The *Cr. raddeana* clade contained alleles from *Cr. raddeana*, *Cr. sitchensis* and *Cr. acrostichoides* (MPBS = 99 %, MLBS = 100 % and B/MCMC PP = 1.00). Additionally, the ML analysis recovered *Cr. cascadensis* and *Cr. acrostichoides* alleles as sister clades with 100% MLBS support while MP and B/MCMC did not recover this node.

The *gapCp* "long" copy analysis was of more limited value due to alleles only being recovered from five species (results not shown; Table 2.2). The ML and B/MCMC analyses recovered *Cr. acrostichoides* and *Cr. crispa* as significantly supported sister taxa (MLBS = 100 %, B/MCMC PP = 1.00). Three species formed reciprocally monophyletic clades, while *Cr. acrostichoides* and *Cr. sitchensis* alleles were recovered as most closely related to each another.

2.4.3. chromEvol analysis

All four permutations of the chromEvol analysis (using topologies generated by ML and B/MCMC analyses of a reduced data set with one examplar accession per species and using topologies generating by pruning excess accessions from the optimal consensus from the ML and B/MCMC analyses and reestimating the branch lengths) had an optimal AIC score for the "Constant rate" model of chromosome evolution. All four analyses inferred a base chromosome number of 30 for the *Llavea*/*Coniogramme*/ *Cryptogramma* clade (Fig. 2.1). One chromosome loss event was inferred; this was the loss of a single chromosome on the branch leading to

Llavea. Three genome duplication events were inferred by all four chromEvol analyses: a duplication was inferred on each of the branches leading to the tetraploid *Cr. crispa* and *Cr. sitchensis* (Fig. 2.1) and a genome duplication event was inferred on the branch leading to *Coniogramme*, which was inferred to have a base number of n = 60.

2.5 **Discussion**

2.5.1 Intergeneric phylogenetic relationships

We have demonstrated the monophyly of both *Coniogramme* and *Cryptogramma* for the first time (Fig. 2.1). Although their circumscription has not generated controversy previously, their relationship as sister taxa was not suggested until the advent of molecular research (Prado et al., 2007; Schuettpelz et al., 2007; Zhang et al., 2005; but see Gastony and Rollo, 1995, for the first suggestion that *Llavea* and *Coniogramme* are closely related). Little molecular differentiation was found among accessions of *Llavea cordifolia*; however, our sampling was restricted to central Mexico and does not include possible variation across its geographic range (Table 2.1). Sampling within *Coniogramme* was limited and relationships and species boundaries within the genus remain enigmatic. The inferred base chromosome number of n = 30 for the cryptogrammoid clade is consistent with general patterns within Pteridaceae (Tryon and Tryon, 1990) but the inferred base number of $n = 60$ for *Coniogramme* may be an artifact of limited sampling in that genus.

2.5.2 Phylogenetic relationships within Cryptogramma

Our study recovers both sections within *Cryptogramma* as monophyletic in accordance with previous classification systems (Alverson, 1989a; Hultén, 1968; Lellinger, 1985; Tryon and Tryon, 1990; Vaganov et al., 2010) and the numerous morphological characters distinguishing the sections. Within monotypic section *Homopteris*, populations of *Cr. stelleri* from Taiwan and Alaska were found to be more closely related to one another than to a population from Ontario. However, this relationship was only well-supported in the maximum likelihood analysis and potential divergence within this taxon should be investigated with more thorough geographic sampling.

Within section *Cryptogramma*, the disjunct South American taxon *Cr. fumariifolia* (Phil.) Christ. is the earliest diverging member of the lineage although it is unclear whether this has

resulted from a recent or ancient dispersal event. Most relationships are geographically unsurprising, with the Asian taxa *Cr. raddeana* and *Cr. brunoniana* being closely related and the western North American taxa *Cr. acrostichoides* and *Cr. sitchensis* forming a paraphyletic grade. One exception is the close relationship of the western North American *Cr. cascadensis* and the European *Cr. crispa*.

Most published species included in the data set are found to be reciprocally monophyletic. The lone exception is *Cr. acrostichoides*, which is polyphyletic due to the inclusion of allotetraploid *Cr. sitchensis* accessions. Thus, we support the recognition of all eight published *Cryptogramma* taxa in our data set at the species level (Fig. 2.1), including both tetraploid taxa as they represent reproductively autonomous, discrete genetic lineages and can be diagnosed morphologically (Barrington et al., 1989). Two taxa were not assessed in this study due to a lack of suitable material; the Turkish *Cr. bithynica* and the Russian Far Eastern and Japanese *Cr. gorovoii* (formerly *Cr. crispa* var. *japonica*) remain in need of inclusion in future molecular studies.

2.5.3 Deciphering the history of tetraploid Cr. crispa

Long established as a tetraploid (Manton, 1950; Löve, 1970; Löve et al., 1971; Pajarón et al., 1999), little else has been known regarding the history or formation of the European *Cr. crispa.* Our plastid and nuclear genetic data both indicate that this species is most closely related to only *Cr. cascadensis*, from northwestern North America (Fig. 2.1; Fig. 2.2). While geographically distant, *Cr. cascadensis* and *Cr. crispa* do share morphological synapomorphies such as deciduous fronds with a thin lamina (Alverson, 1989b). We hypothesize that *Cr. crispa* is an autotetraploid whose progenitor was the now extinct or undiscovered European diploid sister species of *Cr. cascadensis*. This is supported by the geographic distance separating tetraploid *Cr. crispa* and diploid *Cr. cascadensis*, as well as several known genetic and mating system characteristics of *Cr. crispa*.

Previous research on the mating system and allozyme diversity within *Cr. crispa* reveal that its genome has been partially diploidized, as the species has an outcrossing mating system and greater genetic variability than associated with self-crossing polyploid taxa (Pajarón et al., 1999; Pangua et al., 1999). Branch lengths separating *Cr. crispa* and *Cr. cascadensis* are more similar in length to those separating other diploid *Cryptogramma* species, implying an older

origin of this tetraploid or, minimally, of the unknown diploid that formed *Cr. crispa* (Fig. 2.1; Fig. 2.2). Although dating the origin of polyploid taxa is notoriously difficult (Doyle and Egan, 2010), the unique, easily distinguished haplotypes and alleles of *Cr. crispa* (Fig. 2.1; Fig. 2.2) also lead us to conclude that it is a paleopolyploid taxon with an unknown progenitor (Stein et al., 2010). Although presumed extinct, this ancestral diploid could still be undetected within the known range of *Cr. crispa*, as evidenced by the recent discovery of an octoploid *Cryptogramma* from Turkey (Jessen et al., 2010). The current inability to disentangle the effects of evolutionary rates and time within *Cryptogramma* illustrates the need for a robust, fossil-calibrated estimate of divergence times for key parsley fern nodes.

2.5.4 Deciphering the history of tetraploid Cr. sitchensis

Previous research using morphology, spore measurement and allozyme data indicated that *Cr. sitchensis* is an allotetraploid and one of its progenitors was *Cr. acrostichoides* (Alverson, 1989b). The other progenitor was hypothesized to be the Russian *Cr. raddeana* based on morphology (Alverson, 1989a). Our plastid results (Fig. 2.1) confirm the role of *Cr. acrostichoides* as the maternal parent in this cross, as the plastid is maternally inherited in Pteridaceae (Gastony and Yatskievych, 1992) and the nuclear data (Fig. 2.2) confirm the morphological hypothesis that *Cr. raddeana* is the other progenitor. Interestingly, all sampled accessions of *Cr. sitchensis* form a single clade in the plastid data analysis (Fig. 2.1), implying a single origin of this taxon as opposed to the multiple origins typically observed in polyploid taxa (Soltis and Soltis, 2000).

A recent origin of this allopolyploid could be implied by the short branch lengths in the *Cr. sitchensis* clade (Fig. 2.1), although estimating polyploid lineage ages is fraught with difficulty (Doyle and Egan, 2010). The Beringian distribution of allotetraploid *Cr. sitchensis* and one diploid progenitor (*Cr. acrostichoides*) combined with the proximity of the other diploid progenitor (*Cr. raddeana*) suggests that *Cr. sitchensis* is another polyploid taxon formed during glacial maxima or subsequent recolonization (Consaul et al., 2010; Garcia-Jacas et al., 2009; Schmickl et al., 2010). Increased population-level sampling coupled with divergence time estimates and ecological niche modeling will refine this hypothesis (Metzgar, unpublished data).

2.5.5 Introgression within the Cr. acrostichoides complex

Our *gapCp* analysis identified a clade of *Cr. acrostichoides* alleles and a clade of *Cr. raddeana*, with alleles from the allotetraploid *Cr. sitchensis* occuring in both clades (Fig. 2.2). However, the *Cr. raddeana* clade also contains alleles from some populations of *Cr. acrostichoides*. Lineage sorting is unlikely, as a gene duplication event would have had to occur deep in the history of section *Cryptogramma* (Fig. 2.1) and would require an unparsimonious number of losses in various taxa and populations and an unreasonably slow coalescence time (Brokaw and Hufford, 2010). Our chromosome evolution reconstruction also rejects a whole genome duplication event predating extant *Cryptogramma* diversity (Fig. 2.1). We hypothesize that the presence of *gapCp* alleles from two populations of *Cr. acrostichoides* in a clade with *Cr. raddeana* and *Cr. sitchensis* alleles (Fig. 2.2) results from the introgression of *Cr. raddeana* alleles into some *Cr. acrostichoides* populations via backcrossing between *Cr. sitchensis* and *Cr. acrostichoides* (Fig. 2.3). One *Cr. acrostichoides* population that does not demonstrate any evidence of introgression is from Washington State, USA (Fig. 2.2; Fig. 2.3) and its allopatry with respect to *Cr. sitchensis* would preclude any chance of backcrossing. A triploid hybrid bridge could be the mechanism for backcrossing between *Cr. sitchensis* and diploid *Cr. acrostichoides*, as the two species frequently form a triploid hybrid, which produces some spores that appear normal and could produce viable sperm (DeBenedictis, 1969; Husband, 2004). Introgression has also been found to occur at the *gapCp* locus in other fern taxa (Nitta et al., 2011; Yatabe et al., 2009).

2.6 Conclusions

We have established the monophyly of *Coniogramme* and *Cryptogramma*, as well as both sections within *Cryptogramma*. Additionally, all included *Cryptogramma* species in our study represent monophyletic lineages (*Cr. acrostichoides* is monophyletic only when allotetraploid *Cr. sitchensis* is not considered). We support the recognition of these eight taxa at the species level. We have also confirmed or identified the parentage of allotetraploid *Cr. sitchensis* and autotetraploid *Cr. crispa* for the first time.

This study serves as the first rigorous molecular assessment of relationships within *Cryptogramma*. By independently analyzing monophyly and reticulation, we have identified numerous areas of interest or need for future study. The timing and direction of dispersal events

and genome duplications in the genus are in need of more rigorous estimation, as well as possible correlations with climatic fluctuations such as interglacial cycles. Additionally, several *Cryptogramma* species would make ideal candidates for detailed molecular and ecological reconstructions of survival strategies used by free-sporing monilophytes during the Last Glacial Maximum in North America.

2.7 Acknowledgments

We thank Ellen Anderson, Polly Bass, David Boufford (collecting with support from National Science Foundation DEB-0321846), David Gernandt, Li-Yaung Kuo, Juan Larraín, Manuel González Ledesma, Phan Ke Loc, Alicia Marticorena, Emily Metzgar, Santiago Pajarón, Emilia Pangua, Georg Pflugbeil, Kathleen Pryer, Richard Ree, Carl Rothfels, Erin Sigel, A. Shmakov, Mary Stensvold, Stacy Studebaker, Andreas Tribsch, Mike Windham, Valentin Yakubov and Peter Zika for providing specimens. The U.S. National Park Service is thanked for granting a research collection permit. We also thank Mac Campbell, Itay Mayrose, Carl Rothfels, Eric Schuettpelz and Diana Wolf for laboratory advice or technical expertise. Partial funding was provided by the Alaska Experimental Program to Stimulate Competitive Research Landscape Genetics Student Research Award, Alaska Quaternary Center Hopkins Fellowship, American Society of Plant Taxonomists Graduate Student Research Award, University of Alaska Center for Global Change Student Research Grant and University of Alaska Ted McHenry Biology Field Research Award.

2.8 Figures

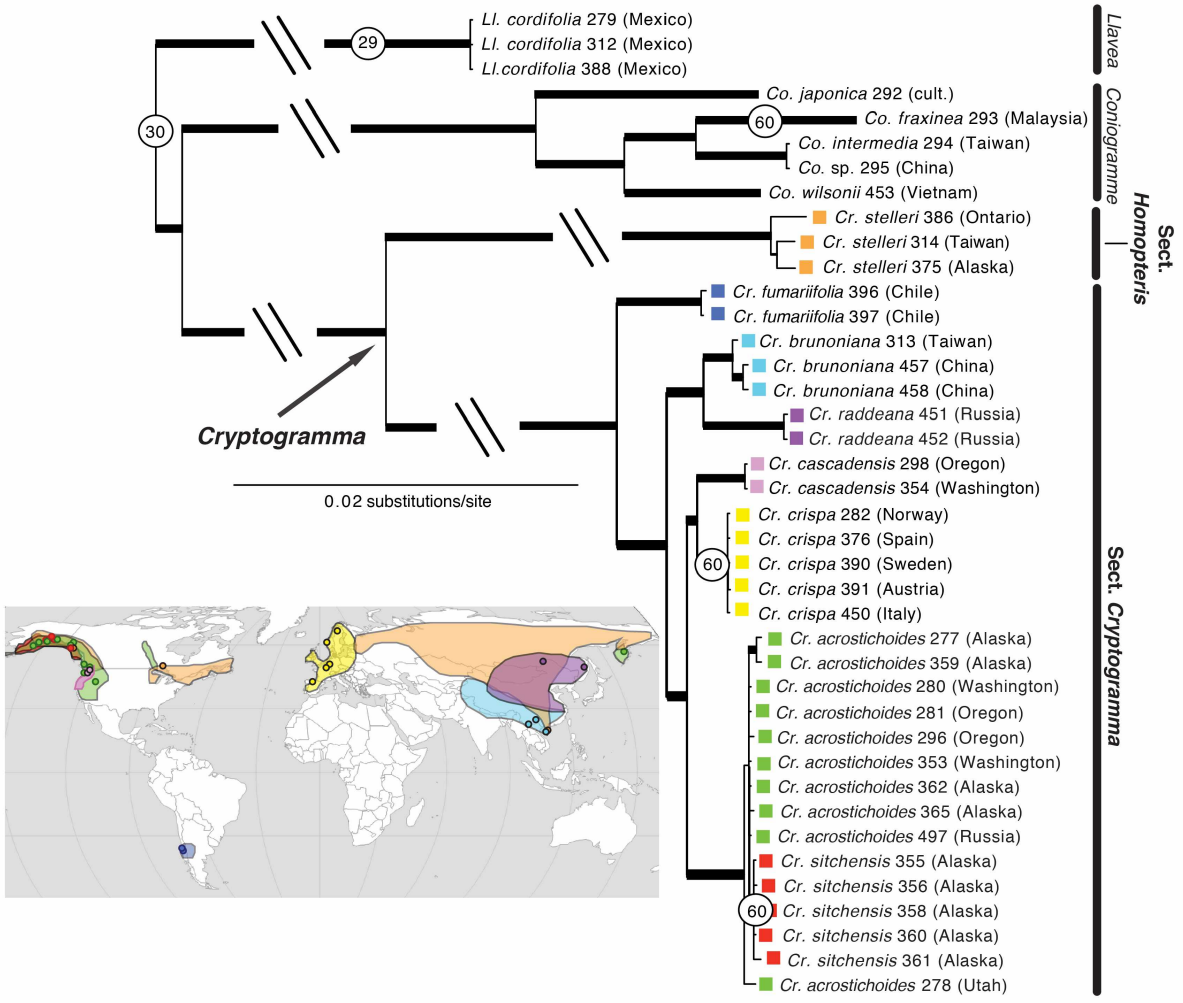

Fig. 2.1. Plastid phylogeny of cryptogrammoid ferns. Consensus phylogeny generated using a combined, six-locus plastid data set analyzed by Bayesian Markov chain Monte Carlo (B/MCMC). Thickened branches indicate relationships significantly supported by B/MCMC, maximum likelihood (ML) and maximum parsimony (MP) analyses (B/MCMC PP = 1.00; MLBS ≥ 95 %; MPBS ≥ 91 %). Branches shortened for clarity are indicated by hash marks. Inferred haploid chromosome numbers for the ancestral node and branches with chromosome transitions are indicated by circled numbers. Distribution map shows approximate range of each *Cryptogramma* species (colors correspond to those used in phylogeny) with sampled localities indicated with colored circles (Table 2.1).

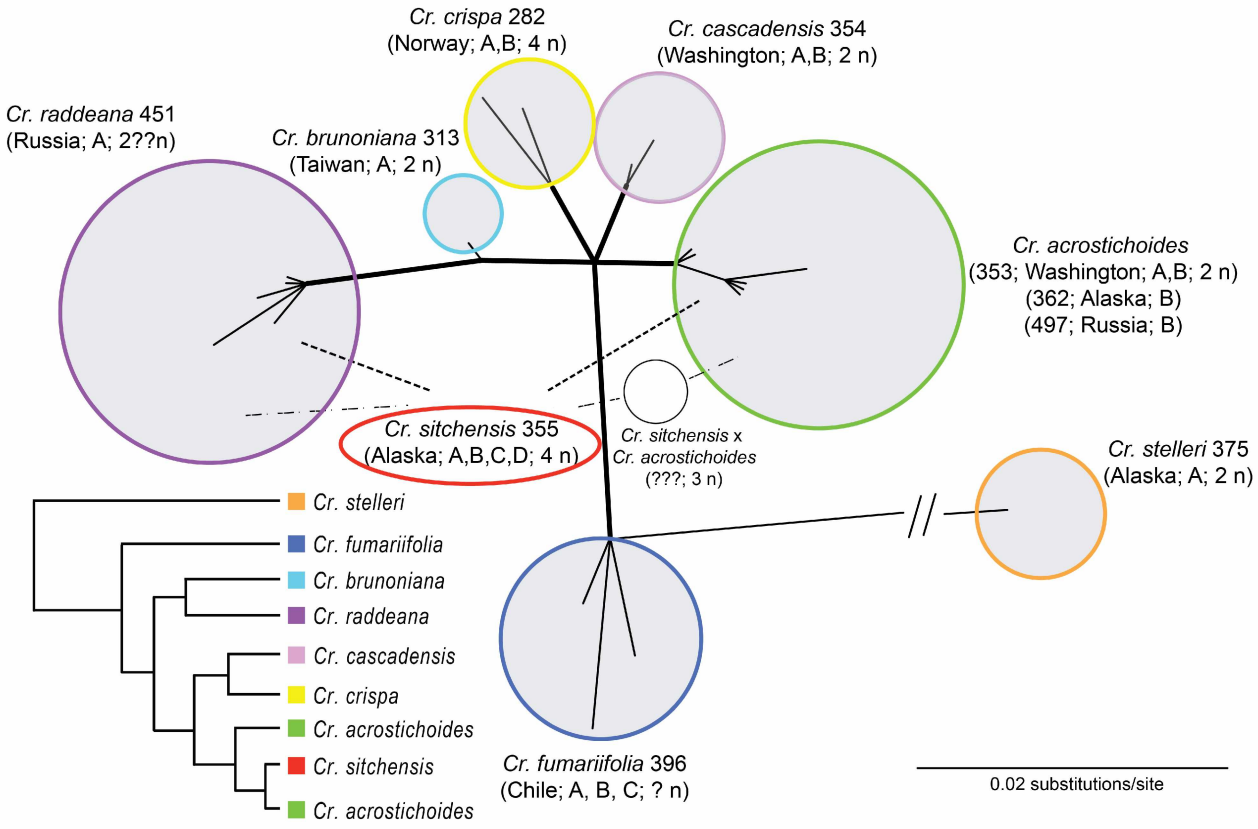

Fig. 2.2. Nuclear *gapCp* phylogeny of *Cryptogramma* species. Consensus phylogeny generated from *gapCp* "short" data set analyzed by Bayesian Markov chain Monte Carlo (B/MCMC). Thickened branches indicate relationships significantly supported by B/MCMC, maximum likelihood (ML) and maximum parsimony (MP) analyses (B/MCMC PP = 0.99; MLBS ≥ 100 %; MPBS ≥ 70 %). The branch leading to *Cr. stelleri* is shortened for clarity, as indicated by hash marks. Bubbles containing alleles represent taxa and are labeled with taxon name, DNA extraction number (Table 2.1), allele identifier and ploidy level. Alleles from allotetraploid *Cr. sitchensis* are found in multiple clades, indicated by dashed lines leading to *Cr. sitchensis*. Hypothesized position and role of the unsampled triploid hybrid between *Cr. sitchensis* and *Cr. acrostichoides* is depicted to illustrate its potential role in facilitating introgression (Fig. 2.3). A simplified cladogram depicts major relationships inferred from combined plastid loci analysis (Fig. 2.1).

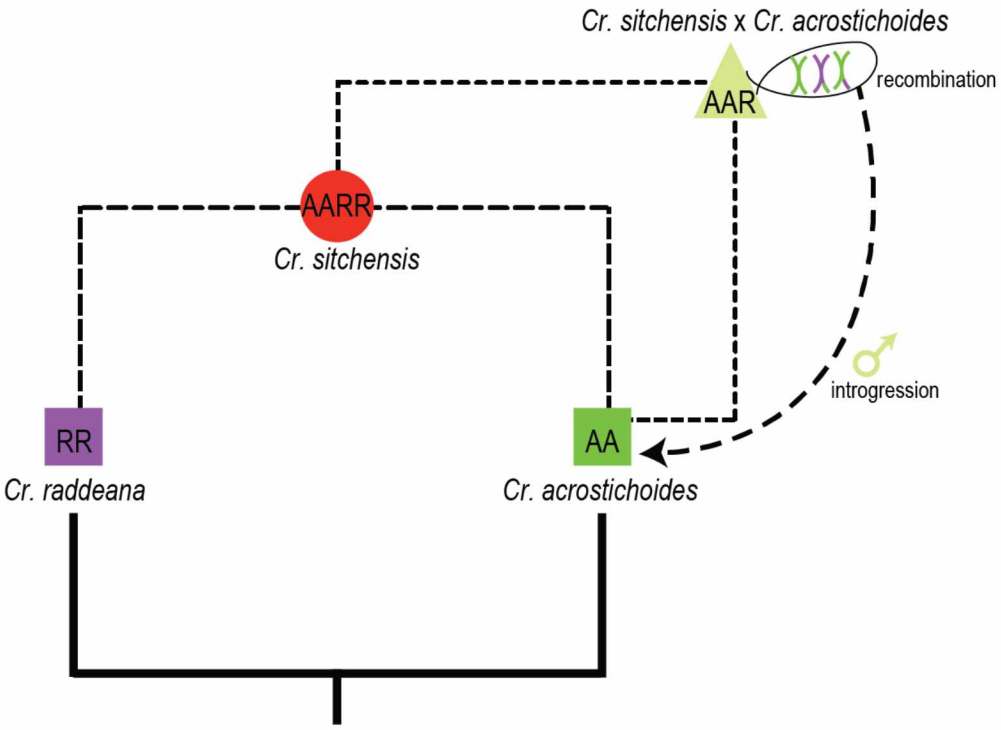

Fig. 2.3. Simplified phyloreticulogram demonstrating hypothesized introgression. *Cryptogramma acrostichoides* complex taxa are labeled with genomic constitution, with diploid taxa depicted as squares; triploid taxa as triangles and tetraploid taxa as circles. A simplified recombination event in triploid hybrid is shown. Known hybridization events are depicted as dashed lines and hypothesized backcrossing between triploid hybrid and diploid *Cr. acrostichoides* is depicted with a dashed arrow.

2.9 Tables

Table 2.1. Voucher information with sampling localities, specimen voucher and GenBank accession numbers. Herbarium acronyms in "Collector/No." field follow Index Herbariorum.

Ext. No.	Taxon	Locality	Collector/No.	GenBank accession no.						
				rbcL	*rbcL-accD*	*rbcL-atpB*	*rps4-trnS*	*trnG-trnR*	*trnP-petG*	*gapCp* short
279	*Llavea cordifolia*	Mexico: Hidalgo: Municipio Nicolas Flores. On road to Nicolas Flores from Cardonal	Rothfels 3025 (ALA, DUKE, MEXU)	KC700108	KC700148	KC700186	KC700225	KC700263	KC700299	-
312	*Llavea cordifolia*	Mexico: Hidalgo: Municipio Zimapán, Los Mármoles gorge.	Ledesma 2113 (HGOM)	KC700109	KC700150	KC700187	KC700226	KC700264	KC700300	-
388	*Llavea cordifolia*	Mexico: Guerrero: On outskirts of Fila De Caballos	Dyer 61 (MEXU, BM)	KC700110	KC700149	KC700188	KC700227	KC700265	KC700301	-
292	*Coniogramme japonica*	USA: North Carolina: Plant in cultivation at Juniper Level Botanic Garden	Schuettpelz 386 (DUKE)	KC700111	KC700151	KC700189	KC700228	KC700266	KC700302	-
293	*Coniogramme fraxinea*	Malaysia: Pahang: Cameron Highlands:	Schuettpelz 836 (DUKE,	KC700112	-	KC700190	KC700229	KC700267	KC700303	-

Table 2.1 continued

		Robinson Falls	KEP)							
294	*Coniogramme intermedia*	Taiwan: Nantou County: Mei-Feng Experimental Farm Reserve	Schuettpelz 1052A (DUKE, TAIF, BM)	KC700113	-	KC700191	KC700230	KC700268	KC700304	-
295	*Coniogramme* sp.	China: Guizhou: Shuicheng, Yushe	Zhang 246 (MO)	KC700114	KC700152	KC700192	KC700231	KC700269	KC700305	-
453	*Coniogramme wilsonii*	Vietnam: Bac Kan Province, Cho Don District, Ban Thi Community, Phia Khao Village	Hieu CPC1240 (ALA)	KC700115	KC700153	-	KC700232	KC700270	KC700306	-
277	*Cryptogramma acrostichoides*	USA: Alaska: Kodiak, near the transient boat harbor	Studebaker 09-473 (ALA)	KC700093	KC700133	KC700171	KC700210	KC700248	KC700284	-
278	*Cryptogramma acrostichoides*	USA: Utah: Salt Lake County, Little Cottonwood Canyon, near Snowbird	Rothfels 2979 (ALA, DUKE, NHIC)	KC700094	KC700134	KC700172	KC700211	KC700249	KC700285	-
280	*Cryptogramma acrostichoides*	USA: Washington: Mason County: N of Lake Cushman along the Mt.	Windham 3624 (DUKE, UT)	KC700095	KC700135	KC700173	KC700212	KC700250	KC700286	-

Table 2.1 continued

		Ellinor trail in the Olympic Mtns.								
281	*Cryptogramma acrostichoides*	USA: Oregon: Linn Co., Horse Rock Ridge, SW of Crawfordsville.	Pryer 06-04 (DUKE)	KC70 0096	KC70 0136	KC70 0174	KC70 0213	KC70 0251	KC70 0287	-
296	*Cryptogramma acrostichoides*	USA: Oregon: Lane County: Trail to Proxy Falls	Alverson s.n. (ALA)	KC70 0097	KC70 0137	KC70 0175	KC70 0214	KC70 0252	KC70 0288	-
353	*Cryptogramma acrostichoides*	USA: Washington: King County: Source Lake Lookout Trail, above Source Lake, Cascade Range.	Zika 25403 (ALA)	KC70 0098	KC70 0138	KC70 0176	KC70 0215	KC70 0253	KC70 0289	KC70 0066, KC70 0071
359	*Cryptogramma acrostichoides*	USA: Alaska: Seward: Kenai Fjords National Park: Harding Icefield Trail	Metzgar 247 (ALA)	KC70 0099	KC70 0139	KC70 0177	KC70 0216	KC70 0254	KC70 0290	-
362	*Cryptogramma acrostichoides*	USA: Alaska: Southeast Alaska: 10 miles northwest of Juneau, Mendenhall Lake, behind	Anderson 745 (ALA)	KC70 0100	KC70 0140	KC70 0178	KC70 0217	KC70 0255	KC70 0291	KC70 0070, KC70 0058

Table 2.1 continued

		Mendenhall Glacier Visitor Center								
365	*Cryptogramma acrostichoides*	USA: Alaska: Sitkalidak Island: Sitkalida Lagoon, cliffs along east side of lagoon	Studebaker 10-61 (ALA)	KC70 0101	KC70 0141	KC70 0179	KC70 0218	KC70 0256	KC70 0292	-
497	*Cryptogramma acrostichoides*	Russia: Kamchatka, north of Kamchatka peninsula, near Karaginskij	Chernyagina s.n. (ALA)	KC70 0102	KC70 0142	KC70 0180	KC70 0219	KC70 0257	KC70 0293	KC70 0059, KC70 0067
313	*Cryptogramma brunoniana*	Taiwan: NanTou County, Mt. ShihMen.	Kuo 455 (TAIF)	KC70 0081	KC70 0121	KC70 0159	KC70 0198	KC70 0238	KC70 0273	KC70 0061
457	*Cryptogramma brunoniana*	China: Xizang (Tibet) Province: Baxoi Xian: Anjiu La (pass), N of Rawu (Raog)	Boufford 29733 (GH)	KC70 0082	KC70 0122	KC70 0160	KC70 0199	KC70 0239	KC70 0274	-
458	*Cryptogramma brunoniana*	China: Gansu Province: Wen Xian: Motianling Shan, Baishui Jiang Nature Reserve	Boufford 37747 (GH)	KC70 0083	KC70 0123	KC70 0161	KC70 0200	KC70 0240	KC70 0275	-
298	*Cryptogramma*	USA: Oregon:	Alverson s.n.	KC70	KC70	KC70	KC70	KC70	KC70	-

Table 2.1 continued

	cascadensis	Deschutes/Linn County boundary: McKenzie Pass	(ALA)	0086	0126	0164	0203	0241	0277	
354	*Cryptogramma cascadensis*	USA: Washington: King County: Source Lake Lookout Trail, above Source Lake,	Zika 25404 (ALA)	KC70 0087	KC70 0127	KC70 0165	KC70 0204	KC70 0242	KC70 0278	KC70 0064, KC70 0065
282	*Cryptogramma crispa*	Norway: Hordaland: Bergen	Reeb VR4-VIII-02/11 (DUKE)	KC70 0088	KC70 0128	KC70 0166	KC70 0205	KC70 0243	KC70 0279	KC70 0062, KC70 0063
376	*Cryptogramma crispa*	Spain: Madrid Province, Sierra de Guadarrama, Siete Picos	Pajarón s.n. (ALA)	KC70 0089	KC70 0129	KC70 0167	KC70 0206	KC70 0244	KC70 0280	-
390	*Cryptogramma crispa*	Sweden: Norrbotten Gällivare County. Dundret, Gällivare.	Larsson 333 (DUKE, UPS)	KC70 0090	KC70 0130	KC70 0168	KC70 0207	KC70 0245	KC70 0281	-
391	*Cryptogramma crispa*	Austria: Steiermark, Niedere Tauern/Seckauer Alpen: Maierangerkogel - Vorwitzsattel	Pflugbeil 111847 (ALA)	KC70 0091	KC70 0131	KC70 0169	KC70 0208	KC70 0246	KC70 0282	-
450	*Cryptogramma crispa*	Italy: northwest of Brunico, Astnerberg	Shmakov s.n. (ALTB)	KC70 0092	KC70 0132	KC70 0170	KC70 0209	KC70 0247	KC70 0283	-

Table 2.1 continued

396	*Cryptogramma ˙fumariifolia*	Chile: Provincia de Ñuble: Comuna de Pinto, Shangri-La	Larraín 34009 (ALA, CONC)	KC70 0079	KC70 0119	KC70 0157	KC70 0196	KC70 0236	KC70 0271	KC70 0073, KC70 0074, KC70 0075
397	*Cryptogramma ˙fumariifolia*	Chile: Provincia de Ñuble: Comuna de Pinto, Shangri-La	Larraín 34010 (ALA, CONC)	KC70 0080	KC70 0120	KC70 0158	KC70 0197	KC70 0237	KC70 0272	-
451	*Cryptogramma raddeana*	Russia: Republic of Buryatia, Severo-Muisky range, Samokuya	Naumov 1989 (NS)	KC70 0084	KC70 0124	KC70 0162	KC70 0201	-	-	KC70 005
452	*Cryptogramma raddeana*	Russia: Khabarovsky krai, 30km north of Sofiysk	Netchaev s.n. (NS)	KC70 0085	KC70 0125	KC70 0163	KC70 0202	-	KC70 0276	-
355	*Cryptogramma sitchensis*	USA: Alaska: between Portage and Whittier: Bering Glacier	Metzgar 248 (ALA)	KC70 0103	KC70 0143	KC70 0181	KC70 0220	KC70 0258	KC70 0294	KC70 0057, KC70 0056, KC70 0060, KC70 0068

Table 2.1 continued

356	*Cryptogramma sitchensis*	USA: Alaska: Taku Glacier	Bass s.n. (ALA)	KC70 0104	KC70 0144	KC70 0182	KC70 0221	KC70 0259	KC70 0295	-
358	*Cryptogramma sitchensis*	USA: Alaska: Seward: Kenai Fjords National Park	Metzgar 246 (ALA)	KC70 0105	KC70 0145	KC70 0183	KC70 0222	KC70 0260	KC70 0296	-
360	*Cryptogramma sitchensis*	USA: Alaska: Palmer: Hatcher Pass	Metzgar 249 (ALA)	KC70 0106	KC70 0146	KC70 0184	KC70 0223	KC70 0261	KC70 0297	-
361	*Cryptogramma sitchensis*	USA: Alaska: Valdez: Thompson Lake	Metzgar 257 (ALA)	KC70 0107	KC70 0147	KC70 0185	KC70 0224	KC70 0262	KC70 0298	-
314	*Cryptogramma stelleri*	Taiwan: NanTou County, Hohuan Shelter.	Kuo 492 (TAIF)	KC70 0076	KC70 0116	KC70 0154	KC70 0193	KC70 0233	-	-
375	*Cryptogramma stelleri*	USA: Alaska: Alexander Archipelago: Prince of Wales Island	Johnson 20104 (ALA)	KC70 0077	KC70 0117	KC70 0155	KC70 0194	KC70 0234	-	KC70 0072
386	*Cryptogramma stelleri*	Canada: Ontario. Thunder Bay District: Talbot Island	Oldham 23697 (OAC, BAB, DUKE)	KC70 0078	KC70 0118	KC70 0156	KC70 0195	KC70 0235	-	-

Table 2.2. Primer names and sequences used.

Locus	Primer name	Sequence (5'-3')	Reference
rbcL	ESRBCL1F[a]	ATG TCA CCA CAA ACG GAG ACT AAA GC	Korall et al., 2006
rbcL	ESRBCL645F	AGA YCG TTT CYT ATT YGT AGC AGA AGC	Korall et al., 2006
rbcL	ESRBCL663R	TAC RAA TAR GAA ACG RTC TCT CCA ACG	Korall et al., 2006
rbcL	ESRBCL1361R[a]	TCA GGA CTC CAC TTA CTA GCT TCA CG	Korall et al., 2006
rbcL-accD	RBCL1187F[a]	GGA ACY TTG GGA CAT CCT TGG	Korall et al., 2007
rbcL-accD	ACCDHIF4	GAA GAT AAA CGA AAA TTG GGT GG	Ebihara et al., 2003
rbcL-accD	ACCD887R	TTA TCA CAB CGM GCC CAT AAT CC	Korall et al., 2007
rbcL-accD	ACCD816R[a]	CCA TGA TCG AAT AAA GAT TCA GC	Ebihara et al., 2003
rbcL-atpB	ESRBCL26R[a]	GCT TTA GTC TCC GTT TGT GGT GAC AT	Korall et al., 2007
rbcL-atpB	ATPB609R[a]	TCR TTD CCT TCR CGT GTA CGT TC	Pryer et al., 2004
rbcL-atpB	ATPBSPACER703R	CCA ATG ATC TGA GTA ATS TAT CC	Korall et al., 2007
rps4-trnS^{GGA}	trnS^{GGAa}	TTA CCG AGG GTT CGA ATC CCT C	Shaw et al., 2005
rps4-trnS^{GGA}	rps4.5'[a]	ATG TCS CGT TAY CGA GGA CCT	Souza-Chies et al., 1997
trnG-trnR	TRNGR1F[a]	GCG GGT ATA GTT TAG TGG TAA	Nagalingum et al., 2007
trnG-trnR	TRNGR353F	TTG CTT MTA YGA CTC GGT G	Korall et al., 2007
trnG-trnR	TRNG63R	GCG GGA ATC GAA CCC GCA TCA	Nagalingum et al., 2007
trnG-trnR	TRNR22R[a]	CTA TCC ATT AGA CGA TGG ACG	Nagalingum et al.,

Table 2.2 continued

			2007
trnP^{UGG}*-petG*	trnP^{UGGa}	TGT AGC GCA GCY YGG TAG CG	Small et al., 2005
trnP^{UGG}*-petG*	petG2[a]	CAA TAY CGA CGK GGY GAT CAA TT	Small et al., 2005
gapCp	ESGAPCP8F1[a]	ATY CCA AGY TCA ACT GGT GCT GC	Schuettpelz et al., 2008
gapCp	ESGAPCP11R1[a]	GTA TCC CCA YTC RTT GTC RTA CC	Schuettpelz et al., 2008

[a]Primer used for both amplification and sequencing.

Table 2.3. Models of DNA sequence evolution. Models used in maximum likelihood (ML) and Bayesian inference (B/MCMC) analyses as selected by Akaike Information Criterion (AIC) scores in MrModeltest (Nylander et al., 2004).

Data set	**ML model**	**B/MCMC model**
rbcL	SYM + G	SYM + G
rbcL-accD	GTR + G	GTR + G
rbcL-atpB	GTR + G	GTR + G
rps4-trnS^{GGA}	HKY + I	HKY + I
trnG-trnR	GTR + G	GTR + G
trnP^{UGG}-petG	GTR + I	GTR + I
combined plastid	GTR + G	GTR + G
***gapCp* "short"**	GTR + I	GTR + I
***gapCp* "long"**	GTR	GTR

Table 2.4. Haploid (*n*) chromosome numbers used in chromosome number evolution analysis.

Taxon	Chromosome number	Reference
Llavea cordifolia	29	Mickle et al., 1966; Knobloch, 1967
Co. fraxinea	30,60[a]	Singh and Roy, 1988; Matsumoto and Nakaike, 1990; Kato et al., 1992
Co. intermedia	30,60[a]	Matsumoto and Nakaike, 1990; Kato et al., 1992
Co. japonica	60	Weng and Qui, 1988
Co. wilsonii	X[b]	N/A
Cr. acrostichoides	30	Taylor and Lang, 1963; Löve and Löve, 1976; Alverson, 1989a
Cr. brunoniana	30	Khullar et al., 1988
Cr. cascadensis	30	Alverson, 1989a
Cr. crispa	60	Manton, 1950; Löve, 1970; Löve et al., 1971; Pajarón et al., 1999
Cr. fumariifolia	X[b]	N/A
Cr. raddeana	X[b]	N/A
Cr. sitchensis	60	Alverson, 1989a;
Cr. stelleri	30	Wagner, 1963; Britton, 1964; Gervais et al., 1999

[a] See Materials and Methods for details on coding taxa with conflicting counts.

[b] No published chromosome count available.

2.10 References

Alverson, E.R., 1988. Biosystematics of North American parsley ferns, *Cryptogramma* (Adiantaceae). Am. J. Bot. 75, 136–137.

Alverson, E.R., 1989a. Biosystematics of Parsley-ferns, *Cryptogramma* R. Br., in Western North America. Master's thesis, Oregon State University.

Alverson, E.R., 1989b. *Cryptogramma cascadensis*, a new parsley fern from Western North America. Am. Fern. J. 79, 95–102.

Alverson, E.R., 1993. *Cryptogramma*, in: Flora of North America Editorial Committee (Eds.), The Flora of North America, Vol. 2. Oxford University Press, New York, NY, pp. 137–139.

Barrington, D.S., Haufler, C.H., Werth, C.R., 1989. Hybridization, reticulation and species concepts in the ferns. Am. Fern J. 79, 55–64.

Beck, J.B., Windham, M.D., Pryer, K.M., 2011. Do asexual lineages lead short evolutionary lives? A case-study from the fern genus *Astrolepis*. Evol. 65, 3217–3229.

Britton, D.M., 1964. Chromosome numbers of ferns in Ontario. Canad. J. Bot. 42, 1349–1354.

Brokaw, J.M., Hufford, L., 2010. Origins and introgression of polyploid species in *Mentzelia* section *Trachyphytum* (Loasaceae). Am. J. Bot. 97, 1457–1473.

Consaul, L.L., Gillespie, L.J., Waterway, M.J., 2010. Evolution and polyploid origins in North American Arctic *Puccinellia* (Poaceae) based on nuclear ribosomal spacer and chloroplast DNA sequences. Am. J. Bot. 97, 324–336.

DeBenedictis, V.M.M., 1969. Apomixis in ferns with special reference to sterile hybrids. Ph.D. dissertation, University of Michigan.

Doyle, J.J., Egan, A.N., 2010. Dating the origins of polyploidy events. New Phytol. 186, 73–85.

Ebihara, A., Iwatsuki, K., Ohsawa, T.A., Ito, M., 2003. *Hymenophyllum paniense* (Hymenophyllaceae), a new species of filmy fern from New Caledonia. Syst. Bot. 28, 228–235.

Fraser-Jenkins, C.R., 2008. Taxonomic revision of three hundred Indian subcontinental Pteridophytes with a revised census-list: a new picture of fern-taxonomy and nomenclature in the Indian subcontinent. Bishen Singh Mahendra Pal Singh, Dehra Dun, India.

Garcia-Jacas, N., Soltis, P.S., Font, M., Soltis, D.E., Vilatersana, R., Susanna, A., 2009. The polyploid series of *Centaurea toletana*: glacial migrations and introgression revealed by nrDNA and cpDNA sequences analyzes. Mol. Phylogenet. Evol. 52, 377–394.

Gastony, G.J., Rollo, D.R., 1995. Phylogeny and generic circumscriptions of cheilanthoid ferns (Pteridaceae: Cheilanthoideae) inferred from *rbcL* nucleotide sequences. Am. Fern J. 85, 341–360.

Gastony, G.J., Yatskievych, G., 1992. Maternal inheritance of the chloroplast and mitochondrial genomes in cheilanthoid ferns. Am. J. Bot. 79, 716–722.

Gervais, C., Trahan, R., Gagnon, J., 1999. IOPB chromosome data 14. Newslett. Int. Organ. Pl. Biosyst. (Oslo) 30, 10–15.

Grusz, A.L., Windham, M.D., Pryer, K.M., 2009. Deciphering the origins of apomictic polyploids in the *Cheilanthes yavapensis* complex (Pteridaceae). Am. J. Bot. 96, 1636–1645.

Huelsenbeck, J.P., Ronquist, F., 2001. MRBAYES: Bayesian inference of phylogeny. Bioinformatics 17, 754–755.

Hultén, E., Fries, M., 1986. Atlas of North European vascular plants: north of the Tropic of Cancer, vol. 1–3. Königstein, Koeltz.

Hultén, E., 1968. Flora of Alaska and Neighboring Territories. Stanford University Press, Stanford, CA.

Husband, B.C., 2004. The role of triploid hybrids in the evolutionary dynamics of mixed-ploidy populations. Biol. J. Linn. Soc. 82, 537–546.

Jessen, S., Lehmann, L., Bujnoch, W., 2012. *Cryptogramma bithynica* sp. nov. (Pteridaceae, Pteridophyta)—a new fern species from northwestern Anatolia/Turkey. Fern Gaz. 19, 47–54.

Kato, M., Nakato, N., Cheng, X., Iwatsuki, K., 1992. Cytotaxonomic study of ferns of Yunnan, southwestern China. Bot. Mag. (Tokyo) 105, 105–124.

Kirkpatrick, R.E.B., 2007. Investigating the monophyly of *Pellaea* (Pteridaceae) in the context of a phylogenetic analysis of cheilanthoid ferns. Syst. Bot. 32, 504–518.

Khullar, S.P., Sharma, S.S., Verma, S.C., 1988. SOCGI plant chromosome number reports – VI. J. Cytol. Genet. 23, 38–52.

Knobloch, I.W., 1967. Chromosome Numbers in *Cheilanthes*, *Notholaena*, *Llavea* and *Polypodium*. Am. J. Bot., 54, 461–464.

Korall, P., Pryer, K.M., Metzgar, J.S., Schneider, H., Conant, D.S., 2006. Tree ferns: monophyletic groups and their relationships as revealed by four protein-coding plastid loci. Mol. Phylogenet. Evol. 39, 830–845.

Korall, P., D.S. Conant, J.S. Metzgar, H. Schneider, K.M. Pryer. 2007. A molecular phylogeny of scaly tree ferns (Cyatheaceae). Am. J. Bot. 94: 873–886.

Larkin, M.A., Blackshields, G., Brown, N.P., Chenna, R., McGettigan, P.A., McWilliam, H., Valentin, F., Wallace, I.M., Wilm, A., Lopez, R., Thompson, J.D., Gibson, T.J., Higgins, D.G., 2007. Clustal W and Clustal X version 2.0. Bioinformatics 23, 2947–2948.

Lellinger, D.B., 1985. A Field Manual of the Ferns & Fern-Allies of the United States & Canada. Smithsonian Institution Press, Washington, DC.

Löve, A., 1970. Islenzk ferdaflora. Almenna Bokfelagid, Reykjavik.

Löve, A., Löve, D., Kapoor, B.M., 1971. Cytotaxonomy of a century of Rocky Mountain orophytes. Arctic and Alpine Res. 3, 139–165.

Löve, A., Löve, D., 1976. In IOPB chromosome number reports LIII. Taxon 25, 483–500.

Manton, I., 1950. Problems of Cytology and Evolution in the Pteridophyta. Cambridge University Press, London.

Mason-Gamer, R.J., Burns, M.M., Naum, M., 2008. Allohexaploidy, introgression, and the complex phylogenetic history of *Elymus repens* (Poaceae). Mol. Phylogenet. Evol. 47, 598–611.

Mason-Gamer, R. J., Kellogg, E. A., 1996. Testing for phylogenetic conflict among molecular data sets in the tribe Triticeae (Gramineae). Syst. Biol. 45, 524–545.

Matsumoto, S., Nakaike, T., 1990. Cytological observations of some ferns in Nepal (1). On the related taxa in Japan. In: M. Watanabe & S. B. Malla (editors), Cryptog. Himalayas 2: 163–178.

Mayrose, I., Barker, M.S., Otto, S.P., 2010. Probabilistic models of chromosome number evolution and the inference of polyploidy. Syst. Biol. 59, 132–144.

McGrath, J. M., Hickok, L.G., 1999. Multiple ribosomal RNA gene loci in the genome of the homosporous fern *Ceratopteris richardii*. Can. J. Bot. 77, 1199–1202.

Mickle, J.T., Wagner, W.H., Chen, K.L., 1966. Chromosome observations on the ferns of Mexico. Caryologia 19, 85–94.

Miller, M.A., Pfeiffer, W., Schwartz, T., 2010. Creating the CIPRES Science Gateway for inference of large phylogenetic trees, in: Proceedings of the Gateway Computing Environments Workshop (GCE), 14 Nov. 2010, New Orleans, LA, pp 1–8.

Nagalingum, N.S., Schneider, H., Pryer, K. M., 2007. Molecular phylogenetic relationships and morphological evolution in the heterosporous fern genus *Marsilea*. Syst. Bot. 32, 16–25.

Nakazato, T., Jung, M.-K., Housworth, E.A., Rieseberg, L.H., Gastony, G.J., 2007. A genome-wide study of reproductive barriers between allopatric populations of a homosporous fern, *Ceratopteris richardii*. Genetics 177, 1–10.

Nitta, J.H., Ebihara, A., Ito, M., 2011. Reticulate evolution in the *Crepidomanes minutum* species complex (Hymenophyllaceae). Am. J. Bot. 98, 1782–1800.

Nylander, J.A.A., Ronquist, F., Huelsenbeck, J.P., Nieves Aldrey, J.L., 2004. Bayesian phylogenetic analysis of combined data. Syst. Biol. 53, 47–67.

Pajarón, S., Pangua, E., García-Álvarez, L., 1999. Sexual expression and genetic diversity in populations of *Cryptogramma crispa* (Pteridaceae). Am. J. Bot. 86, 964–973.

Pangua, E., García-Álvarez, L., Pajarón, S., 1999. Studies on *Cryptogramma crispa* Spore Germination. Am. Fern J., 89, 159–170.

Prado, J., Rodrigues, C.D.N., Salatino, A., Salatino, M.L.F., 2007. Phylogenetic relationships among Pteridaceae, including Brazilian species, inferred from *rbcL* sequences. Taxon 56, 355–368.

Pryer, K.M., Schuettpelz, E., Wolf, P.G., Schneider, H., Smith, A.R., Cranfill, R., 2004. Phylogeny and evolution of ferns (monilophytes) with a focus on the early leptosporangiate divergences. Am. J. Bot. 91, 1582–1598.

Rambaut, A., Drummond, A.J., 2007. Tracer v1.4, http://beast.bio.ed.ac.uk/Tracer.

Raven, P.H., 1963. Amphitropical relationships in the floras of North and South America. Q. Rev. Biol. 38, 151–177.

Ronquist, F., Huelsenbeck, J.P., 2003. MrBayes3: Bayesian phylogenetic inference under mixed models. Bioinformatics 19: 1572–1574.

Ronquist, F., Teslenko, M., van der Mark, P., Ayres, D.L., Darling, A., Höhna, S., Larget, B., Liu, L., Suchard, M.A., Huelsenbeck, J.P., 2012. MrBayes 3.2: efficient Bayesian phylogenetic inference and model choice across a large model space. Syst. Biol. 61, 539–542.

Rothfels, C.J., Windham, M.D., Grusz, A.L., Gastony, G.J., Pryer, K.M., 2008. Toward a monophyletic *Notholaena* (Pteridaceae): Resolving patterns of evolutionary convergence in xeric-adapted ferns. Taxon 57, 712–724.

Schmickl, R., Jørgensen, M.H., Brysting, A.K. Koch, M.A., 2010. The evolutionary history of the *Arabidopsis lyrata* complex: a hybrid in the amphi-Beringian area closes a large distribution gap and builds up a genetic barrier. BMC Evol. Biol. 10, 98.

Schuettpelz, E., Pryer, K.M., 2007. Fern phylogeny inferred from 400 leptosporangiate species and three plastid genes. Taxon 56, 1037–1050.

Schuettpelz, E., Schneider, H., Huiet, L., Windham, M.D., Pryer, K.M., 2007. A molecular phylogeny of the fern family Pteridaceae: assessing overall relationships and the affinities of previously unsampled genera. Mol. Phylogenet. Evol. 44, 1172–1185.

Schuettpelz, E., Grusz, A.L., Windham, M.D., Pryer, K.M., 2008. The utility of nuclear *gapCp* in resolving polyploid fern origins. Syst. Bot. 33, 621–629.

Scott, R.J., Gastony, G.J., Weatherford, J.W., Nakazato, T., 2007. Characterization of four members of the alpha-tubulin gene family in *Ceratopteris richardii*. Am. Fern J. 97, 47–65.

Shaw, J., Lickey, E.B., Beck, J.T., Farmer, S.B., Liu, W., Miller, J., Siripun, K. C., Winder, C.T., Schilling, E.E., Small, R.L., 2005. The tortoise and the hare II: Relative utility of 21 noncoding chloroplast DNA sequences for phylogenetic analysis. Am. J. Bot. 92, 142–166.

Sigel, E.M., Windham, M.D., Huiet, L., Yatskievych, G., Pryer, K.M., 2011. Species relationships and farina evolution in the cheilanthoid fern genus *Argyrochosma* (Pteridaceae). Syst. Bot. 36, 554–564.

Singh, V.P., Roy, S.K., 1988. Cytology of forty four species from Sikkim, Himalaya. Indian Fern J. 5, 162–169.

Small, R.L., Lickey, E.B., Shaw, J., Hauk, W.D., 2005. Amplification of noncoding chloroplast DNA for phylogenetic studies in lycophytes and monilophytes with a comparative example of relative phylogenetic utility from Ophioglossaceae. Mol. Phylogenet. Evol. 36, 509–522.

Smith, A.R., Pryer, K.M., Schuettpelz, E., Korall, P., Schneider, H., Wolf, P.G., 2006. A classification for extant ferns. Taxon 55, 705–731.

Soltis, P.S., Soltis, D.E., 2000. The role of genetic and genomic attributes in the success of polyploids. Proc. Nat. Acad. Sci. USA 97, 7051–7057.

Stein, D.B., Hutton, C., Conant, D.S., Haufler, C.H., Werth, C.R., 2010. Reconstructing *Dryopteris "semicristata"* (Dryopteridaceae): molecular profiles of tetraploids verify their undiscovered diploid ancestor. Am. J. Bot. 97, 998–1004.

Swofford, D.L., 2002. PAUP*: phylogenetic analysis using parsimony (*and other models), v. 4.0 beta 10. Sunderland, Sinauer Associates.

Taylor, T.M.C., Lang, F., 1963. Chromosome counts in some British Columbia Ferns. Amer. Fern J. 53, 123–126.

Tryon, R.M., Tryon, A.F., 1990. *Pteridaceae, in*: K. U. Kramer and P. S. Green [eds.], The families and genera of vascular plants, vol. I, Pteridophytes and gymnosperms. Springer-Verlag, Berlin, pp. 230–256.

Vaganov, A., Shmakov, A., 2007. New species of *Cryptogramma* (Cryptogrammaceae) from the Far East. Turcz. 10, 5–8.

Vaganov, A.V., Shmakov, A.I., Kuznetsov, A.A., Gureeva, I.I., 2010. Spore morphology of *Cryptogramma* R. Br. ex Richards species (Cryptogrammaceae). Turcz. 13, 50–58.

Wagner, W.H., 1963. A biosystematic study of United States ferns. A preliminary abstract. Amer. Fern J. 56, 1–16.

Weng, R.F., Qiu, S.P., 1988. Chromosome counts of some ferns from Zhejiang. Invest. Stud. Nat. 8, 43–52.

Winkworth, R.C., Bell, C.D., Donoghue, M.J., 2008. Mitochondrial sequence data and Dipsacales phylogeny: Mixed models, partitioned Bayesian analyses, and model selection. Mol. Phylogenet. Evol. 46, 830–843.

Yatabe, Y., Tsutsumi, C., Hirayama, Y., Mori, K., Murakami, N., Kato, M., 2009. Genetic population structure of *Osmunda japonica*, rheophilous *Osmunda lancea* and their hybrids. J. Plant Res. 122, 585–95.

Zhang, G.M., Alverson, E.R., Metzgar, J. S., 2013. *Cryptogramma* R. Brown, in: Wu, Z.Y., Raven, P.H., Hong, D.Y. (Eds.), Flora of China Volume 2-3 (Lycopodiaceae through Polypodiaceae). Science Press, Beijing, and Missouri Botanical Garden Press, St. Louis.

Zhang, G-M., Zhang, X-C., 2003. Taxonomic revision of the genus *Cryptogramma* R.Br. from China. Acta Phyto. Sin. 41, 475–482.

Zhang, G., Zhang, X., Chen, Z., 2005. Phylogeny of cryptogrammoid ferns and related taxa based on *rbcL* sequences. Nord. J. Bot. 23, 485–493.

Zwickl, D. J., 2006. Genetic algorithm approaches for the phylogenetic analysis of large biological sequence datasets under the maximum likelihood criterion. Ph.D. dissertation, University of Texas at Austin.

Chapter 3. Genetic differentiation and polyploid formation within the *Cryptogramma crispa* (Polypodiales: Pteridaceae) complex[1]

3.1 Abstract

The tetraploid fern *Cryptogramma crispa* (L.) R.Br. ex Hook. is distributed across alpine and high latitude regions of Europe and western Asia and is sympatric with the recently described octoploid *C. bithynica* S. Jess., L. Lehm. & Bujnoch in northcentral Turkey. Our analysis of a 6-region plastid DNA sequence dataset comprising 39 accessions of *Cryptogramma* R.Br., including 14 accessions of *C. crispa* and one accession of *C. bithynica*, revealed a deep genetic division between the accessions of *C. crispa* from western, northern and central Europe and the accessions of *C. crispa* and *C. bithynica* from Turkey and the Caucasus Mountains. This legacy likely results from Pleistocene climate fluctuations and appears to represent incipient speciation between the eastern and western clades. These plastid DNA sequence data also demonstrate that the western clade of *C. crispa*, specifically the western Asian clade, is the maternal progenitor of *C. bithynica*. Our analysis of DNA sequence data from the biparentally inherited nuclear locus *gapCp* supports an autopolyploid origin of *C. bithynica*, with *C. crispa* as the sole progenitor.

3.2 Introduction

The repeated range contractions and expansions caused by Pleistocene climate oscillations have long been recognized as an important driver of genetic diversity and differentiation in European biota (Hewitt, 2004). Several regions have been repeatedly identified as important refugia for taxa during glacial maxima, such as the Iberian Peninsula, the Italian Peninsula and the Balkans (Taberlet et al., 1998; Hewitt, 2004; Schmitt, 2007), and each region may comprise numerous additional small-scale refugia (see Médail and Diadema, 2009). Some organisms also show evidence of refugia in Turkey and/or the Caucasus Mountains (King and Ferris, 1998; Michaux et al., 2004; Gömöry et al., 2007; Grassi et al., 2008; Ansell et al., 2011). Glaciation and associated climate shifts also appear to increase the rate of polyploid formation in refugial areas and subsequent contact zones (Parisod et al., 2010). European fern taxa have also

[1] Metzgar, J.S., M. Stamey, and S.M. Ickert-Bond. In press. Genetic differentiation and polyploid formation within the *Cryptogramma crispa* (Polypodiales: Pteridaceae) complex. *Turkish Journal of Botany*.

been shown to use these same refugia and also show an increase in the formation of polyploid lineages in response to glacial climate cycles (Vogel et al., 1999; Trewick et al., 2002).

The fern genus *Cryptogramma* R. Br. (Pteridaceae) consists of ten mainly boreal species, of which three are known to be polyploid taxa (i.e, *C. bithynica*, *C. crispa* and *C. sitchensis*; (Figure 3.1; Metzgar et al., 2013). Previous research on the genus using a combined plastid and nuclear DNA dataset has shown diploid taxa to be genetically distinct, mostly allopatric lineages and revealed that the Beringian tetraploid *Cryptogramma sitchensis* is an allopolyploid (Metzgar et al., 2013). The European and southwest Asian tetraploid *C. crispa* was shown to be an autopolyploid based on all its nuclear alleles being recovered in a single clade with no other taxon's alleles present (Metzgar et al., 2013). The recently described southwest Asian octoploid *C. bithynica* S. Jess., L. Lehm. & Bujnoch (Jessen et al., 2012) is endemic to north-central Turkey and has never been included in a previous phylogenetic or molecular study including that of Metzgar et al. (2013). Therefore, it is unknown if *C. bithynica* is an auto- or allopolyploid lineage and which species were involved in its formation. Sympatry and some shared morphological characters (i.e., deciduous leaves) suggest that *C. crispa* may have been involved in the formation of *C. bithynica*, but several other morphological characters such as leaf thickness vary and are used to distinguish these two taxa (Jessen et al., 2012).

Cryptogramma has not been previously used to study phylogeographical patterns in Europe and southwest Asia, although its distribution patterns and the frequent occurrence of polyploidy make it well-suited to an examination of the role of Pleistocene refugia on genetic divergence, incipient speciation and polyploid formation in a free-sporing vascular plant lineage. Here we characterize genetic diversity across the range of *C. crispa*, identify possible Pleistocene refugia, and identify the progenitor species of *C. bithynica*. This study expands on the nuclear and plastid datasets previously used to study phylogenetic relationships within *Cryptogramma* (Metzgar et al., 2013).

3.3 Materials and Methods

3.3.1 Taxon sampling

The phylogenetic position of *Cryptogramma* within the Pteridaceae is well-established (Zhang et al., 2005; Prado et al., 2007; Schuettpelz et al., 2007; Metzgar et al., 2013) and the genus has two reciprocally monophyletic sections, *Homopteris* and *Cryptogramma*, with one and

nine species, respectively (Metzgar et al., 2013). Due to the well-established intergeneric relationships within the cryptogrammoid ferns (Zhang et al., 2005; Prado et al., 2007; Schuettpelz et al., 2007; Metzgar et al., 2013) and the strongly supported position of *Cryptogramma fumariifolia* (Phil.) Christ as the sister lineage to all remaining *Cryptogramma* sect. *Cryptogramma* taxa (Metzgar et al., 2013), we only included *Cryptogramma* sect. *Cryptogramma* accessions in the current study and used *C. fumariifolia* as the outgroup. *Cryptogramma stelleri*, the sole taxon in section *Homopteris*, was not included in this study as it is genetically isolated from all other *Cryptogramma* species and its exclusion greatly reduced the amount of excluded data in the sequence alignments. The current study included 39 accessions from nine species of *Cryptogramma*, including 14 accessions of *C. crispa* and one accession of *C. bithynica* (Table 3.1).

3.3.2 DNA amplification and sequencing

Six plastid DNA regions were used in this study (*rbcL*, *rbcL-accD*, *rbcL-atpB*, *rps4-trnS*, *trnG-trnR* and *trnP-petG*), and the *gapCp* "short" nuclear locus (henceforth *gapCp*) was sequenced for a subset of accessions (Table 3.1). The Invitrogen TOPO TA Cloning kit (Invitrogen, Carlsbad, California, USA) was used to clone nuclear PCR products, and clones were amplified using the Invitrogen M13 primer pair. *Cryptogramma crispa* accessions each had 25 clones and the *C. bithynica* accession was sequenced for 44 clones. Primers, PCR conditions, cloning, sequencing and matrix construction followed established protocols (Metzgar et al., 2013). For *gapCp* sequences, the sequence correction procedure first involved the examination of contigs formed by all sequences from a single accession in Sequencher version 4.10.1 (Gene Codes Corporation, Ann Arbor, Michigan, USA). All mutations and indels were mapped across the length of the putative allele and compared to identify and remove chimeric sequences and Taq error, with the resulting consensus sequence(s) exported as separate alleles (Grusz et al., 2009; Metzgar et al., 2013). Of the 254 sequences used here, 63 were generated expressly for this study and were deposited in GenBank (Table 3.1).

3.3.3 Phylogenetic analyses

Sequences were added to existing datasets (Metzgar et al., 2013) and aligned by eye using MacClade 4.08 (Maddison and Maddison, 2005). We excluded a total of 331 basepairs

due to ambiguously aligned portions of the 6827 bp plastid alignment (66 bp in *rbcL-accD*, 15 bp in *rbcL-atpB*, 67 bp in *rps4-trnS*, 84 bp in *trnG-trnR* and 88 bp in *trnP-petG*). The resulting gapCp alignment was 599 bp long with no excluded characters. Alignments are available in TreeBASE (study ID 17439; http://treebase.org).

For model-based phylogenetic analyses, the appropriate model of sequence evolution was selected using Akaike Information Criterion scores calculated in MrModeltest 2.3 (Nylander et al., 2004). Prior to combining the six plastid region datasets, each region was analyzed separately using Bayesian Markov chain Monte Carlo (B/MCMC) and maximum parsimony bootstrap (MPBS) methods. The B/MCMC analyses were conducted in MrBayes version 3.2 (Huelsenbeck and Ronquist, 2001; Ronquist and Huelsenbeck, 2003; Ronquist et al., 2012). Each of these analyses was run for 10 million generations and implemented using default priors on four runs with four chains a piece. Tracer v1.5 (Rambaut and Drummond, 2009) was used to inspect parameter convergence with the first 2 million generations discarded as the burn-in. The majority-rule consensus tree, posterior probabilities and average branch lengths were calculated from the resulting 32,000 trees. The MPBS analyses consisted of 500 bootstrap replicated with 10 random addition sequence replicates implemented in PAUP* 4.0b10 (Swofford, 2002). The majority-rule consensus trees for the six plastid datasets were then inspected for supported (PP $\geq$ 0.95; MPBS $\geq$ 70) topological conflicts (Mason-Gamer and Kellogg, 1996). One conflict was detected with the *rbcL-atpB* B/MCMC topology supporting the inclusion of *C. crispa* + *C. bithynica* in a clade with *Cryptogramma brunoniana* Wall. ex Hook. & Grev. + *Cryptogramma raddeana* Fomin (PP = 0.98) rather than as the sister lineage to *Cryptogramma cascadensis* E.R. Alverson. This relationship was not significantly supported in the *rbcL-atpB* MPBS analysis, so all six plastid data sets were combined into a single 6827 base pair alignment.

Phylogenetic analyses of both the *gapCp* alignment and the combined plastid alignment were conducted using maximum parsimony (MP), maximum likelihood (ML) and B/MCMC. MP tree searches were run for 1000 heuristic replicates, using the random addition sequence (RAS) starting tree and tree-bisection-reconnection (TBR) branch swapping options in PAUP* 4.0b10 (Swofford, 2002). MP support values were calculated using 500 bootstrap replicates, each with 10 random addition sequence replicates.

ML analyses used region-specific models of sequence evolution implemented in Garli 2.0 (Zwickl, 2006) on the CIPRES Science Gateway computational portal (Miller et al., 2010). ML

analyses were ran twice for eight replicates, using random starting trees and using stepwise addition starting trees. All ML bootstrap (MLBS) analyses were run for 100 replicates. B/MCMC analyses were as previously described.

3.3.4 Spore measurements

Spores were removed from five herbarium specimens and mounted in glycerol on slides and examined using a Nikon Eclipse 80i compound microscope. 18-46 spores from each specimen were measured at 400X magnification. Each spore was measured along its longest axis (Alverson, 1989) and both standard deviation and mean spore size were calculated for each specimen. Additional spore measurements values were culled from the primary literature (Table 3.2).

3.4 Results

3.4.1 Plastid DNA analyses

The combined six-region plastid dataset contained 185 variable sites and 172 parsimony informative characters. Maximum parsimony (MP), ML and B/MCMC analyses recovered congruent, well-supported (PP $\geq$ 0.95; MLBS $\geq$ 90%; MPBS $\geq$ 90%) phylogenies for the combined six-region plastid dataset (Figure 3.2). The MP analysis identified two equally most parsimonious trees with a length of 205. The ML analysis identified a most-likely topology with a likelihood of -10406.891151, with no topological differences between searches using random or stepwise starting trees. The B/MCMC topology was calculated from 32,000 post-burnin trees and was well resolved with strong support for most relationships (Figure 3.2). All three methods recovered all diploid species as monophyletic (including polyploid progeny where relevant) with strong support. The *C. bithynica* accession was consistently recovered in a clade of *C. crispa* haplotypes from eastern Europe and western Asia. These inferred relationships are all congruent with previous phylogenetic assessments of *Cryptogramma* (Metzgar et al., 2013).

3.4.2 Nuclear DNA analyses

Tree topologies recovered from our MP, ML and B/MCMC analyses of the *gapCp* dataset were congruent with one another and with previous research (Metzgar et al., 2013). We found eight most parsimonious trees in the MP search with a length of 60. The optimal ML

topology had a likelihood of -1233.560927, with identical topologies recovered using random or stepwise starting trees. The B/MCMC analysis generated a strongly supported topology that was congruent with the MP and ML analyses (Figure 3.3). Alleles of *C. bithynica* were recovered in a clade containing alleles of European and Caucasian *C. crispa* specimens with strong support (Figure 3.3).

3.4.3 Spore measurements

The mean spore lengths in *C. crispa* from the Caucasus Mountains (48-57 μm) fell within the observed range of variation for other *C. crispa* samples from across Europe (47.1-58.6 μm) from the current and previous studies and were considerably smaller than in *C. bithynica* (70.87 μm) (Jessen et al., 2012; Table 3.2).

3.5 Discussion

3.5.1 Formation of C. bithynica

Our results suggest that the Turkish octoploid *C. bithynica* originated as an autopolyploid within the Caucasian clade of *C. crispa* (Figure 3.2; Figure 3.3; Figure 3.4). In the phylogeny derived from our plastid DNA data (Figure 3.2), *C. bithynica* was nested within a well-supported clade of *C. crispa* accessions from the Caucasian Mountains (Figure 3.4). Since plastids in ferns are typically inherited maternally (Gastony and Yatskievych, 1992), western Asian *C. crispa* probably acted as the maternal parent of *C. bithynica*. In our phylogeny based on the biparentally inherited nuclear locus *gapCp*, *C. bithynica* was nested within *C. crispa* (Figure 3.3), indicating an autopolyploid origin of *C. bithynica*. An autopolyploid origin of *C. bithynica* is also concordant with current distributional patterns, as *C. crispa* is its only sympatric congener (Figure 3.1; Metzgar et al., 2013). Shared morphological characters such as deciduous leaves, ovate leaf segments and sterile leaf shape also support this hypothesis, although *C. crispa* and *C. bithynica* can be distinguished based on leaf size, spore length (Table 3.2) and some subtle leaf characteristics such as leaf thickness and size (Jessen et al., 2012). The spore measurements and chromosome counts of *C. crispa* accessions across Europe and western Asia suggest that it is consistently tetraploid, 2n = 4x = 120, with spore measurements (47.1-58.6 μm) easily distinguished from the isolated ocotoploid *C. bithynica* lineage (70.87 μm; Manton, 1950; Löve, 1970; Pajarón et al., 1999; Jessen et al., 2012; Alverson, unpub. data; Table 3.2). Spore

measurement data, when assessed in a phylogenetic context, have been used previously as a proxy for ploidy in Pteridaceae (Barrington et al. 1986; Grusz et al. 2009; Beck et al., 2011), although it is not reliable in at least one fern lineage (*Asplenium* L.; Dyer et al., 2013).

3.5.2 Genetic partitioning within Cryptogramma crispa

A sharp plastid DNA division is apparent within *C. crispa* (Figure 3.2), with the accessions from Turkey and the Caucasus Mountains clearly distinct from those of western and central Europe (Figure 3.1). The considerable sequence divergence observed between these clades is nearly equivalent to that separating sister species in *Cryptogramma*, although there appears to be no morphological distinction (including spore size; Table 3.2) between them (Figure 3.2; Metzgar et al., 2013). This genetic division could be indicative of incipient speciation occurring within *C. crispa*. Diversification following climate-induced range shifts have been commonly documented in temperate plants in general (e.g., Qiu et al., 2009) and in temperate ferns specifically (Haufler et al., 2008). Sequencing of additional loci would quantify gene flow between the two clades. Analysis of the nuclear locus *gapCp* revealed no division into eastern and western clades among *C. crispa* and *C. bithynica* alleles (Figure 3.3). The reason for this discrepancy between plastid and nuclear sequence data is unclear, but additional nrDNA sequencing of additional accessions of *C. bithynica* and *C. crispa* could be beneficial in resolving it.

The genetic distinctness of the Turkey + Caucasus Mountains clade (Figure 3.2) suggests a second Pleistocene refugium. Numerous plant and animal lineages show evidence of surviving climatic fluctuations in Turkish and/or Caucasian refugia (King and Ferris, 1998; Petit et al., 2002; Seddon et al., 2002; Rokas et al., 2003; Dubey et al., 2005; Kučera et al., 2006; Challis et al., 2007; Gömöry et al., 2007; Naydenov et al., 2007; Grassi et al., 2008; Ansell et al., 2011). The recent history of *C. crispa* appears to be most similar to that of *Vitis vinifera* L. ssp. *silvestris* (C.C. Gmel.) Hegi (Grassi et al., 2008) and *Arabis alpina* L. (Ansell et al., 2011). All three taxa display shared Turkish and Caucasian haplotypes that have not recolonized any additional regions.

The restricted range of eastern *C. crispa* haplotypes suggests that the Caucasus Mountains could have served as a barrier to recolonization, similar to other lineages (Figure 3.4; Seddon et al., 2002; Dubey et al., 2005), but future research efforts sampling accessions north

and northwest of the Caucasus Mountains would be needed to better evaluate this possibility. Phylogeographic patterns involving Turkey have been previously characterized into several broad categories (Bilgin, 2011) based on the geographic boundaries of genetic diversity. *Cryptogramma crispa* is an example of Bilgin's (2011) "Pattern I" with western and eastern clades that are divided between the Balkans and Anatolia. This divide between Anatolian and Balkan accessions was likely caused by the Sea of Marmara (Ansell et al., 2011) or western Anatolia (Bilgin, 2011).

This clear geographic separation of plastid genetic diversity within *C. crispa* probably reflects use of at least two different refugia during the Pleistocene glaciations. There is little differentiation between accessions across western, northern and central Europe in the plastid phylogeny (Figure 3.2) with the exception of one moderately supported early divergence in Spain. Iberia has commonly been inferred as a refugium for other vascular plant lineages (Taberlet et al., 1998; Hewitt, 2004; Schmitt, 2007) including ferns (Trewick et al., 2002; Jiménez et al., 2009). Our results could be suggestive that Iberia was a source for recolonization of deglaciated regions, but other potential sources cannot be eliminated. Unlike the pattern previously shown for some European ferns (Vogel et al., 1999; Trewick et al., 2002), the higher ploidy lineage (*C. bithynica*) is geographically restricted to a glacial refugium rather than having recolonized deglaciated regions. The small geographic range of *C. bithynica* suggests that it has formed recently, although future research could assess this hypothesis using divergence time estimation. The divergence between *C. crispa* clades is similar to that separating other species within *Cryptogramma*, although there is no apparent morphological differentiation. This taxon could be undergoing incipient speciation.

This study illustrates the genetic isolation and incipient speciation that can result from climate change cycles. The use of the Caucasus Mountains as a refugium is a novel finding for a free-sporing fern lineage. The octoploid *C. bithynica* will benefit from additional research, especially to determine if it has arisen multiple times.

3.6 Acknowledgments

We thank Stefan Jessen, Anders Larsson, Yulia Mikhaylova, Santiago Pajarón, Emilia Pangua and Walter Bujnoch for providing voucher specimens and silica-dried leaf tissue. We thank ALA and LE for allowing us to sample herbarium specimens. We thank Tzu-Tong Kao,

Margaret Oliver, Kathleen Pryer and Carl Rothfels for assistance with laboratory and morphological procedures. We thank Stina Weststrand for providing photographs and habitat information, Lisa Strecker for translation of Russian labels and Ed Alverson for sharing unpublished spore measurement data. We thank two anonymous reviewers for many helpful comments on the manuscript. Funding was provided in part by a University of Alaska Fairbanks Undergraduate Research and Scholarly Activity award to MRS and National Science Foundation Division of Environmental Biology Doctoral Dissertation Improvement Grant award 1311685 to SMI-B and JSM.

3.7 Figures

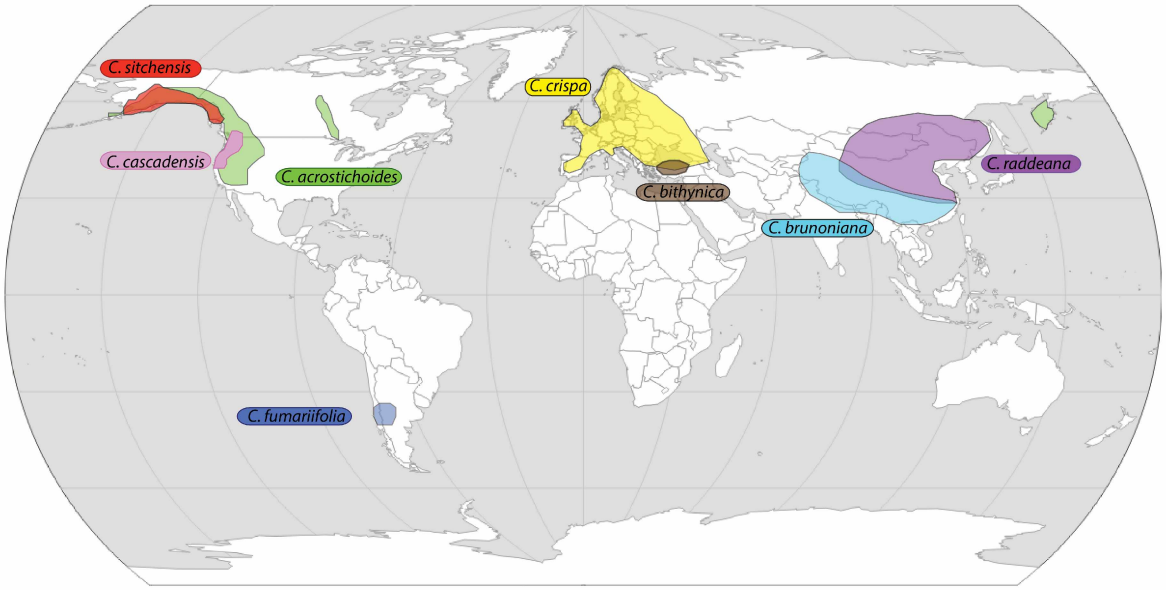

Fig. 3.1. Approximate distributions of species of *Cryptogramma* sect. *Cryptogramma*. Colors reflect those used in plastid and nuclear phylogenies for each of the taxa (Figures 3.2, 3.3).

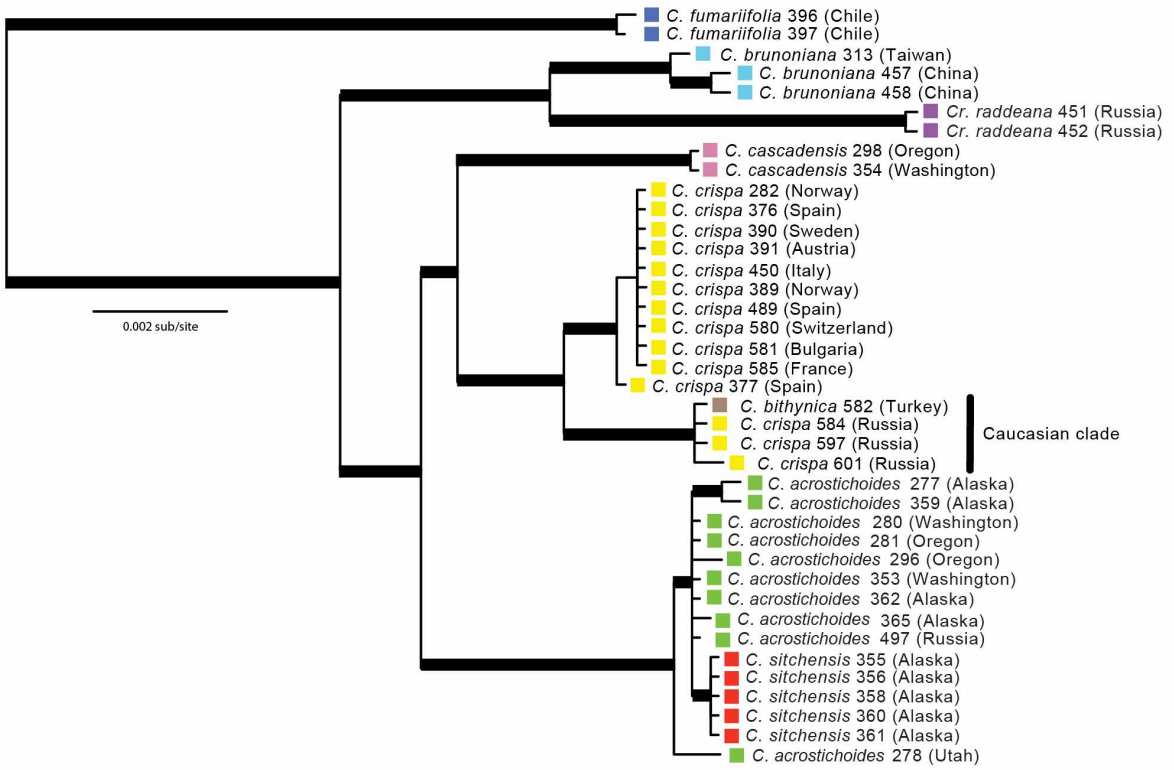

Fig. 3.2. Plastid phylogeny of *Cryptogramma* sect. *Cryptogramma.* Phylogeny generated using a Bayesian Markov chain Monte Carlo (B/MCMC) analysis of a combined 6-region plastid data set. 63 of the 254 sequences used here were generated expressly for this study and were deposited in GenBank (Table 3.1). Interspecific relationships are congruent with previous research (Metzgar et al., 2013) but new sequence data has expanded sampling within the C. *crispa* clade. Strongly supported relationships (B/MCMC PP = 1.00; MLBS ≥ 95 %; MPBS ≥ 91 %) are depicted with thickened branches. Numbers following taxon names refer to extraction numbers (Table 3.1). The Caucasian clade of *C. crispa* and *C. bithynica* is marked by a vertical black bar. Colors as in Figure 3.1.

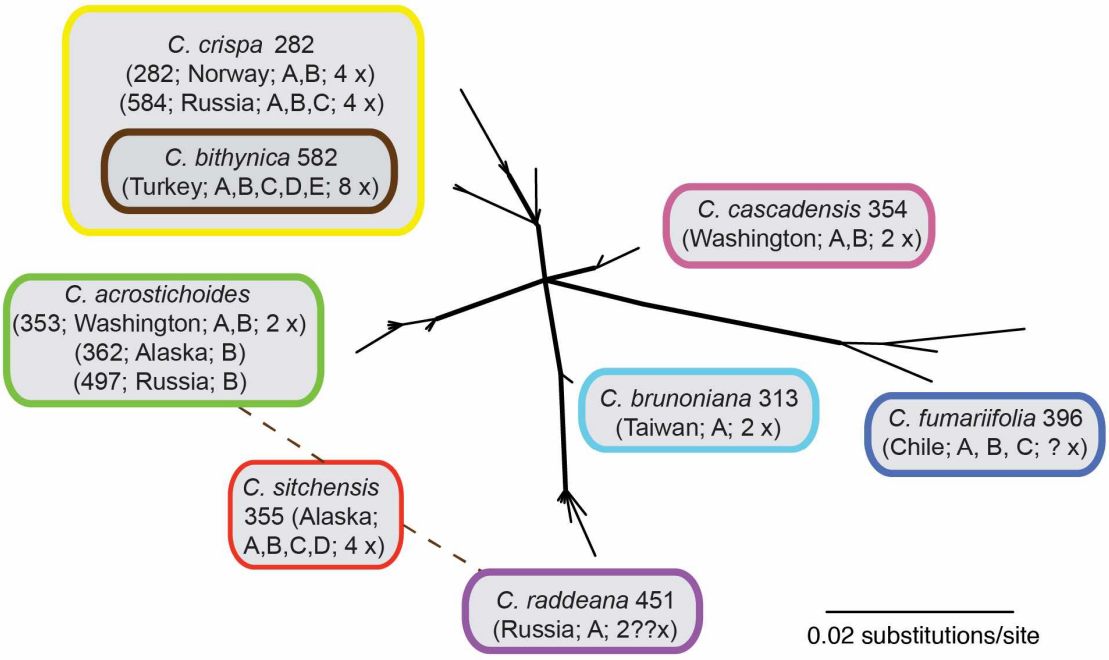

Fig. 3.3. Unrooted nuclear *gapCp* phylogeny. Phylogeny of nuclear *gapCp* "short" alleles of species of *Cryptogramma* sect. *Cryptogramma* analyzed by Bayesian Markov chain Monte Carlo (B/MCMC). Branches that represent strongly supported relationships (B/MCMC PP = 0.99; MLBS ≥ 100 %; MPBS ≥ 70 %) are thickened. Taxa present in clades are noted in color-coded bubbles along with taxon name, DNA extraction number, allele identifier and estimated ploidy level. Colors as in Figure 3.1.

Fig. 3.4. Distribution and sampling localities for *C. crispa* and *C. bithynica.* Plastid clades (Figure 3.2) indicated by red dotted lines. Accessions sampled for DNA analysis are shown as colored circles with solid borders. Accessions included in spore size analysis (Table 3.2) are shown as colored circles with dashed borders. The Caucasus Mountains are depicted by inverted triangles.

3.8 Tables

Table 3.1. Sampling data for specimen vouchers, including locality, herbarium (*sensu* Thiers, 2014), and GenBank accession numbers.

DNA Ext. No.	Taxon	Locality	Collector/No. (herbarium acronym)	GenBank accession no.						
				rbcL	*rbcL-accD*	*rbcL-atpB*	*rps4-trnS*	*trnG-trnR*	*trnP-petG*	*gapCp* "short"
277	*Cryptogramma acrostichoides* R.Br.	USA, Alaska, Kodiak, near the transient boat harbor	*Studebaker 09-473* (ALA)	KC700093	KC700133	KC700171	KC700210	KC700248	KC700284	-
278	*Cryptogramma acrostichoides*	USA, Utah, Salt Lake County, Little Cottonwood Canyon, near Snowbird	*Rothfels 2979* (ALA, DUKE, NHIC)	KC700094	KC700134	KC700172	KC700211	KC700249	KC700285	-
280	*Cryptogramma acrostichoides*	USA, Washington, Mason County, N of Lake Cushman	*Windham 3624* (DUKE, UT)	KC700095	KC700135	KC700173	KC700212	KC700250	KC700286	-

Table 3.1 continued

		along the Mt. Ellinor trail in the Olympic Mtns.								
281	*Cryptogramma acrostichoides*	USA, Oregon, Linn Co., Horse Rock Ridge, SW of Crawfordsville .	*Pryer 06-04* (DUKE)	KC700096	KC700136	KC700174	KC700213	KC700251	KC700287	-
296	*Cryptogramma acrostichoides*	USA, Oregon, Lane County, Trail to Proxy Falls	*Alverson s.n.* (ALA)	KC700097	KC700137	KC700175	KC700214	KC700252	KC700288	-
353	*Cryptogramma acrostichoides*	USA, Washington, King County, Source Lake Lookout Trail, above Source Lake, Cascade Range	*Zika 25403* (ALA)	KC700098	KC700138	KC700176	KC700215	KC700253	KC700289	KC700066,KC700071

Table 3.1 continued

359	*Cryptogramma acrostichoides*	USA, Alaska, Seward, Kenai Fjords National Park, Harding Icefield Trail	*Metzgar 247* (ALA)	KC70009	KC700139	KC700177	KC70021	KC700254	KC700290	-
362	*Cryptogramma acrostichoides*	USA, Alaska, Southeast Alaska, 10 miles northwest of Juneau, Mendenhall Lake, behind Mendenhall Glacier Visitor Center	*Anderson 745* (ALA)	KC70010	KC700140	KC700178	KC70021	KC700255	KC700291	KC700070,KC700058

Table 3.1 continued

365	*Cryptogramma acrostichoides*	USA, Alaska, Sitkalidak Island, Sitkalida Lagoon, cliffs along east side of lagoon	*Studebaker 10-61* (ALA)	KC700101	KC700141	KC700179	KC700218	KC700256	KC700292	-
582	*Cryptogramma bithynica* S.	Turkey, Uludag, silicate scree slope on NNE side of mountain	*Jessen SJ-3820* (ALA)	KT000629[a]	KT000649[a]	KT000639[a]	KT221146[a]	KT221156[a]	KT221165[a]	KT000619[a] ,KT000620[a]
313	*Cryptogramma brunoniana*	Taiwan, NanTou County, Mt. ShihMen.	*Kuo 455* (TAIF)	KC700081	KC700121	KC700159	KC700198	KC700238	KC700273	KC700061
457	*Cryptogramma brunoniana*	China, Xizang (Tibet) Province,	*Boufford 29733* (GH)	KC700082	KC700122	KC700160	KC700199	KC700239	KC700274	-

Table 3.1 continued

		Baxoi Xian, Anjiu La (pass), N of Rawu (Raog)								
458	*Cryptogramma brunoniana*	China, Gansu Province, Wen Xian, Motianling Shan, Baishui Jiang Nature Reserve	*Boufford 37747* (GH)	KC700083	KC700123	KC700161	KC700200	KC700240	KC700275	-
298	*Cryptogramma cascadensis*	USA, Oregon, Deschutes/Linn County boundary, McKenzie Pass	*Alverson s.n.* (ALA)	KC700086	KC700126	KC700164	KC700203	KC700241	KC700277	-
354	*Cryptogramma cascadensis*	USA, Washington, King County, Source Lake Lookout Trail,	*Zika 25404* (ALA)	KC700087	KC700127	KC700165	KC700204	KC700242	KC700278	KC700064,KC700065

Table 3.1 continued

		above Source Lake,								
282	*Cryptogramma crispa* (L.) R.Br. ex Hook	Norway, Hordaland, Bergen	*Reeb VR4-VIII-02/11* (DUKE)	KC700088	KC700128	KC700166	KC700205	KC700243	KC700279	KC700062,KC700063
376	*Cryptogramma crispa*	Spain, Madrid Province, Sierra de Guadarrama, Siete Picos	*Pajarón s.n.* (ALA)	KC700089	KC700129	KC700167	KC700206	KC700244	KC700280	-
377	*Cryptogramma crispa*	Spain, Soria Province, Sierra de Urbión, Laguna Negra, cracks and between blocks of sandstone	*Pajarón s.n.* (ALA)	KT000624[a]	KT000644[a]	KT000634[a]	KT221141[a]	KT221151[a]	KT221160[a]	-
389	*Cryptogramma crispa*	Norway, Troms	*Larsson 307* (DUKE,	KT000625[a]	KT000645[a]	KT000635[a]	KT221142[a]	KT221152[a]	KT221161[a]	-

Table 3.1 continued

		Skjervøy County. Storfjellet, Aarviksand. In rocky depression on northern part of bare mountain region	UPS)							
390	*Cryptogramma crispa*	Sweden, Norrbotten Gällivare County. Dundret, Gällivare	*Larsson 333* (DUKE, UPS)	KC70 0090	KC70 0130	KC70 0168	KC70 0207	KC70 0245	KC70 0281	-
391	*Cryptogramma crispa*	Austria, Steiermark, Niedere Tauern/Secka uer Alpen,	*Pflugbeil 111847* (ALA)	KC70 0091	KC70 0131	KC70 0169	KC70 0208	KC70 0246	KC70 0282	-

Table 3.1 continued

		Maierangerko gel – Vorwitzsattel								
450	*Cryptogramma crispa*	Italy, northwest of Brunico, Astnerberg	*Shmakov s.n.* (ALTB)	KC700092	KC700132	KC700170	KC700209	KC700247	KC700283	-
489	*Cryptogramma crispa*	Spain, Ávila Province, Sierra de Gredos, Arroyo y Circo de los Pozas	*Pajarón s.n.* (ALA)	KT000626[a]	KT000646[a]	KT000636[a]	KT221143[a]	KT221153[a]	KT221162[a]	-
580	*Cryptogramma crispa*	Switzerland, Tessin, Val Serdena bei Isone, S-Abhang der Cima Calesco	*Jessen SJ-3892* (ALA)	KT000627[a]	KT000647[a]	KT000637[a]	KT221144[a]	KT221154[a]	KT221163[a]	-
581	*Cryptogramma*	Bulgaria,	*Jessen SJ-*	KT000	KT00	KT00	KT22	KT22	KT22	-

Table 3.1 continued

	crispa	Pirin Mountains, south of Dautovo Lake	*3891* (ALA)	628[a]	0648[a]	0638[a]	1145[a]	1155[a]	1164[a]	
584	*Cryptogramma crispa*	Russia, Dombai, North Caucasus	*Jessen SJ-3099* (ALA)	KT000630[a]	KT000650[a]	KT000640[a]	KT221147[a]	KT221157[a]	KT221166[a]	KT000621[a] ,KT000622[a] ,KT000623[a]
585	*Cryptogramma crispa*	France, Pyrenees Mountains, Cirque de Troumouse	*Jessen SJ-2920* (ALA)	KT000631[a]	KT000651[a]	KT000641[a]	KT221148[a]	KT221158[a]	KT221167[a]	-
597	*Cryptogramma crispa*	Russia, North Ossetia, Iravskii region	*Shilnikov s.n.* (LE)	KT000632[a]	KT000652[a]	KT000642[a]	KT221149[a]	KT221159[a]	KT221168[a]	-
601	*Cryptogramma crispa*	Russia, Dagestan,	*Popova 695* (LE)	KT000633[a]	-	KT000643[a]	KT221150[a]	-	KT221169[a]	-

Table 3.1 continued

		Samur River								
396	*Cryptogramma fumariifolia*	Chile, Provincia de Ñuble, Comuna de Pinto, Shangri-La	*Larraín 34009* (ALA, CONC)	KC700079	KC700119	KC700157	KC700196	KC700236	KC700271	KC700073,KC700074,KC700075
397	*Cryptogramma fumariifolia*	Chile, Provincia de Ñuble, Comuna de Pinto, Shangri-La	*Larraín 34010* (ALA, CONC)	KC700080	KC700120	KC700158	KC700197	KC700237	KC700272	-
451	*Cryptogramma raddeana*	Russia, Republic of Buryatia, Severo-Muisky range, Samokuya	*Naumov 1989* (NS)	KC700084	KC700124	KC700162	KC700201	-	-	KC70005
452	*Cryptogramma*	Russia,	*Netchaev*	KC70	KC70	KC70	KC70	-	KC70	-

Table 3.1 continued

	raddeana	Khabarovsky krai, 30km north of Sofiysk	*s.n.* (NS)	0085	0125	0163	0202		0276	
355	*Cryptogramma sitchensis* (Rupr.) T. Moore	USA, Alaska, between Portage and Whittier, Bering Glacier	*Metzgar 248* (ALA)	KC700103	KC700143	KC700181	KC700220	KC700258	KC700294	KC700057,KC700056,KC700060,KC700068
356	*Cryptogramma sitchensis*	USA, Alaska, Taku Glacier	*Bass s.n.* (ALA)	KC700104	KC700144	KC700182	KC700221	KC700259	KC700295	-
358	*Cryptogramma sitchensis*	USA, Alaska, Seward, Kenai Fjords National Park	*Metzgar 246* (ALA)	KC700105	KC700145	KC700183	KC700222	KC700260	KC700296	-
360	*Cryptogramma sitchensis*	USA, Alaska, Palmer, Hatcher Pass	*Metzgar 249* (ALA)	KC700106	KC700146	KC700184	KC700223	KC700261	KC700297	-

Table 3.1 continued

361	*Cryptogramma sitchensis*	USA, Alaska, Valdez, Thompson Lake	*Metzgar 257* (ALA)	KC70 0107

[a]Indicates sequences generated for this study.

KC70 0147	KC70 0185	KC70 0224	KC70 0262	KC70 0298	-

Table 3.2. Mean spore size and chromosome numbers in the *Cryptogramma crispa* complex. Sample size for species measured by the present study range from 18-46 spores/specimen. Missing data indicated by dashes.

Sample No.	**Species**	**Locality**	**Mean spore size (µm)**	**Standard Deviation (µm)**	**Chromosome count**	**Number of spores measured**	**Reference**
1	*Cryptogramma crispa*	Great Britain, Wales	-	-	$n = 60$	-	Manton, 1950
2	*C. crispa*	Iceland	-	-	$2n = 120$	-	Löve, 1970
3	*C. crispa*	England	54.8	2.23	-	26	Alverson, unpub.
4	*C. crispa*	England	57.5	1.56	-	25	Alverson, unpub.
5	*C. crispa*	England	53.7	1.60	-	25	Alverson, unpub.
6	*C. crispa*	Finland	58.6	2.20	-	25	Alverson, unpub.
7	*C. crispa*	France	49.8	1.30	-	25	Alverson, unpub.
8	*C. crispa*	France	54.1	1.79	-	25	Alverson, unpub.

Table 3.2 continued

9	*C. crispa*	Germany	50.9	1.72
10	*C. crispa*	Switzerland	49.8	1.30
11	*C. crispa*	Switzerland	55.3	1.75
12	*C. crispa*	Spain, Huesca Province; Scotland, Central Region	49.3-54.8	-
13	*C. crispa*	Switzerland, Tocino; Turkey, Artvin Province	48-57	-
582	*C. bithynica*	Turkey, Uludag	70.87	-
376	*C. crispa*	Spain, Madrid Province	47.1	3.98

-	25	Alverson, unpub.
-	25	Alverson, unpub.
-	25	Alverson, unpub.
$2n = 120$	10	Pajarón et al., 1999
$2n = 120$	-	Jessen et al., 2012
$2n = 240$	-	Jessen et al., 2012
-	37	Present study

Table 3.2 continued

377	*C. crispa*	Spain, Soria Province	49.4	5.39
489	*C. crispa*	Spain, Ávila Province	53.3	4.94

-	18	Present study
-	46	Present study

3.9 References

Alverson ER (1989). Biosystematics of Parsley-ferns, *Cryptogramma* R. Br., in Western North America. Master's thesis, Oregon State University.

Ansell SW, Stenøien HK, Grundmann M, Russell SJ, Koch M, Schneider H, Vogel JC (2011). The importance of Anatolian mountains as the cradle of global diversity in *Arabis alpina*, a key arctic-alpine species. Ann Bot-London 108: 241–252.

Barrington DS, Paris CA, Ranker TA (1986). Systematic inferences from spore and stomate size in the ferns. Am Fern J 76: 149-159.

Beck JB, Windham MD, Pryer KM (2011). Do asexual lineages lead short evolutionary lives? A case-study from the fern genus *Astrolepis*. *Evolution* 65: 3217–3229.

Bilgin R (2011). Back to the suture: the distribution of intraspecific genetic diversity in and around Anatolia. Int J Mol Sci 12: 4080–4103.

Challis RJ, Mutun S, Nieves-Aldrey J-L, Preuss S, Rokas A, Aebi A, Sadeghi E, Tavakoli M, Stone GN (2007). Longitudinal range expansion and cryptic eastern species in the western Palaearctic oak gallwasp, *Andricus coriarius*. Mol Ecol 16: 2103–2114.

Dubey S, Zaitsev M, Cosson J-F, Abdukadier A, Vogel P (2005). Pliocene and Pleistocene diversification and multiple refugia in a Eurasian shrew (*Crocidura suaveolens* group). Mol Phylogenet Evol 38: 635–647.

Dyer RJ, Pellicer J, Savolainen V, Leitch IJ, Schneider H (2013). Genome size expansion and the relationship between nuclear DNA content and spore size in the *Asplenium monanthes* fern complex (Aspleniaceae). BMC Plant Biol 13: 219.

Gastony GJ, Yatskievych G (1992). Maternal inheritance of the chloroplast and mitochondrial genomes in cheilanthoid ferns. Am J Bot 79: 716–722.

Gömöry D, Paule L, Vyšný J (2007). Patterns of allozyme variation in western Eurasian *Fagus*. Bot J Linn Soc 154: 165–174.

Grassi F, de Mattia F, Zecca G, Sala F, Labra, M (2008). Historical isolation and Quaternary range expansion of divergent lineages in wild grapevine. Biol J Linn Soc 95: 611–619.

Grusz AL, Windham MD, Pryer KM (2009). Deciphering the origins of apomictic polyploids in the *Cheilanthes yavapensis* complex (Pteridaceae). Am J Bot 96:1636–1645.

Haufler CH, Hooper EA, Thierren JA (2008). Modes and mechanisms of speciation in pteridophytes: Implications of contrasting patterns in ferns representing temperate and tropical habitats. Plant Spec Biol 15:223-236.

Hewitt GM (2004). Genetic consequences of climatic oscillations in the Quaternary. Philos T Roy Soc B 359: 183–195.

Huelsenbeck JP, Ronquist F (2001). MRBAYES: Bayesian inference of phylogeny. Bioinformatics 17: 754–755.

Jessen S, Lehmann L, Bujnoch W (2012). *Cryptogramma bithynica* sp. nov. (Pteridaceae, Pteridophyta)a new fern species from northwestern Anatolia/Turkey. Fern Gazette 19: 47–54.

Jiménez A, Quintanilla A, Pajarón S, Pangua E (2009). Genetic variation in the allotetraploid *Dryopteris corleyi* (Dryopteridaceae) and its diploid parental species in the Iberian Peninsula. Am J Bot 96: 1880–1886.

King RA, Ferris C (1998). Chloroplast DNA phylogeography of *Alnus glutinosa* (L.) Gaertn. Mol Ecol 7: 1151–1161.

Kučera J, Lihová J, Marhold K (2006). Taxonomy and phylogeography of *Cardamine impatiens* and *C. pectinata* (Brassicaceae). Bot J Linn Soc 152: 169–195.

Löve A (1970). Islenzk ferdaflora. Almenna Bokfelagid, Reykjavik.

Maddison DR, Maddison WP (2005). MacClade 4: Analysis of phylogeny and character evolution. Version 4.08a. http://macclade.org.

Manton I (1950). Problems of Cytology and Evolution in the Pteridophyta. Cambridge University Press, London.

Mason-Gamer RJ, Kellogg EA (1996). Testing for phylogenetic conflict among molecular data sets in the tribe Triticeae (Gramineae). Syst Biol 45: 524–545.

Médail F, Diadema K (2009). Glacial refugia influence plant diversity patterns in the Mediterranean Basin. J Biogeogr 36: 1333–1345.

Metzgar JS, Alverson ER, Chen S, Vaganov AV, Ickert-Bond SM (2013). Diversification and reticulation in the circumboreal fern genus *Cryptogramma*. Mol Phylogenet Evol 67: 589–599.

Michaux JR, Libois R, Paradis E, Filippucci M-G (2004). Phylogeographic history of the yellow-necked fieldmouse (*Apodemus flavicollis*) in Europe and in the Near and Middle East. Mol Phylogenet Evol 32: 788–798.

Miller MA, Pfeiffer W, Schwartz T (2010). Creating the CIPRES Science Gateway for inference of large phylogenetic trees. In: *Proceedings of the Gateway Computing Environments Workshop (GCE)*, 14 November 2010, New Orleans, LA, pp. 1–8.

Naydenov K, Senneville S, Beaulieu J, Tremblay F, Bousquet J (2007). Glacial vicariance in Eurasia: mitochondrial DNA evidence from Scots pine for a complex heritage involving genetically distinct refugia at mid-northern latitudes and in Asia Minor. BMC Evol Biol doi:10.1186/1471-2148-7-233.

Nylander JAA, Ronquist F, Huelsenbeck JP, Nieves Aldrey JL (2004). Bayesian phylogenetic analysis of combined data. Syst Biol 53: 47–67.

Pajarón S, Pangua E, García-Álvarez L (1999). Sexual expression and genetic diversity in populations of *Cryptogramma crispa* (Pteridaceae). Am J Bot 86: 964–973.

Parisod C, Holderegger R, Brochmann C (2010). Evolutionary consequences of autopolyploidy. New Phytol 186: 5–17.

Petit RJ, Brewer S, Bordács S, Burg K, Cheddadi R, Coart E, Cottrell J, Csaikl UM, van Dam B, Deans JD, Espinel S, Fineschi S, Finkeldey R, Glaz I, Goicoechea PG, Jensen JS, Konig AO, Lowe AJ, Madsen SF, Matyas G, Munro RC, Popescu F, Slade D, Tabbener H, de Vries SGM, Ziegenhagen B, de Beaulieu J-L (2002). Identification of refugia and post-glacial colonization routes of European white oaks based on chloroplast DNA and fossil pollen evidence. Forest Ecol Manag 156: 49–74.

Prado J, Rodrigues CDN, Salatino A, Salatino MLF (2007). Phylogenetic relationships among Pteridaceae, including Brazilian species, inferred from *rbcL* sequences. Taxon 56: 355–368.

Qiu, Y.-X., Guan B.-C., Fu C.-X., Comes, HP (2009). Did glacials and/or interglacials promote allopatric incipient speciation in East Asian temperate plants? Phylogeographic and coalescent analyses on refugial isolation and divergence in *Dysosmaversipellis*. Mol Phylogenet Evol 51 281-293.

Rambaut A, Drummond AJ (2009). Tracer v1.5. Available from http://beast.bio.ed.ac.uk/Tracer.

Ronquist F, Huelsenbeck JP (2003). MrBayes3: Bayesian phylogenetic inference under mixed models. Bioinformatics 19: 1572–1574.

Ronquist F, Teslenko M, van der Mark P, Ayres DL, Darling A, Höhna S, Larget B, Liu L, Suchard MA, Huelsenbeck JP (2012). MrBayes 3.2: efficient Bayesian phylogenetic inference and model choice across a large model space. Syst Biol 61: 539–542.

Rokas A, Atkinson RJ, Webster LMI, Csókas G, Stone GN (2003). Out of Anatolia: longitudinal gradients in genetic diversity support an eastern origin for a circum-Mediterranean oak gallwasp *Andricus quercustozae*. Mol Ecol 12: 2153–2174.

Seddon JM, Santucci F, Reeve N, Hewitt GM (2002). Caucasus Mountains divide postulated postglacial colonization routes in the white-breasted hedgehog, *Erinaceus concolor*. J Evolution Biol 15: 463–467.

Schmitt T (2007). Molecular biogeography of Europe: Pleistocene cycles and postglacial trends. Front Zool 4: 11.

Schuettpelz E, Schneider H, Huiet L, Windham MD, Pryer KM (2007). A molecular phylogeny of the fern family Pteridaceae: assessing overall relationships and the affinities of previously unsampled genera. Mol Phylogenet Evol 44: 1172–1185.

Swofford DL (2002). PAUP*: phylogenetic analysis using parsimony (*and other models), v. 4.0 beta 10. Sunderland, Sinauer Associates.

Taberlet P, Fumagelli L, Wust-Saucy A-G, Cosson JF (1998). Comparative phylogeography and postglacial colonization routes in Europe. Mol Ecol 7: 453–464.

Thiers B (2014). Index Herbariorum, A global directory of public herbaria and associated staff. New York Botanical Garden's Virtual Herbarium. http,//sweetgum.nybg.org/ih/

Trewick SA, Morgan-Richards M, Russell SJ, Henderson S, Rumsey FJ, Pintér I, Barrett JA, Gibby M, Vogel JC (2002). Polyploidy, phylogeography and Pleistocene refugia of the rockfern *Asplenium ceterach*: evidence from chloroplast DNA. Mol Ecol 11: 2003–2012.

Vogel JC, Rumsey FJ, Schneller JJ, Barrett JA, Gibby M (1999). Where are the glacial refugia in Europe? Evidence from pteridophytes. Biol J Linn Soc 66: 23–37.

Zhang G, Zhang X, Chen Z (2005). Phylogeny of cryptogrammoid ferns and related taxa based on *rbcL* sequences. Nord J Bot 23: 485–493.

Zwickl DJ (2006). Genetic algorithm approaches for the phylogenetic analysis of large biological sequence datasets under the maximum likelihood criterion. Ph.D. dissertation, University of Texas at Austin.

Chapter 4. Slow and steady wins the race: the fern genus *Cryptogramma* survives climatic fluctuations with little apparent morphological or molecular diversification since the Oligocene[1]

4.1 Abstract

Cold-tolerant species are potentially susceptible to rapid habitat shifts caused by anthropogenic climate change. Here, we use divergence time estimation, ancestral area reconstruction and speciation rate analysis to examine the ability of the broadly distributed boreal fern genus *Cryptogramma* to persist in high-latitude and high-altitude environments. We find that crown group *Cryptogramma* diversity originated in east Asia during the Oligocene and that most extant diversity within *Cryptogramma* was generated during the Pliocene and Pleistocene, with multiple colonization events of the New World from east Asia. Speciation rate analysis infers no significant changes in rate across time or the phylogeny, suggesting that *Cryptogramma* could have experienced morphological stasis, perhaps due to being well-suited to surviving shifting habitats.

4.2 Introduction

Climate regime shifts caused by anthropogenic climate change are regarded as a serious danger to numerous taxa worldwide, including cold-loving taxa occurring at high altitude or high latitude (Thomas & al., 2004; Engler & al., 2011; Urban, 2015). Projections from future climate scenarios show elevated extinction risks for these regions (Engler & al., 2011; Maclean and Wilson, 2011; Thuiller & al., 2011; Zhang & al., 2015), with extinction probability estimates ranging from 0.9-24.2% (Thomas & al., 2004). These threats have led to suggestions for assisted migration and additional conservation measures to increase these lineages' survival probabilities before global climate is altered heavily (Hoegh-Guldberg & al., 2008; Gray & al., 2011).

Considerable phylogenetic variability exists among these climate-associated extinction estimates (Thuiller & al., 2011; Zhang & al., 2015), with little information available for some lineages, such as leptosporangiate ferns. These free-sporing vascular plants have minute, wind-borne spores that have left clear evidence of frequent, long distance dispersal events (e.g., Tryon,

[1] Metzgar, J.S., and S.M. Ickert-Bond. In prep. Slow and steady wins the race: the fern genus *Cryptogramma* survives climatic fluctuations with little morphological or molecular diversification since the Oligocene. To be submitted to: *Taxon*.

1970), although the importance of vicariance has been demonstrated as well (Haufler, 2007). This dispersal capability could potentially give these lineages an advantage in quickly colonizing new suitable habitat in rapidly changing environments. Furthermore, an easily dispersed clade that has been long-established in high altitude and high latitude regions could have been further pre-adapted by previous glacial cycles to survive widespread, dramatic climate shifts.

The leptosporangiate fern genus *Cryptogramma* R.Br. is ideally suited to evaluating the potential stability of cold-loving taxa to climatic fluctuations. This genus contains nine species that are predominantly found in high altitude or high latitude environments (Alverson, 1989; Tryon and Tryon, 1990). Most species are predominantly boreal, although one taxon occurs in mountainous terrain in southern South America (Tryon and Tryon, 1990). Phylogenetic relationships within the genus have been well characterized, with parentage of all polyploid taxa established (Metzgar & al., 2013; Metzgar & al., 2016). This includes the suggestion that the allotetraploid *C. sitchensis* was formed by climate-induced range shifts during the Pleistocene (Metzgar & al., 2013). *Cryptogramma* is one of three genera in the cryptogrammoid clade, which is the sister lineage to the rest of the diverse, cosmopolitan Pteridaceae (Prado & al., 2007; Schuettpelz & al., 2007; Metzgar & al., 2013). This clade also consists of the monotypic Central American genus *Llavea* Lag. and the approximately 30 species of *Coniogramme* that have an Asian center of diversity (Tryon and Tryon, 1990; Prado & al., 2007; Schuettpelz & al., 2007).

Here we examine the history of the cryptogrammoid ferns by applying divergence time estimation, biogeographic analysis of ancestral areas, and Bayesian analysis of speciation rates across a well-supported plastid phylogeny. By adding a temporal axis to the phylogeny and inferring ancestral areas we can establish the long-term preference of *Cryptogramma* species for high altitude and high latitude regions. Recent advances in analyzing speciation rate heterogeneity (Rabosky and Huang, 2016) will allow us to identify any potential radiation events (Orr and Smith, 1998). This approach has been used to dectect geographic patterns, directional trends and assessing morphological evolution in radiation events (Patiño and Vanderpoorten, 2015; Rabosky & al., 2013; Rabosky & al., 2014). We will use the findings from speciation rate analysis to provide a historical perspective on the relative ability of free-sporing, cold-tolerant taxa to respond to climate shifts and by extension, the relative need for conservation concern for such taxa in the face of anthropogenic climate change.

4.3 Materials and methods

4.3.1. Taxon sampling and DNA sequence alignments

The dataset of 40 accessions sequenced for 7143 basepairs (Appendix 1) was generated in a previous study of phylogenetic relationships within *Cryptogramma* (Metzgar & al., 2013). This dataset is comprised of six plastid loci (*rbc*L, *rbc*L–*acc*D, *rbc*L–*atp*B, *rps*4–*trn*S, *trn*G–*trn*R and *trn*P–*pet*G) and includes 32 *Cryptogramma* accessions representing eight species. Three accessions of *Llavea cordifolia* were used as the outgroup and five accessions of *Coniogramme* were also included. DNA sequence alignments are identical to an earlier study (Metzgar & al., 2013) and are available in TreeBASE (treebase.org; study #18991).

4.3.2 Phylogenetic analyses and divergence time estimation

The phylogeny and divergence time estimates were calculated simultaneously using Bayesian inference implemented in BEAST v.1.7.5 (Drummond and Rambaut, 2007; Drummond & al., 2012). Molecular rates were estimated using an uncorrelated lognormal relaxed-clock model (Drummond and Rambaut, 2007). Each locus was treated as a separate partition and substitution models and clock models were unlinked across partitions. All partitions were assigned a substitution model of HKY to avoid possible over-parameterization of the analysis associated with using the general time reversible model (Bryson & al., 2014). The analysis was conducted using four separate chains, each running for 10 million generations with a sampling frequency of every 1000 generations. The BEAST input file was generated in BEAUti v.1.8.0 (Drummond & al., 2012). The initial 25% of generations were discarded as the burn-in period. Tree files and run statistics from the four chains were combined using LogCombiner v.1.8.0 (Drummond & al., 2012).

The fossil record of the cryptogrammoid ferns (*Llavea*, *Coniogramme* and *Cryptogramma*) is remarkably depauperate with no assignable fossils available to integrate with this analysis (Collinson, 2001). Instead, two secondary constraints were used to calibrate our phylogeny. These constraints were obtained from a robust, large-scale study of phylogenetic divergences and divergence times across leptosporangiate ferns (Schuettpelz and Pryer, 2009). The prior on the root of our tree (i.e., the divergence of *Llavea* from the *Coniogramme*+*Cryptogramma* clade) was given a normal distribution with a mean of 58.5 Ma with a standard deviation of 2.0 to correspond to the previously published estimate of 58.5 Ma

(Node 107; Schuettpelz and Pryer, 2009). The divergence of *Coniogramme* from *Cryptogramma* was assigned a prior with a normal distribution and a mean of 44.3 Ma and standard deviation of 2.0 to correspond to the previously published estimate of 44.3 Ma (Node 108; Schuettpelz and Pryer, 2009).

4.3.3 Likelihood biogeographical reconstruction

Ancestral area reconstruction was performed using the dispersal-extinction-cladogenesis (DEC) model implemented in Lagrange (Ree and Smith, 2008). One time slice was used for our analysis in Lagrange as most divergences in the phylogeny are relatively recent and older time slices would contain few nodes and produce skewed estimates (Chacón and Renner, 2014). Species ranges were divided into seven distributions: Europe, western North America, eastern North America, southern South America, central America, southeastern Asia and east-central Asia (Fig. 4.1). To test the effect of range delimitation on inferred ancestral area ranges, separate Lagrange analyses were run with the western North American and east-central Asian ranges subdivided into two additional areas. The effect of varying the maximum range size was explored using analyses that set the maximum number of ancestral areas at two or three. The dispersal matrix was set to 1.0 for all values, although setting the dispersal probability to 0.1 for all migration to and from the isolated southern South American range was also examined. All Lagrange input files were constructed using the Lagrange configurator v.20130526 (http://www.reelab.net/lagrange/configurator/index).

4.3.4 Bayesian diversification analysis

Speciation rates were estimated using BAMM (Bayesian analysis of macroevolutionary rates; Rabosky, 2014). BAMM employs reversible jump Markov chain Monte Carlo to infer speciation rates on a phylogeny, allowing for intra- and inter-clade rate variation (Rabosky, 2014). We used the chronogram generated by BEAST as the input phylogeny. Rates were allowed to vary across the phylogeny. The analysis was run for five million generations, with a burn-in fraction of 0.25. Prior probabilities were set using the setBAMMpriors tool in the BAMMtools software package (Rabosky, 2014). All output from BAMM was also processed using the BAMMtools software package (Rabosky, 2014).

4.4 Results

4.4.1 Phylogenetic analyses and divergence time estimation

The combined, post-burnin four chain BEAST analysis converged onto a mean posterior likelihood of -19552.091. All run statistics possessed an ESS well in excess of 200. The inferred age of constrained nodes converged on 52.954 Ma for the root node and 46.918 Ma for the *Cryptogramma* + *Coniogramme* node (Fig. 4.1). The low values obtained for the coefficient of variation and covariance statistics for each partition support our use of an uncorrelated lognormal model distribution. Phylogenetic relationships generally agreed with previous estimates generated from this dataset using maximum parsimony, maximum likelihood and Bayesian inference (Metzgar & al., 2013).

4.4.2 Likelihood biogeographical reconstruction

Reconstructions using Lagrange (Ree and Smith, 2008) infer that east-central Asia was the most likely ancestral area for all deep nodes in the tree (i.e., divergences occurring before 10 Ma; Fig. 4.1). Within *Cryptogramma*, the first divergence in sect. *Cryptogramma* infers a single long-distance dispersal event from Asia to South America for the ancestor of *C. fumariifolia* and infers an east Asian range for the remainder of sect. *Cryptogramma*. The subsequent divergence event (*C. cascadensis* + *C. acrostichoides* clade) shows a dispersal event from east Asia to North America (Fig. 4.1). Further radiation in this clade included a single dispersal of the *C. crispa* lineage to Europe. Altering the number of ancestral areas allowed and varying the dispersal probability did not affect the results (results not shown).

4.4.3 Bayesian diversification analysis

The BAMM analysis identified no distinct rate shifts within the same 40-accession phylogeny (Fig. 4.2), with an effective sample size of over 1600. However, some authors have suggested a reduced ability to detect rate variation in smaller phylogenies (e.g., Villarreal & al., 2015). The fastest rates were inferred to occur within the *Cryptogramma* sect. *Cryptogramma* clade and the slowest rates in the *Llavea* clade. Cohort analysis also demonstrated the broad similarity of rates across the phylogeny (Fig. 4.2).

4.5 Discussion

4.5.1 Origin of the cryptogrammoid ferns

Most diversification within the cryptogrammoid ferns is relatively recent (Fig. 4.1), echoing a pattern shown across leptosporangiate ferns (Schuettpelz and Pryer, 2009). Intergeneric divergences are shown to have occurred in the Paleocene and Eocene, with both sections of *Cryptogramma* diverging from each other in the late Oligocene. *Llavea* is monotypic and occupies a small range with little known morphological diversity (Tryon and Tryon, 1990), so it is not surprising that our results show all crown group diversity originated in the late Pleistocene or later (Fig. 4.1). Taxonomic sampling within *Coniogramme* is limited (approximately 10% of extant species), but our results demonstrate that crown group diversification began at least in the mid-Miocene and highlights the need for detailed examination of this group.

All deep nodes in the phylogeny were inferred to have been present in east Asia. The conclusion that east Asia was the cradle of diversity for this lineage has also been inferred for many other plant lineages (e.g., Wen & al., 2010; Sessa & al., 2012; Wen & al., 2014), with a suggestion that uplift events in the Himalayan Plateau during the Miocene may have driven diversification there (Fan & al., 2013; Wen & al., 2014). The allotetraploid *C. sitchensis* was formed during Pleistocene glacial cycles in Beringia (Fig. 4.1; Metzgar & al., 2013). This is another example of glaciation cycles inducing the formation of polyploids (Brochmann & al., 2004). These studies have also demonstrated the frequency of dispersal from Asia to North America (Wen & al., 2010).

The sole member of *Cryptogramma* sect. *Homopteris*, *C. stelleri*, diversified in the Pleistocene. This is most likely due to repeated dispersal events from one or multiple refugia to colonize deglaciated regions, similar to that seen in other northern fern lineages (e.g, *Dryopteris carthusiana*; Sessa & al., 2012) as the short time scale would preclude vicariance.

4.5.2 Colonization events by Cryptogramma

The cryptogrammoid ferns show clear evidence supporting the role of east Asia as a source for colonization events of the New World. Sect. *Cryptogramma* reveals one long distance dispersal event early in its history during the late Miocene, with *C. fumariifolia* or its ancestor dispersing from east Asia to South America (Fig. 4.1). A direct dispersal from east Asia to South

America is difficult to explain, with few known pathways. Only one forest-dwelling bird species is known to migrate between Asia and South America (*Catharus minimus aliciae*; Winker and Gibson, 2016), although its present day range in South American is farther north in Peru (Kevin Winker, pers. comm.) than that of *C. fumariifolia* in Chile and Argentina. Other plant lineages occur disjunctly distributed between South America and Asia (Sessa & al., 2012; McHenry and Barrington, 2014; Wen & al., 2014), although with no long-distance dispersal mechanism suggested other than light-weight propagules having been carried by wind currents (e.g., *Nanoglottis*; Wen & al., 2014).

With an inferred ancestral area of east Asia for the root node, a dispersal event to North America occurred along the branch leading to extant *Llavea* (Fig. 4.1). Additionally, a colonization event from east Asia to North America led to subsequent speciation in the *C. cascadensis* + *C. acrostichoides* clade (Fig. 4.1) during the Pliocene. This colonization event, most likely by vicariance via the Bering Land Bridge, is a common pathway for Asian taxa to reach North America during the Miocene and Pliocene (Tiffney, 1985; Wen & al., 2010; Sessa & al., 2012; Wen & al., 2014). The *C. crispa* lineage reached Europe from North America during the Pliocene. This could represent a long-distance dispersal event, but also could represent vicariance using the North American Land Bridge. Palynological findings support the existence of the North American Land Bridge at least as recently as 5.5 mya (Tiffney, 1985; Manchester, 1999; Tiffney and Manchester, 2001; Denk & al., 2010), leaving this possibility open as a mechanism for *C. crispa* to reach Europe. Plastid sequence data support further diversification occurring in the *C. crispa* clade, perhaps in response to Pleistocene glacial cycles (Metzgar & al., 2016). *Cryptogramma acrostichoides* also recolonized Asia from western North America during the Quaternary, with vicariance due to the disappearance of the Bering Land Bridge the most likely explanation (Metzgar & al., 2013; Ickert-Bond and Wen, 2006).

4.5.3 Stability of speciation rate and morphology in Cryptogramma

The lack of speciation rate shifts across the phylogeny and across time (Fig. 4.2) could suggest a tendency towards stability within *Cryptogramma*. This lineage has occupied regions heavily impacted by glacial climate cycles (e.g., Beatty and Provan, 2010; Wen & al., 2014) yet has steadily persisted across these regions with little morphological change (Tryon and Tryon, 1990; Metzgar & al., 2013). Ferns are capable of rapid dispersal via minute spores (Tryon,

1970), and high amounts of dispersal have been correlated with low speciation rates (Birand & al., 2012). Some fern lineages have also been demonstrated to not rely on morphological innovation for diversification (Sundue et al., 2015). This could explain the lack of any significant rate changes across the phylogeny (Fig. 4.2). Geographic and altitudinal clines should offer reservoirs of genetic variability to better cope with climate-induced range shifts (Aitkin & al., 2008), a strategy used by many arctic plants (Crawford and Abbott, 1994). Dispersal ability would also have been critical in pre-adapting *Cryptogramma* to climate cycles by quickly responding to newly available habitat from receding glaciers (Crawford and Abbott, 1994). Speciation in montane taxa has also previously been attributed to these rapid range shifts (*Koenigia*; Fan & al., 2013). Boreal taxa also possibly possess a greater tolerance to higher temperatures than expected (Aitken & al., 2008). The small number of *Cryptogramma* species hinders our ability to draw firm conclusions from the speciation rate analysis, however (Rabosky, 2014).

The lack of morphological variation seen in *Cryptogramma* could imply pre-adaptation for these climatically variable areas. Sections *Homopteris* and *Cryptogramma* differ in traits such as soil preference, rhizome type, lamina thickness and degree of leaf dimorphism (Alverson, 1989; Tryon and Tryon, 1990). In the more species-rich sect. *Cryptogramma*, taxa are distinguished only by small differences such as pinnule shape, hydathode position, and herbaceous or wintergreen life history (Alverson, 1989; Tryon and Tryon, 1990). This conservative body plan across the genus could be an example of morphological stasis enabling long-term occupation of an environmental niche (Estes and Arnold, 2007). Long-term morphological stasis has been reported previously for globally distributed plant lineages (McDaniel and Shaw, 2003), including fern lineages that have undergone modest diversification since the Oligocene (Schneider & al., 2015). Morphological stasis has also been shown to result from natural selection (Davis & al., 2014). Modeling experiments suggest that stabilizing selection is the most important factor in maintaining the stasis (Estes and Arnold, 2007). Future morphological studies with large sample sizes could assess this possible morphological stasis from a robust statistical perspective.

Cryptogramma originated in east Asia and multiple colonization events have led to its present-day circumboreal and austral range. This lineage appears to have evolved a successful morphological strategy for long-term survival in high-altitude, high-latitude habitats that are

subject to dramatic climate cycles. It is likely pre-adapted to changing climates and morphological stasis is preserving its ecological strategy. *Cryptogramma* does not appear to be a boreal lineage in higher need of conservation efforts to survive anthropogenic climate change.

4.6 Acknowledgements

We thank Katie Everson, Petra Korall, Israel Loera, Carl Rothfels, Eric Schuettpelz and Diana Wolf for laboratory advice or technical expertise. This research was funded in part by the Alaska Experimental Program to Stimulate Competitive Research Landscape Genetics Student Research Award, Alaska Quaternary Center Hopkins Fellowship, American Society of Plant Taxonomists Graduate Student Research Award, University of Alaska Center for Global Change Student Research Grant, University of Alaska Ted McHenry Biology Field Research Award, and a National Science Foundation Division of Environmental Biology Doctoral Dissertation Improvement Grant award 1311685 to SMI-B and JSM.

4.7 Figures

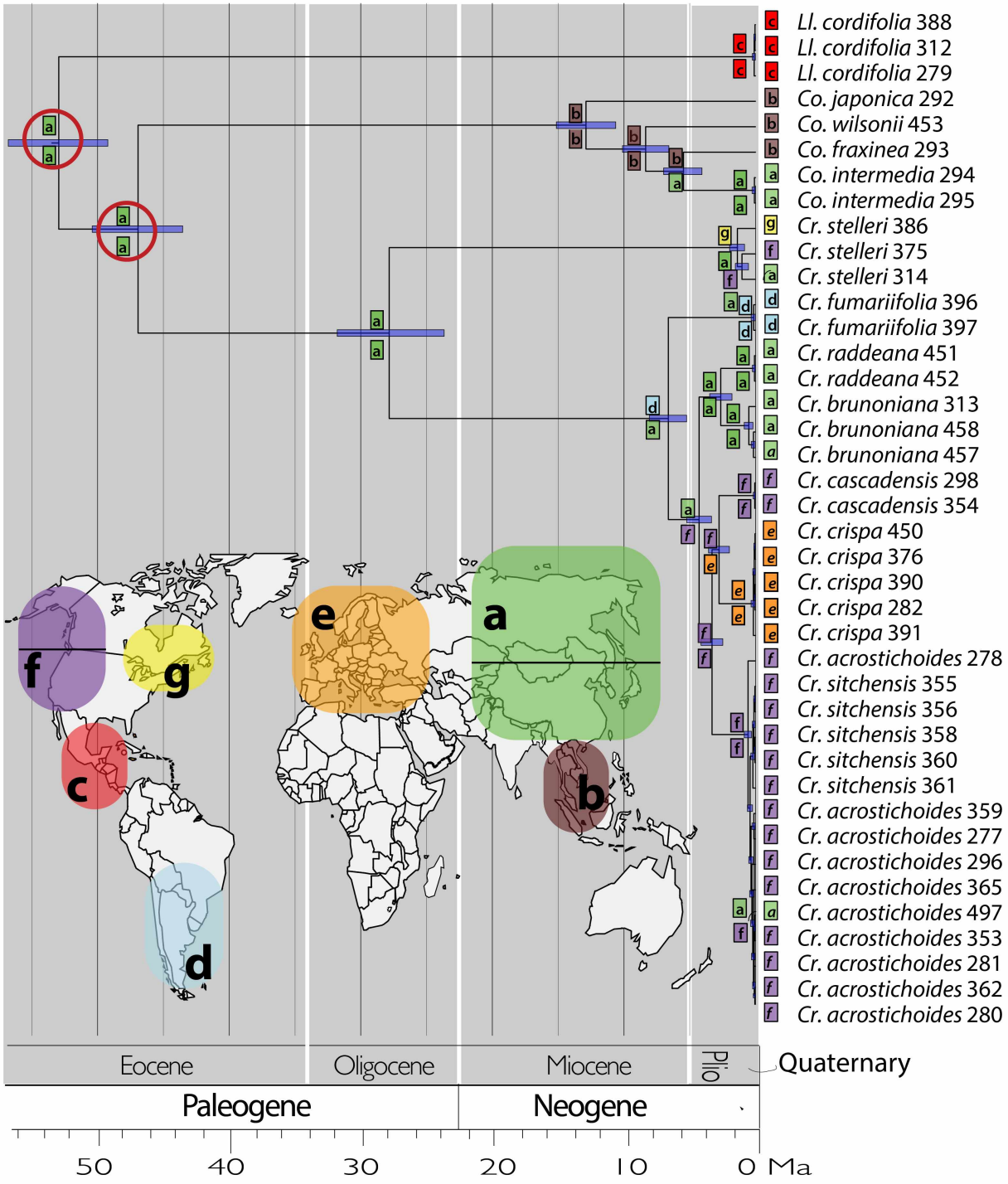
Ll. cordifolia 388
Ll. cordifolia 312
Ll. cordifolia 279
Co. japonica 292
Co. wilsonii 453
Co. fraxinea 293
Co. intermedia 294
Co. intermedia 295
Cr. stelleri 386
Cr. stelleri 375
Cr. stelleri 314
Cr. fumariifolia 396
Cr. fumariifolia 397
Cr. raddeana 451
Cr. raddeana 452
Cr. brunoniana 313
Cr. brunoniana 458
Cr. brunoniana 457
Cr. cascadensis 298
Cr. cascadensis 354
Cr. crispa 450
Cr. crispa 376
Cr. crispa 390
Cr. crispa 282
Cr. crispa 391
Cr. acrostichoides 278
Cr. sitchensis 355
Cr. sitchensis 356
Cr. sitchensis 358
Cr. sitchensis 360
Cr. sitchensis 361
Cr. acrostichoides 359
Cr. acrostichoides 277
Cr. acrostichoides 296
Cr. acrostichoides 365
Cr. acrostichoides 497
Cr. acrostichoides 353
Cr. acrostichoides 281
Cr. acrostichoides 362
Cr. acrostichoides 280
a
b
c
d
e
f
g
Eocene
Oligocene
Miocene
Plio
Quaternary
Paleogene
Neogene
50
40
30
20
10
0 Ma

Fig. 4.1. Divergence time estimates and inferred ancestral areas for cryptogrammoid ferns. Divergence time estimates are shown in millions of years and were calculated using BEAST. Red circles depict secondary constraints used to calibrate the analysis. Purple bars reflect 95% HPD of estimate at each node. Ancestral areas were reconstructed at each node using Lagrange. Boxes at nodes depict the inferred area for respective daughter lineages. Boxes are color-coded and correspond with possible range areas used in the analysis depicted on the map.

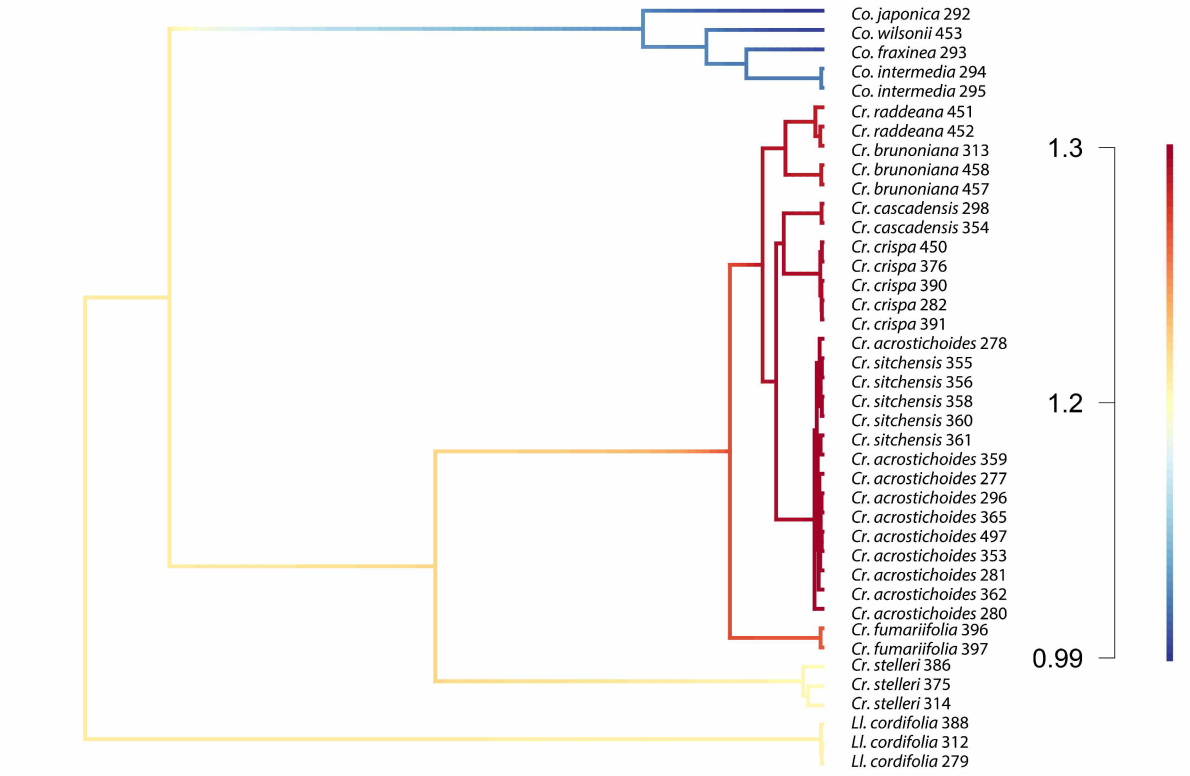
Co. japonica 292
Co. wilsonii 453
Co. fraxinea 293
Co. intermedia 294
Co. intermedia 295
Cr. raddeana 451
Cr. raddeana 452
Cr. brunoniana 313
Cr. brunoniana 458
Cr. brunoniana 457
Cr. cascadensis 298
Cr. cascadensis 354
Cr. crispa 450
Cr. crispa 376
Cr. crispa 390
Cr. crispa 282
Cr. crispa 391
Cr. acrostichoides 278
Cr. sitchensis 355
Cr. sitchensis 356
Cr. sitchensis 358
Cr. sitchensis 360
Cr. sitchensis 361
Cr. acrostichoides 359
Cr. acrostichoides 277
Cr. acrostichoides 296
Cr. acrostichoides 365
Cr. acrostichoides 497
Cr. acrostichoides 353
Cr. acrostichoides 281
Cr. acrostichoides 362
Cr. acrostichoides 280
Cr. fumariifolia 396
Cr. fumariifolia 397
Cr. stelleri 386
Cr. stelleri 375
Cr. stelleri 314
Ll. cordifolia 388
Ll. cordifolia 312
Ll. cordifolia 279
1.3
1.2
0.99

A

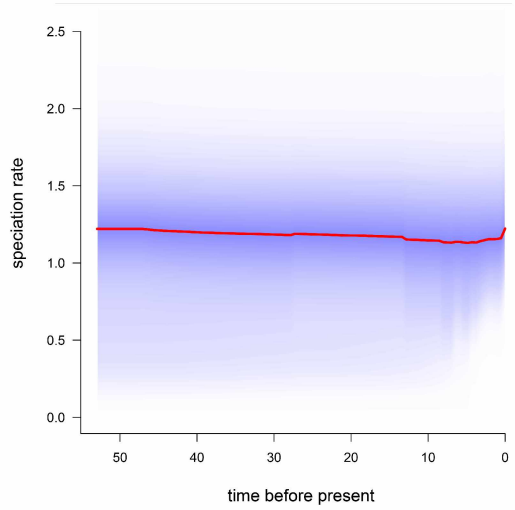
speciation rate
2.5
2.0
1.5
1.0
0.5
0.0
50
40
30
20
10
0
time before present

B

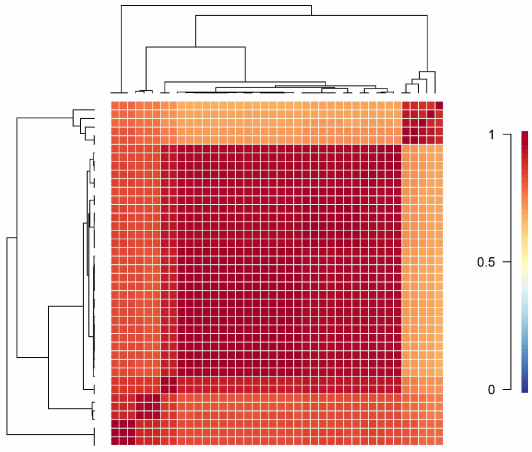
1
0.5
0

C

Fig. 4.2. Estimates of speciation rate variability across the cryptogrammoid ferns. A. Cryptogrammoid fern chronogram as in fig. 4.1 with shading of branches reflective of estimated diversification rates (see scale at right) estimated in BAMM. Diversifications are the means of the marginal densities of the rates. B. Estimates of speciation rate variability across the cryptogrammoid ferns (red line), with average global climate overlain (Zachos & al., 2001; purple line). C. Cohort analysis comparing similarity of rates between lineages. Pairs of taxa with highly similar rates are depicted in hotter colors (i.e., red) and dissimilar rates are shown as colder colors (i.e., blue).

4.8 References

Aitkin, S.N., Yeaman, S., Holliday, J.A., Wang, T., & Curtis-McLane, S. 2008. Adaptation, migration or extirpation: climate change outcomes for tree populations. *Evol. Appl.* 1: 95—111.

Alverson, E.R. 1989. *Biosystematics of Parsley-ferns,* Cryptogramma *R. Br., in Western North America.* Master's thesis, Oregon State University, Corvallis, Oregon, U.S.A.

Beatty, G.E., & Provan, J. 2010. Refugial persistence and postglacial recolonization of North America by the cold-tolerant herbaceous plant *Orthilia secunda*. *Mol. Ecol.* 2010, 19: 5009—5021.

Birand, A., Vose, A., & Gavrilets, S. 2012. Patterns of species ranges, speciation, and extinction. *Am. Nat.* 179: 1—21.

Brochmann, C., Brysting, A.K., Alsos, I.G., Borgen, L., Grundt, H.H., Scheen, A.-C., & Elven, R. 2004. Polyploidy in Arctic plants. *Biol. J. Linn. Soc.* 82: 521—536.

Bryson, R.W., Prendini, L., Savary, W.E., & Pearman, P.B. 2014. Caves as microrefugia: Pleistocene phylogeography of the troglophilic North American scorpion *Pseudouroctonus reddelli. BMC Evol Biol.* 14: 9. doi: 10.1186/1471-2148-14-9

Chacón, J., & Renner, S.S. 2014. Assessing model sensitivity in ancestral area recontruction using LaGRANGE: a case study using the Colchicaceae family. *J. Biogeogr.* 41: 1414—1427.

Collinson, M.E. 2001. Cainozoic ferns and their distribution. *Britt.* 53: 173—235.

Crawford, R.M.M. & Abbott, R.J. 1994. Pre-adaptation of Arctic plants to climate change. *Bot. Acta.* 107: 271—278.

Davis, C.C., Schaefer, H., Xi, Z., Baum, D.A., Donoghue, M.J., & Harmon, L.J. 2014. Long-term morphological stasis maintained by a plant–pollinator mutualism. *Proc. Nat. Acad. Sci. U.S.A.* 111: 5914—5919.

Denk, T., Grimsson, F., & Zetter, R. 2010. Episodic migration of oaks to Iceland: Evidence for a North Atlantic "land bridge" in the latest Miocene. *Am. J. Bot.* 97: 276—287.

Drummond, A., & Rambaut, A. 2007. BEAST: bayesian evolutionary analysis sampling trees. *BMC Evol. Biol.* 7: 214. doi:10.1186/1471-2148-7-214

Drummond, A., Suchard, M.A., Xie, D., & Rambaut, A. 2012. Bayesian phylogenetics with BEAUti and the BEAST 1.7. *Mol. Bio. Evol.* 29: 1969—73.

Engler, R., Randin, C.F., Thuiller, W., Dullinger, S., Zimmermann, N.E., Araújo, M.B., Pearman, P.B., Le Lay, G., Piedallu, C., Choler, P., De Lamo, X., Dirnböck, T., Gégout, J.-C., Gómez-García, D., Grytnes, J.-A., Heegaard, E., Høistad, F., Nogués-Bravo, D., Normand, S., Puşcaş, M., Sebastià, M.-T., Stanisci, A., Theurillat, J.-P., Trivedi, M.R., Vittoz, P., & Guisan, A. 2011. 21st century climate change threatens mountain flora unequally across Europe. *Global Change Biology* 17: 2330—2341. doi:10.1111/j.1365-2486.2010.02393.x.

Estes, S., & Arnold, S.J. 2007. Resolving the paradox of stasis: models with stabilizing selection explain evolutionary divergence on all timescales. *Am. Nat.* 169: 227—244.

Fan, D.-M., Chen, J.-H., Meng, Y., Wen, J., Huang, J.-L., & Yang, Y.-P. 2013. Molecular phylogeny of *Koenigia* L. (Polygonaceae: Persicarieae): Implications for classification, character evolution and biogeography. *Mol. Phylogenet. Evol.* 69: 1093—1100.

Gray, L.K., Gylander, T., Mbogga, M.S., Chen, P., & Hamann, A. 2011. Assisted migration to address climate change: recommendations for aspen reforestation in western Canada. *Ecol. Appl.* 21: 1591—1603.

Haufler, C.H. 2007. Genetics, phylogenetics, and biogeography: Considering how shifting paradigms and continents influence fern diversity. *Britt.* 59: 108—114 .

Hoegh-Guldberg, O., Hughes, L., McIntyre, S., Lindenmayer, D.B., Parmesan, C., Possingham, H.P. & Thomas, C.D. 2008. Assisted colonization and rapid climate change. *Science* 321: 345—346.

Ickert-Bond, S.M., & Wen, J. 2006. Phylogeny and biogeography of Altingiaceae: Evidence from combined analysis of five non-coding chloroplast regions. *Mol. Phylogenet. Evol.* 39: 512—528.

Maclean, I.M.D. & Wilson, R.J. 2011. Recent ecological responses to climate change support predictions of high extinction risk. *Proc. Nat. Acad. Sci. U.S.A.* 108: 12337—12342.

Manchester, S.R. 1999. Biogeographical relationships of North American Tertiary floras. *Ann. Miss. Bot. Gard.* 86: 472—522.

McDaniel, S.F., & Shaw, A.J. 2003. Phylogeographic structure and cryptic speciation in the trans-Antarctic moss *Pyrrhobryum mnioides*. *Evol.* 57: 205—215.

McHenry, M.A., & Barrington, D.S. 2014. Phylogeny and biogeography of exindusiate Andean *Polystichum* (Dryopteridaceae). *Am. J. Bot.* 101: 365—375.

Metzgar, J.S., Alverson, E.R., Chen, S., Vaganov, A.V., & Ickert-Bond S.M. 2013. Diversification and reticulation in the circumboreal fern genus *Cryptogramma*. *Mol. Phyl. Evol.* 67: 589—599.

Metzgar, J.S., Stamey, M., & Ickert-Bond, S.M. 2016. Genetic differentiation and polyploid formation within the Cryptogramma crispa (Polypodiales: Pteridaceae) complex. *Turkish J. Bot.* doi:10.3906/bot-1501-54

Orr, M.R., & Smith, T.B. 1998. Ecology and speciation. *Trends Ecol. Evol.* 13: 502—506.

Patiño, J., & Vanderpoorten, A. 2015. Macaronesia is a departure gate of anagenetic speciation in the moss genus *Rhynchostegiella*. *J. Biogeog.* 42: 2122—2130.

Prado J., Rodrigues, C.D.N., Salatino, A., & Salatino, M.L.F. 2007. Phylogenetic relationships among Pteridaceae, including Brazilian species, inferred from *rbcL* sequences. *Taxon* 56: 355—368.

Rabosky, D.L. 2014. Automatic detection of key innovations, rate shifts, and diversity-dependence on phylogenetic trees. *PLOS One* 9(2): e89543.

Rabosky, D.L., Santini, F., Eastman, J., Smith, S.A., Sidlauskas, B., Chang, J., & Alfaro, M.E. 2013. Rates of speciation and morphological evolution are correlated across the largest vertebrate radiation. *Nature Comm.* 4: 10.1038/ncomms2958.

Rabosky, D.L., Title, P.O., & Huang, H. 2014. Minimal effects of latitude on present-day speciation rates in New World birds. *Proc. R. Soc. B.* 282:20142889.

Rabosky, D.L., & Huang, H. 2016. A robust semi-paremetric test for detecting trait-dependent diversification. *Syst. Biol.* 65:181—193.

Ree, R.H., & Smith, S.A. 2008. Maximum likelihood inference of geographic range evolution by dispersal, local extinction, and cladogenesis. *Syst. Biol.* 57: 4—14.

Schneider, H., Liu, H., Clark, J., Hidalgo, O., Pellicer, J., Zhang, S., Kelly, L.J., Fay, M.F. & Leitch, I.L. 2015. Are the genomes of royal ferns really frozen in time? Evidence for coinciding genome stability and limited evolvability in the royal ferns. *New Phyt.* 1: 1—4.

Schuettpelz, E., Schneider, H., Huiet, L., Windham, M.D., & Pryer, K.M. 2007. A molecular phylogeny of the fern family Pteridaceae: assessing overall relationships and the affinities of previously unsampled genera. *Mol. Phylogenet. Evol.* 44: 1172—1185.

Schuettpelz, E., & Pryer, K.M. 2009. Evidence for a Cenozoic radiation of ferns in an angiosperm-dominated canopy. *Proc. Nat. Acad. Sci. U.S.A.* 106: 11200—11205.

Sessa, E.B., Zimmer, E.A., & Givnish, T.J. 2012. Phylogeny, divergence times and historical biogeography of New World *Dryopteris* (Dryopteridaceae). *Am. J. Bot.* 99: 730—750.

Tiffney, B.H. 1985 . The Eocene North Atlantic Land Bridge: Its importance in Tertiary and modern phytogeography of the northern hemisphere. *J. Arnold Arboretum* 66: 243—273.

Tiffney, B.H., & Manchester, S.R. 2001. The use of geological and paleontological evidence in evaluating plant phylogeographic hypotheses in the northern hemisphere Tertiary. *Int. J. Plant Sci.* 162: S3—S17.

Thomas, C.D., Cameron, A., Green, R.E., Bakkenes, M., Beaumont, L.J., Collingham, Y.C., Erasmus, B.F.N., Ferreira de Siqueira, M., Grainger, A., Hannah, L., Hughes, L., Huntley, B., van Jaarsveld, A.S., Midgley, G.F., Miles, L., Ortega-Huerta, M.A., Peterson, A.T., Phillips, O.L., & Williams, S.E. 2004. Extinction risk from climate change. *Nature* 427: 145—148.

Thuiller, W., Lavergne, S., Roquet, C., Boulangeat, I., Lafourcade, B., & Araujo, M.B. 2011. Consequences of climate change on the tree of life in Europe. *Nature* 470: 531—534.

Tryon, R.M., & Tryon, A.F. 1990. *Pteridaceae. Pp. 230—256. in*: Kramer, K.U. & Green, P.S. (eds.), *The families and genera of vascular plants, vol. I, Pteridophytes and gymnosperms.* Berlin: Springer-Verlag.

Tryon, R.M. 1970. Development and evolution of fern floras of oceanic islands. *Biotropica* 2: 76—84.

Urban, M.C. 2015. Accelerating extinction risk from climate change. *Science* 348: 571—573.

Villarreal, J.C., Cusimano, N., & Renner, S.S. 2015. Biogeography and diversification rates in hornworts: The limitations of diversification modeling. *Taxon* 64: 229—238.

Wen, J., Ickert-Bond, S.M., Nie, Z.-L., & Li, R. 2010. Timing and Modes of Evolution of Eastern Asian–North American Biogeographic Disjunctions in Seed Plants. Pp. 252—269 in: Long, M., Gu, H., & Zhou, Z. *Darwin's Heritage Today: Proceedings of the Darwin 2010 Beijing International Conference.* Beijing: Higher Education Press.

Wen, J., Zhang, J.-Q., Nie, Z.-L., Zhong, Y., & Sun, H. 2014. Evolutionary diversifications of plants on the Qinghai-Tibet Plateau. *Frontiers in Gen.* 4: doi: 10.3389/fgene.2014.00004.

Winker, K., & Gibson, D.D. 2016. Some broad-scale effects of recent and future climate change among migratory birds in Beringia. In: Shuford, W.D., & R. Gill, R.. 2016. *Avifaunal Change in Western North America. Studies of Western Birds 1*. Los Angeles: Western Field Ornithologists.

Zachos, J., Pagani, M., Sloan, L., Thomas, E., Billups, K. 2001. Trends, rhythms, and aberrations in global climate 65 Ma to present. *Science* 292 (5517): 686–693. doi:10.1126/science.1059412

Zhang, J., Nielsen, S.E., Stolar, J., Chen, Y., & Thuiller, W. 2015. Gains and losses of plant species and phylogenetic diversity for a northern high-latitude region. *Diversity and Distributions* 1: 1—14.

4.9 Appendix

Appendix. Voucher specimens, DNA extraction numbers, and GenBank accession numbers for six plastid DNA loci.

Species, DNA extraction number, specimen voucher, rbcL,rbcL-accD,rbcL-atpB,rps4-trnS,trnG-trnR,trnP-petG;

Outgroups: ***Llavea cordifolia,*** 279, Mexico, Hidalgo, Municipio Nicolas Flores. On road to Nicolas Flores from Cardonal, *Rothfels 3025* (ALA, DUKE, MEXU), KC700108, KC700148, KC700186, KC700225, KC700263, KC700299; ***Llavea cordifolia,*** 312, Mexico, Hidalgo, Municipio Zimapán, Los Mármoles gorge., *Ledesma 2113* (HGOM), KC700109, KC700150, KC700187, KC700226, KC700264, KC700300; ***Llavea cordifolia,*** 388, Mexico, Guerrero, On outskirts of Fila De Caballos, *Dyer 61* (MEXU, BM), KC700110, KC700149, KC700188, KC700227, KC700265, KC700301; ***Coniogramme japonica,*** 292, USA, North Carolina, Plant in cultivation at Juniper Level Botanic Garden, *Schuettpelz 386* (DUKE), KC700111, KC700151, KC700189, KC700228, KC700266, KC700302; ***Coniogramme fraxinea,*** 293, Malaysia, Pahang, Cameron Highlands, Robinson Falls, *Schuettpelz 836* (DUKE, KEP), KC700112, -, KC700190, KC700229, KC700267, KC700303; ***Coniogramme intermedia,*** 294, Taiwan, Nantou County, Mei-Feng Experimental Farm Reserve, *Schuettpelz 1052A* (DUKE, TAIF, BM), KC700113, -, KC700191, KC700230, KC700268, KC700304; ***Coniogramme intermedia,*** 295, China, Guizhou, Shuicheng, Yushe, *Zhang 246* (MO), KC700114, KC700152, KC700192, KC700231, KC700269, KC700305; ***Coniogramme wilsonii,*** 453, Vietnam, Bac Kan Province, Cho Don District, Ban Thi Community, Phia Khao Village, *Hieu CPC1240* (ALA), KC700115, KC700153, -, KC700232, KC700270, KC700306; **Ingroup:** ***Cryptogramma acrostichoides,*** 277, USA, Alaska, Kodiak, near the transient boat harbor, *Studebaker 09-473* (ALA), KC700093, KC700133, KC700171, KC700210, KC700248, KC700284; ***Cryptogramma acrostichoides,*** 278, USA, Utah, Salt Lake County, Little Cottonwood Canyon, near Snowbird, *Rothfels 2979* (ALA, DUKE, NHIC), KC700094, KC700134, KC700172, KC700211, KC700249, KC700285; ***Cryptogramma acrostichoides,*** 280, USA, Washington, Mason County, N of Lake Cushman along the Mt. Ellinor trail in the Olympic Mtns., *Windham 3624* (DUKE, UT), KC700095, KC700135, KC700173, KC700212, KC700250, KC700286; ***Cryptogramma acrostichoides,*** 281, USA, Oregon, Linn Co., Horse Rock Ridge, SW of Crawfordsville., *Pryer*

06-04 (DUKE), KC700096, KC700136, KC700174, KC700213, KC700251, KC700287; ***Cryptogramma acrostichoides,*** 296, USA, Oregon, Lane County, Trail to Proxy Falls, *Alverson s.n.* (ALA), KC700097, KC700137, KC700175, KC700214, KC700252, KC700288; ***Cryptogramma acrostichoides,*** 353, USA, Washington, King County, Source Lake Lookout Trail, above Source Lake, Cascade Range, *Zika 25403* (ALA), KC700098, KC700138, KC700176, KC700215, KC700253, KC700289; ***Cryptogramma acrostichoides,*** 359, USA, Alaska, Seward, Kenai Fjords National Park, Harding Icefield Trail, *Metzgar 247* (ALA), KC700099, KC700139, KC700177, KC700216, KC700254, KC700290; ***Cryptogramma acrostichoides,*** 362, USA, Alaska, Southeast Alaska, 10 miles northwest of Juneau, Mendenhall Lake, behind Mendenhall Glacier Visitor Center, *Anderson 745* (ALA), KC700100, KC700140, KC700178, KC700217, KC700255, KC700291; ***Cryptogramma acrostichoides,*** 365, USA, Alaska, Sitkalidak Island, Sitkalidak Lagoon, cliffs along east side of lagoon, *Studebaker 10-61* (ALA), KC700101, KC700141, KC700179, KC700218, KC700256, KC700292; ***Cryptogramma acrostichoides,*** 497, Russia, Kamchatka, north of Kamchatka peninsula, near Karaginskij, *Chernyagina s.n.* (ALA), KC700102, KC700142, KC700180, KC700219, KC700257, KC700293; ***Cryptogramma brunoniana,*** 313, Taiwan, NanTou County, Mt. ShihMen, *Kuo 455* (TAIF), KC700081, KC700121, KC700159, KC700198, KC700238, KC700273; ***Cryptogramma brunoniana,*** 457, China, Xizang (Tibet) Province, Baxoi Xian, Anjiu La (pass), N of Rawu (Raog), *Boufford 29733* (GH), KC700082, KC700122, KC700160, KC700199, KC700239, KC700274; ***Cryptogramma brunoniana,*** 458, China, Gansu Province, Wen Xian, Motianling Shan, Baishui Jiang Nature Reserve, *Boufford 37747* (GH), KC700083, KC700123, KC700161, KC700200, KC700240, KC700275; ***Cryptogramma cascadensis,*** 298, USA, Oregon, Deschutes/Linn County boundary, McKenzie Pass, *Alverson s.n.* (ALA), KC700086, KC700126, KC700164, KC700203, KC700241, KC700277; ***Cryptogramma cascadensis,*** 354, USA, Washington, King County, Source Lake Lookout Trail, above Source Lake, *Zika 25404* (ALA), KC700087, KC700127, KC700165, KC700204, KC700242, KC700278; ***Cryptogramma crispa,*** 282, Norway, Hordaland, Bergen, *Reeb VR4-VIII-02/11* (DUKE), KC700088, KC700128, KC700166, KC700205, KC700243, KC700279; ***Cryptogramma crispa,*** 376, Spain, Madrid Province, Sierra de Guadarrama, Siete Picos, *Pajarón s.n.* (ALA), KC700089, KC700129, KC700167, KC700206, KC700244, KC700280; ***Cryptogramma crispa,*** 390, Sweden, Norrbotten Gällivare County. Dundret, Gällivare, *Larsson 333* (DUKE, UPS), KC700090,

KC700130, KC700168, KC700207, KC700245, KC700281; ***Cryptogramma crispa,*** 391, Austria, Steiermark, Niedere Tauern/Seckauer Alpen, Maierangerkogel - Vorwitzsattel, *Pflugbeil 111847* (ALA), KC700091, KC700131, KC700169, KC700208, KC700246, KC700282; ***Cryptogramma crispa,*** 450, Italy, northwest of Brunico, Astnerberg, *Shmakov s.n.* (ALTB), KC700092, KC700132, KC700170, KC700209, KC700247, KC700283; ***Cryptogramma fumariifolia,*** 396, Chile, Provincia de Ñuble, Comuna de Pinto, Shangri-La, *Larraín 34009* (ALA, CONC), KC700079, KC700119, KC700157, KC700196, KC700236, KC700271; ***Cryptogramma fumariifolia,*** 397, Chile, Provincia de Ñuble, Comuna de Pinto, Shangri-La, *Larraín 34010* (ALA, CONC), KC700080, KC700120, KC700158, KC700197, KC700237, KC700272; ***Cryptogramma raddeana,*** 451, Russia, Republic of Buryatia, Severo-Muisky range, Samokuya, *Naumov 1989* (NS), KC700084, KC700124, KC700162, KC700201, -, -; ***Cryptogramma raddeana,*** 452, Russia, Khabarovsky krai, 30km north of Sofiysk, *Netchaev s.n.* (NS), KC700085, KC700125, KC700163, KC700202, -, KC700276; ***Cryptogramma sitchensis,*** 355, USA, Alaska, between Portage and Whittier, Bering Glacier, *Metzgar 248* (ALA), KC700103, KC700143, KC700181, KC700220, KC700258, KC700294; ***Cryptogramma sitchensis,*** 356, USA, Alaska, Taku Glacier, *Bass s.n.* (ALA), KC700104, KC700144, KC700182, KC700221, KC700259, KC700295; ***Cryptogramma sitchensis,*** 358, USA, Alaska, Seward, Kenai Fjords National Park, *Metzgar 246* (ALA), KC700105, KC700145, KC700183, KC700222, KC700260, KC700296; ***Cryptogramma sitchensis,*** 360, USA, Alaska, Palmer, Hatcher Pass, *Metzgar 249* (ALA), KC700106, KC700146, KC700184, KC700223, KC700261, KC700297; ***Cryptogramma sitchensis,*** 361, USA, Alaska, Valdez, Thompson Lake, *Metzgar 257* (ALA), KC700107, KC700147, KC700185, KC700224, KC700262, KC700298; ***Cryptogramma stelleri,*** 314, Taiwan, NanTou County, Hohuan Shelter., *Kuo 492* (TAIF), KC700076, KC700116, KC700154, KC700193, KC700233, -; ***Cryptogramma stelleri,*** 375, USA, Alaska, Alexander Archipelago, Prince of Wales Island, *Johnson 20104* (ALA), KC700077, KC700117, KC700155, KC700194, KC700234, -; ***Cryptogramma stelleri,*** 386, Canada, Ontario. Thunder Bay District, Talbot Island, *Oldham 23697* (OAC, BAB, DUKE), KC700078, KC700118, KC700156, KC700195, KC700235, -.

Chapter 5. Conclusions

5.1. Broader contributions of dissertation research

This dissertation has advanced our knowledge of the leptopsorangiate ferns in fields including taxonomy, polyploidy, climate response, and biogeography. I have furthered our understanding of the large family Pteridaceae in parallel with the recent interest in this family (Beck et al., 2011; Grusz et al., 2009; Kirkpatrick, 2007; McGrath and Hickok, 1999; Nakazato et al., 2007; Rothfels et al., 2008; Scott et al., 2007; Schuettpelz et al., 2008; Sigel et al., 2011) by producing the first detailed phylogeny of the cryptogrammoid ferns (Chapter 2). I have demonstrated the monophyly of the three cryptogrammoid genera (*Llavea*, *Coniogramme*, and *Cryptogramma*) and further have shown that both sections and most described species of *Cryptogramma* are monophyletic. These findings, including 20 new sequences of *gapCp* and 231 new sequences of six plastid loci, will be invaluable for larger-scale comparative studies of Pteridaceae and the Polypodiales.

My studies have also contributed to research into polyploidization (Chapters 2-3). I have demonstrated two recent polyploid taxa that have arisen in response to climate fluctuations during Pleistocene glacial cycles, in support of previous hypotheses (Brochmann et al. 2004; Haufler et al. 1995). One of these taxa is an allotetraploid from Beringia (*C. sitchensis*) and the other is an autooctoploid from southwest Asia (*C. bithynica*). I also further supported the role of glacial refugia in creating present-day genetic diversity (Hewitt, 2004), specifically in the European and west Asian *C. crispa* (Chapter 3).

DNA sequencing technology has sufficiently progressed that a much more fine-scale examination of the impact of the Last Glacial Maximum on distribution and genetic diversity is now possible. *Cryptogramma* could be used to exploit these techniques and help to usher leptosporangiate ferns into the genomics age (Barker and Wolf, 2010; Sessa et al., 2014). Additionally, our understanding of Asian ferns would benefit from a critical re-examination of *Coniogramme*.

5.2. Phylogeny of *Cryptogramma* and species-level diversity

This research adds to a recent tradition of molecular studies understanding and untangling the evolution of clades within the Pteridaceae (Beck et al., 2011; Grusz et al., 2009; Kirkpatrick,

2007; McGrath and Hickok, 1999; Nakazato et al., 2007; Rothfels et al., 2008; Scott et al., 2007; Schuettpelz et al., 2008; Sigel et al., 2011). I used DNA sequence data from six plastid loci and one low-copy nuclear locus to reconstruct the phylogeny of the cryptogrammoid ferns, a clade of approximately 40 species comprised of the monotypic genus *Llavea* from central America, approximately 30 species of the Asian *Coniogramme* and 9 species of *Cryptogramma* (Chapter 2; Alverson, 1989; Gangmin and Ranker, 2013). This dissertation research represented the first examination of infra-generic relationships within the cryptogrammoid ferns and the first study of intergeneric relationships in this group with multiple accessions per genus (Prado et al., 2007; Schuettpelz et al., 2007; Zhang et al., 2005). Samples of four *Coniogramme* species from southeast Asia, *Llavea* populations from Mexico and eight species of *Cryptogramma* representing the geographic and morphological diversity of the genus were included. Multiple population samples of each *Cryptogramma* species were used. Phylogenetic analysis of the plastid data set confirmed the monophyly of all three genera. Within *Cryptogramma*, the two sections were reciprocally monophyletic. In addition, the results showed strong support for recognizing all eight included species.

This study provided the first conclusive evidence to fully explain the origin of polyploid taxa within the genus (Alverson, 1989; Pajarón et al., 1999). Plastids are maternally inherited in ferns and the plastid phylogeny determined that *C. acrostichoides* was the maternal parent of *C. sitchensis*. Although less resolved, the nuclear *gapCp* phylogeny was congruent with the plastid phylogeny. It also confirmed that *C. raddeana* was the second parent of *C. sitchensis*. *Cryptogramma crispa* has a partially diploidized genome (Pajarón et al., 1999) and was determined to be of autopolyploid origin and most closely related to the western North American species *C. cascadensis*. Its immediate progenitor is unknown and is assumed to either be extinct or undiscovered. These findings greatly expand upon and are congruent with preliminary findings and predictions based on morphology and cytology (Alverson, 1989).

5.3. Genetic diversity patterns in European *Cryptogramma*

The examination of genetic partitioning in European and western Asian *Cryptogramma* demonstrated a strong glacial influence on the geographic distribution of genetic diversity, similar to patterns seen in other European biota (Chapter 3; Ansell et al., 2011; Hewitt, 2004; Taberlet et al., 1998). The research focused on two taxa from this region, the widespread

autotetraploid *C. crispa* and the newly described Turkish octoploid *C. bithynica*. Using in-depth sampling across their geographic range and a combined nuclear and plastid dataset, we discovered a strong differentiation within *C. crispa*. Populations from western and central Europe were easily distinguished from those in Turkey and the Caucuses Mountains. The latter clade also included *C. bithynica*, implying its origin as an auto-octoploid formed by *C. crispa* and serving as another example of a polyploid taxon generated by glacial cycles (Brochmann et al., 2004). This diversity most likely results from Pleistocene glaciation cycles that repeatedly forced the C. *crispa* lineage to retreat to distant refugia in western Europe and the Caucasus Mountains. My results support the hypothesis that the *C. crispa* lineage represents incipient speciation resulting from this isolation and our findings document the first fern to display a deep divergence between western Europe and the eastern Europe/west Asia region.

5.4. Temporal and biogeographic aspects of diversification

This study added a temporal and geographic perspective to our understanding of the evolution of *Cryptogramma* (Chapter 4). Using a dataset of DNA sequence data for 40 accessions from six plastid loci, I incorporated time constraints on the divergence of *Llavea* from the other two genera and of *Coniogramme* from *Cryptogramma*. Divergence time estimates using BEAST v.1.7.5 (Drummond and Rambaut, 2007; Drummond et al., 2012) infer that crown group *Cryptogramma* originated in the Oligocene and most extant species date to the Pliocene and Pleistocene. My results are congruent with a broader trend of generic diversification of ferns during this period (Schuettpelz and Pryer, 2009). Biogeographic analysis of this chronogram using the dispersal-extinction-cladogenesis (DEC) approach implemented in Lagrange (Ree et al., 2005; Ree and Smith, 2008) finds that east Asia is the most likely ancestral area for the cryptogrammoid ferns and for *Cryptogramma*. These results corroborate the frequently-observed pattern of Asia serving as a source population for colonization of the New World (Wen, 1999; Wen et al., 2014) and is similar to the biogeographic patterns seen in the much larger genus *Dryopteris* (Sessa et al., 2012). Three colonization events to North America from east Asia were inferred, as well as one colonization event of Europe from North America. The lone South American taxon, *C. fumariifolia*, was inferred to have reached South America by long distance dispersal from east Asia. Speciation rates were similar across the phylogeny and morphological variation is low, leading to the possibility that the *Cryptogramma* lineage is among the first

leptosporagiate fern lineages documented to exhibit morphological stasis (Sundue and Rothfels, 2014).

5.5. Future directions

This dissertation has built a solid foundation for understanding the complexity of diversification in the genus *Cryptogramma* and has furthered our understanding of the effects of glacial cycles on leptosporangiate ferns. I have also furthered the discussion on the biogeographic history of ferns, and the roles of Beringia and the North Atlantic Land Bridge in generating species-level diversity. The role of morphological stasis in surviving high-latitude climate shifts was also shown.

There remain, however, more opportunities to characterize biological and ecological processes in this group. Several taxa in *Crypogramma* would be ideal for studying short-term responses (i.e., since the Last Glacial Maximum) in response to rapid climate warming. Additionally, my work has provided an entryway into understanding the systematics of the more species-rich genus *Coniogramme* in southeast Asia.

5.5.1. Population-level responses to climate shifts

This dissertation has demonstrated impacts of Pleistocene glacial cycle range contractions and expansions on generating diversity in *Cryptogramma* (*C. bithynica* and *C. sitchensis*). Longer-term effects were also seen in the genetic partitioning of *C. crispa* populations, but advancements in research techniques have enabled future researchers to detect shorter-term responses to rapid climate shifts. During the Last Glacial Maximum (LGM) rapid climate change drove episodes of biotic expansion, interchange, isolation and diversification (and extinction) on varying temporal and spatial scales. These episodes had large impacts on the genetic and taxonomic diversity of the present-day flora and fauna (Hewitt, 2000). Population-level trends in the partitioning of genetic diversity have been shown to result from LGM survival in climatically stable, unglaciated refugia around the world (Hewitt, 2004; Shafer et al., 2010; Soltis et al., 1997). Subsequent patterns of recolonization into deglaciated areas added additional complexity to species' phylogenetic history (Petit et al., 2002). These refugia also served to reunite previously allopatric sister species, resulting in the production of numerous hybrid and polyploid taxa (Abbott and Brochmann, 2003; Brochmann et al., 2004; Consaul et al., 2010; Haufler et al.,

1995). Beringia is perhaps the most well-known of these refugia, but additional areas were also important harbors for boreal taxa and engines of diversity. These include central China (Chen et al., 2008; Chen et al., 2010; Feng et al., 2009; Liu et al., 2007; Wang et al., 2011; Wang et al., 2012), the Pacific Northwest south of the ice sheet (Shafer et al., 2010; Soltis et al., 1997), the High Arctic (Consaul et al., 2010; Tremblay and Schoen, 1999), and so-called cryptic refugia along North America's Pacific Coast such as Haida Gwaii and the Alexander Archipelago (Beatty and Provan, 2011; Marr et al., 2008).

5.5.1.1. Next-generation DNA sequencing

The widespread distributions of the trans-Beringian *C. acrostichoides* complex make this an ideal case for examining the fine-scale role of refugia for ferns during the LGM. The role of Beringia as a glacial refuge for many plant and animal taxa is long established (Abbott et al., 2000; Abbott and Brochmann, 2003; Hultén, 1937; Tremblay and Schoen, 1999), but the role of these Beringian populations in recolonizing deglaciated land is variable (Hewitt, 2004). *Cryptogramma sitchensis* is a possible candidate for nunatak survival, as allopolyploidy, narrow distribution, self-crossing and extreme cold tolerance are all hypothesized to confer a greater probability of nunatak survival (Brochmann et al., 2003; Brochmann et al., 2004; Westergaard et al., 2011).

Next-generation DNA sequencing technologies offer promise of greatly increased ability to isolate and explain genetic phenomena. Our understanding of the impact of the Last Glacial Maximum (LGM) on present-day genetic diversity could be immensely improved by using one of these techniques. Restriction-associated DNA Sequencing (RADSeq) is a next-generation DNA sequencing method capable of sequencing thousands of SNPs for dozens of populations in one run and has been successful at identifying refugial areas in other taxa (Emerson et al., 2010; Peterson et al., 2012). It has been hypothesized that colonization from glacial refugia is mainly due to a few long-distance dispersal events by single individuals (Rowe et al., 2004). Thus, new populations would undergo a severe bottleneck event, resulting in low genetic diversity in more recent populations and high genetic diversity in refugial source populations.

5.5.1.2. Ecological niche modeling

The use of ecological niche modeling allows for potential glacial refugia to be identified independent of molecular data (Waltari et al., 2007). The *Cryptogramma acrostichoides* polyploid complex and *C. crispa* polyploidy complex would be well suited to this approach. Ecological niche models (ENMs) couple presence-only distribution data from herbarium specimens and online databases with environmental data such as the BIOCLIM climate layers (Hijmans et al., 2005) to produce ecological niche models of predicted possible range for the present-day using the maximum entropy method employed by MaxEnt v3.3.3k (Phillips et al., 2006).

These present day models can then be projected to previous environmental conditions including 10k, 18k and 2.5M years before present. These paleodistribution models can identify potential refugial areas used during the LGM, as well as regions of long-term stability where *Cryptogramma* species could have persisted continuously since the Pleistocene (Carnaval et al., 2009). These ENMs can also test for higher probability of survival in cryptic refugia or nunataks during the LGM by testing the significance of occurrence probabilities of species with varying distributions. Principal component analysis can be used to assess niche conservatism within taxa and integrated with my divergence time estimates to further study incipient speciation and identify past climatic events associated with speciation (Smith and Donoghue, 2010). Present day models can also be projected to future predicted environmental conditions predicted (e.g., 50 or 100 years from now). This method predicts range shifts or contractions caused by anthropogenic climate change and identifies populations susceptible to extinction. Use of this approach would allow for an independent assessment of refugial locations during the Last Glacial Maximum or for expected impacts of anthropogenic climate change on *Cryptogramma* species over short time-scales such as 50 or 100 years.

5.5.2. Systematics of *Coniogramme*

Coniogramme is restricted to southeast Asia and has been shown in this dissertation to be monophyletic and most closely related to *Cryptogramma*. There are an estimated 20-30 extant species (Gangmin and Ranker, 2013; Tryon and Tryon, 1990) and the genus has received minimal regional or comprehensive taxonomic attention for a century, with only two recent morphological summaries of Chinese taxa (Gangmin and Ranker, 2013; Shing, 1990). The only

comprehensive systematic treatment included 17 taxa (Hieronymous, 1916) and a taxonomic revision would be very timely. The phylogenetics of the group will likely be complicated from processes such as hybridization, polyploid complexes, and rapid diversifications since morphological intermediates are frequently encountered and phenotypic plasticity is high across the genus (Gangmin and Ranker, 2013). This dissertation has provided a springboard for evaluating taxonomic decisions and character evolution in *Coniogramme*.

5.6 References

Abbott, R.J., Smith, L.C., Milne, R.I., Crawford, R.M., Wolff, K., Balfour, J., 2000. Molecular analysis of plant migration and refugia in the Arctic. Science 289, 1343–1346.

Abbott, R.J., Brochmann, C., 2003. History and evolution of the Arctic flora: in the footsteps of Eric Hultén. Mol. Ecol. 12, 229–313.

Adams, K.L., 2007. Evolution of duplicate gene expression in polyploid and hybrid plants. J. Hered. 98, 136–141.

Adams, K.L., Wendel, J.F., 2005. Polyploidy and genome evolution in plants. Curr. Opin. Pl. Biol. 8, 135–141.

Aitkin, S.N., Yeaman, S., Holliday, J.A., Wang, T., Curtis-McLane, S., 2008. Adaptation, migration or extirpation: climate change outcomes for tree populations. Evol. Appl. 1, 95–111.

Alverson, E.R., 1989. Biosystematics of Parsley-ferns, *Cryptogramma* R. Br., in Western North America. Master's thesis, Oregon State University, Corvallis, Oregon.

Alverson, E.R., 1993. *Cryptogramma*, in: Flora of North America Editorial Committee (Eds.), The Flora of North America, Vol. 2. Oxford University Press, New York, NY, pp. 137–139.

Ansell, S.W., Stenøien, H.K., Grundmann, M., Russell, S.J., Koch, M., Schneider, H., Vogel, J.C., 2011. The importance of Anatolian mountains as the cradle of global diversity in *Arabis alpina*, a key arctic-alpine species. Ann. Bot. London 108, 241–252.

Barker, M.S., Wolf, P.G., 2010. Unfurling fern biology in the genomics age. BioScience 60, 177–185.

Beatty, G.E., Provan, J., 2011. Phylogeographic analysis of North American populations of the parasitic herbaceous plant *Monotropa hypopitys* L. reveals a complex history of range expansion from multiple late glacial refugia. J. Biogeog. 38, 1585–1599.

Beck, J.B., Windham, M.D., Pryer, K.M., 2011. Do asexual lineages lead short evolutionary lives? A case-study from the fern genus *Astrolepis*. Evol. 65, 3217–3229.

Brochmann, C., Gabrielsen, T.M., Nordal, I., Landvik, J.Y., Elven, R., 2003. Glacial survival or tabula rasa? The history of North Atlantic biota revisited. Taxon 52, 417–450.

Brochmann, C., Brysting, A.K., Alsos, I.G., Borgen, L., Grundt, H.H., Scheen, A.-C., Elven, R., 2004. Polyploidy in Arctic plants. Biol. J. Linn. Soc. 82, 521–536.

Carnaval, A.C., Hickerson, M.J., Haddad, C.F.B., Rodrigues, M.T. Moritz, C. 2009. Stability predicts genetic diversity in the Brazilian Atlantic forest hotspot. Science 323, 785–788.

Chen, S., Wu, G., Zhang, D., Gao, Q., Duan, Y., Zhang, F., Chen, S., 2008. Potential refugium on the Qinghai-Tibet Plateau revealed by the chloroplast DNA phylogeography of the alpine species *Metagentiana striata* (Gentianaceae). Bot. J. Linn. Soc. 157, 125–140.

Chen, W., Liu, S., Liu, Y., Hao, H., Zeng, B., Chen, S., Peng, H., Yue, B., Zhang, X., 2010. Phylogeography of the large white-bellied rat *Niviventer excelsior* suggests the influence of Pleistocene glaciations in the Hengduan Mountains. Zoolog. Sci. 27, 487–493.

Consaul, L.L., Gillespie, L.J., Waterway, M.J., 2010. Evolution and polyploid origins in North American Arctic *Puccinellia* (Poaceae) based on nuclear ribosomal spacer and chloroplast DNA sequences. Am. J. Bot. 97, 324–336.

Crawford, R.M.M., Abbott, R.J., 1994. Pre-adaptation of Arctic plants to climate change. Bot. Acta. 107, 271–278.

Drummond, A., Rambaut, A., 2007. BEAST: bayesian evolutionary analysis sampling trees. BMC Evol. Biol. 7, 214. http://dx.doi:10.1186/1471-2148-7-214.

Drummond, A., Suchard, M.A., Xie, D., Rambaut, A. 2012. Bayesian phylogenetics with BEAUti and the BEAST 1.7. Mol. Bio. Evol. 29, 1969–1973.

Emerson, K.J., Merz, C.R., Catchen, J.M., Hohenlohe, P.A., Cresko, W.A., Bradshaw, W.A., Holzapfel, C.M., 2010. Resolving postglacial phylogeography using high-throughput sequencing. Proc. Nat. Acad. Sci. U.S.A. 107, 16196–16200.

Fan, D.-M., Chen, J.-H., Meng, Y., Wen, J., Huang, J.-L., Yang, Y.-P., 2013. Molecular phylogeny of *Koenigia* L. (Polygonaceae: Persicarieae): Implications for classification, character evolution and biogeography. Mol. Phylogenet. Evol. 69, 1093–1100.

Feng, T., Downie, S.R., Yu, Y., Zhang, X., Chen, W., He, X., Liu, S., 2009. Molecular systematics of *Angelica* and allied genera (Apiaceae) from the Hengduan Mountains of China based on nrDNA ITS sequences: phylogenetic affinities and biogeographic implications. J. Plant. Res. 122, 403–414.

Fraser-Jenkins, C.R., 2008. Taxonomic revision of three hundred Indian subcontinental pteridophytes with a revised census-list: a new picture of fern-taxonomy and nomenclature in the Indian subcontinent. Bishen Singh Mahendra Pal Singh, Dehra Dun, India.

Galtier, J., Phillips, T.L., 1996. Structure and evolutionary significance of Palaeozoic ferns. In: Camus, J.M., Gibby, M., Johns, R.J. (Eds.), Pteridology in Perspective. Royal Botanical Gardens, Kew, pp. 417–483.

Gangmin, Z., Ranker, T.A., 2013. *Coniogramme* Fée. In: Wu, Z.Y., Raven, P.H., Hong, D.Y., (eds.), Flora of China Volume 2-3 (Lycopodiaceae through Polypodiaceae). Science Press, Beijing, and Missouri Botanical Garden Press, St. Louis, pp. 170-171.

Gastony, G.J., Rollo, D.R., 1995. Phylogeny and generic circumscriptions of cheilanthoid ferns (Pteridaceae: Cheilanthoideae) inferred from *rbcL* nucleotide sequences. Am. Fern J. 85, 341–360.

Gifford, E.M., Foster, A.S., 1989. Morphology and evolution of vascular plants. Ed. 3. W.H. Freeman & Co., New York.

Grusz, A.L., Windham, M.D., Pryer, K.M., 2009. Deciphering the origins of apomictic polyploids in the *Cheilanthes yavapensis* complex (Pteridaceae). Am. J. Bot. 96, 1636–1645.

Haufler, C.H., 1987. Electrophoresis is modifying our concepts of evolution in homosporous pteridophytes. Am. J. Bot. 74, 953–966.

Haufler, C.H., Soltis, D.E., 1986. Genetic evidence suggests that homosporous ferns with high chromosome numbers are diploid. Proc. Nat. Acad. Sci. U.S.A. 83, 4389–4393.

Haufler, C.H., Windham, M.D., Rabe, E.W., 1995. Reticulate evolution in the *Polypodium vulgare* complex. Syst. Bot. 20, 110–119.

Hewitt, G.M., 2000. The genetic legacy of the Quaternary ice ages. Nature 405, 907–913.

Hewitt, G.M., 2004. Genetic consequences of climatic oscillations in the Quaternary. Philos. T. Roy. Soc. B 359, 183–195.

Hieronymous, G., 1916. Über die Gattung *Coniogramme* und ihre Arten. Hedwigia 57, 265–328.

Hijmans, R.J., Cameron, S.E., Parra, J.L., Jones, P.G., Jarvis, A., 2005. Very high resolution interpolated climate surfaces for global land areas. Inter. J. Clim. 25, 1965–1978.

Hultén, E., 1937. Outline of the History of Arctic and Boreal Biota during the Quarternary Period. Lehre J Cramer, New York.

Hultén, E., 1968. Flora of Alaska and Neighboring Territories. Stanford University Press, Stanford, CA.

Huttunen, S., Kuznetsova, O., Li, M., Wang, Y.-F., Ignatov, M.S., 2015. East Asian origin and Northern Hemisphere diversification in the *Brachythecium novae-angliae* complex (Bryophyta). Taxon 64, 911–930.

Ickert-Bond, S.M., Wen, J., 2006. Phylogeny and biogeography of Altingiaceae: Evidence from combined analysis of five non-coding chloroplast regions. Mol. Phylogenet. Evol. 39, 512–528.

Jessen, S., Lehmann, L., Bujnoch, W., 2012. *Cryptogramma bithynica* sp. nov. (Pteridaceae, Pteridophyta)—a new fern species from northwestern Anatolia/Turkey. Fern Gaz. 19, 47–54.

Kawai, H., Kanegae, T., Christensen, S., Kiyosue, T., Sato, Y., Imaizumi, T., Kadota, A., Wada, M., 2003. Responses of ferns to red light are mediated by an unconventional photoreceptor. Nature 421, 287–290.

Kenrick, P., Crane, P.R., 1997. The origin and early evolution of plants on land. Nature 389, 33–39.

Kirkpatrick, R.E.B., 2007. Investigating the monophyly of *Pellaea* (Pteridaceae) in the context of a phylogenetic analysis of cheilanthoid ferns. Syst. Bot. 32, 504–518.

Klekowski, E.J., Baker, H.G., 1966. Evolutionary significance of polyploidy in the Pteridophyta. Science 153, 305–307.

Kramer, K.U, Green, P.S. [eds.], 1990. The families and genera of vascular plants, vol. I, Pteridophytes and gymnosperms. Springer-Verlag, Berlin.

Leitch, I.J., Bennett, M.D., 2004. Genome downsizing in polyploid plants. Biol. J. Linn.Soc. 82, 651–663.

Lellinger, D.B., 1985. A Field Manual of the Ferns & Fern-Allies of the United States & Canada. Smithsonian Institution Press, Washington, DC.

Li, Z., Baniaga, A.E., Sessa, E.B., Scascitelli, M., Graham, S.W., Rieseberg, L.H., Barker, M.S., 2015. Early genome duplications in conifers and other seed plants. Science Advances 1, e1501084. DOI: 10.1126/sciadv.1501084.

Liu, X-Q., Gituru, R.W., Chen, L-Q., 2007. Genetic variation in the endangered fern *Adiantum reniforme* var. *sinense* (Adiantaceae) in China. Ann. Bot. Fennici 44, 25–32.

Löve, A., Löve, D., Pichi-Sermolli, R.E.G., 1977. Cytotaxonomical atlas of the Pteridophyta. J. Cramer, Vaduz, Liechtenstein.

Manton, I., 1950. Problems of Cytology and Evolution in the Pteridophyta. Cambridge University Press, London.

Marr, K.L., Allen, G.A., Hebda, R.J., 2008. Refugia in the Cordilleran ice sheet of western North America: chloroplast DNA diversity in the Arctic-alpine plant *Oxyria digyna*. J. Biogeog. 35, 1323–1334.

Mayrose, I., Barker, M.S., Otto, S.P., 2010. Probabilistic models of chromosome number evolution and the inference of polyploidy. Syst. Biol. 59, 132–144.

McDaniel, S.F., Shaw, A.J. 2003. Phylogeographic structure and cryptic speciation in the trans-Antarctic moss *Pyrrhobryum mnioides*. Evol. 57, 205–215.

McGrath, J. M., Hickok, L.G., 1999. Multiple ribosomal RNA gene loci in the genome of the homosporous fern *Ceratopteris richardii*. Can. J. Bot. 77, 1199–1202.

Nakazato, T., Jung, M.-K., Housworth, E.A., Rieseberg, L.H., Gastony, G.J., 2007. A genome-wide study of reproductive barriers between allopatric populations of a homosporous fern, *Ceratopteris richardii*. Genetics 177, 1–10.

Otto, S.P., 2007. The Evolutionary Consequences of Polyploidy. Cell 131, 452–462.

Otto, S.P., Whitton, J., 2000. Polyploid incidence and evolution. Ann. Rev. Genet. 34, 401–437.

Pajarón, S., Pangua, E., García-Álvarez, L., 1999. Sexual expression and genetic diversity in populations of *Cryptogramma crispa* (Pteridaceae). Am. J. Bot. 86, 964–973.

Peterson, B.K., Weber, J.N., Kay, E.H., Fisher, H.S., Hoekstra, H.E., 2012. Double digest RADseq: an inexpensive method for de novo SNP discovery and genotyping in model and non-model species. PLOS One 7, e37135. http://dx.doi.org/10.1371/journal.pone.0037135.

Petit, R.J., Brewer, S., Bordács, S., Burg, K., Cheddadi, R., Coart, E., Cottrell, J., Csaikl, U.M., van Dam, B., Deans, J.D., Espinel, S., Fineschi, S., Finkeldey, R., Glaz, I., Goicoechea, P.G., Jensen, J.S., König, A.O., Lowe, A.J., Madsen, S.F., Mátyás, G., Munro, R.C., Popescu, F., Slade, D., Tabbener, H., de Vries, S.G.M., Ziegenhagen, B., de Beaulieu, J.L., Kremer, A., 2002. Identification of refugia and post-glacial colonization routes of European white oaks based on chloroplast DNA and fossil pollen evidence. Forest Ecol. Manag. 156, 49–74.

Pichi-Sermolli, R.E.G., 1963. Adumbratio florae aethiopicae 9. Cryptogrammaceae. Webbia 17, 299–315.

Phillips, S.J., Dudik, M., Schapire, R.E., 2006. Maximum entropy modeling of species geographic distributions. *Ecol. Model.* 190, 231–259.

Prado, J., Rodrigues, C.D.N., Salatino, A., Salatino, M.L.F., 2007. Phylogenetic relationships among Pteridaceae, including Brazilian species, inferred from *rbcL* sequences. Taxon 56, 355–368.

Pryer, K.M., Schneider, H., Smith, A.R., Cranfill, R., Wolf, P.G., Hunt, J.S., Sipes, S.D., 2001. Horsetails and ferns are a monophyletic group and the closest living relatives to seed plants. Nature 409, 618–622.

Pryer, K.M., Schuettpelz, E., Wolf, P.G., Schneider, H., Smith, A.R., Cranfill, R., 2004. Phylogeny and evolution of ferns (monilophytes) with a focus on the early leptosporangiate divergences. Am. J. Bot. 91, 1582–1598.

Rabosky, D.L., Santini, F., Eastman, J., Smith, S.A., Sidlauskas, B., Chang, J., Alfaro, M.E., 2013. Rates of speciation and morphological evolution are correlated across the largest vertebrate radiation. Nature Comm. 4, 1958. http://dx.doi.org/10.1038/ncomms2958.

Rabosky, D.L., Title, P.O., Huang, H., 2014. Minimal effects of latitude on present-day speciation rates in New World birds. Proc. R. Soc. B. 282, 1809. http://dx.doi.org/10.1098/rspb.2014.2889.

Ree, R.H., Moore, B.R., Webb, C.O., Donoghue, M.J., 2005. A likelihood framework for inferring the evolution of geographic range on phylogenetic trees. Evol. 59, 2299–2311.

Ree, R.H., Smith, S.A., 2008. Maximum likelihood inference of geographic range evolution by dispersal, local extinction, and cladogenesis. Syst. Biol. 57, 4–14.

Rothfels, C.J., Windham, M.D., Grusz, A.L., Gastony, G.J., Pryer, K.M., 2008. Toward a monophyletic *Notholaena* (Pteridaceae): Resolving patterns of evolutionary convergence in xeric-adapted ferns. Taxon 57, 712–724.

Rothwell, G.W., 1987. Complex Paleozoic Filicales in the evolutionary radiation of ferns. Am. J. Bot. 74, 458–461.

Rowe, K.C., E.J. Heske, Brown, P.W., Paige, K.N., 2004. Surviving the ice: Northern refugia and postglacial colonization. Proc. Nat. Acad. Sci. U.S.A. 101, 10355–10359.

Schneider, H., Schuettpelz, E., Pryer, K.M., Cranfill, R., Magallón, S., Lupia, R., 2004. Ferns diversified in the shadow of angiosperms. Nature 428, 553–557.

Schuettpelz, E., Pryer, K.M., 2007. Fern phylogeny inferred from 400 leptosporangiate species and three plastid genes. Taxon 56, 1037–1050.

Schuettpelz, E., Schneider, H., Huiet, L., Windham, M.D., Pryer, K.M., 2007. A molecular phylogeny of the fern family Pteridaceae: assessing overall relationships and the affinities of previously unsampled genera. Mol. Phylogenet. Evol. 44, 1172–1185.

Schuettpelz, E., Grusz, A.L., Windham, M.D., Pryer, K.M., 2008. The utility of nuclear *gapCp* in resolving polyploid fern origins. Syst. Bot. 33, 621–629.

Schuettpelz, E., Pryer, K.M., 2009. Evidence for a Cenozoic radiation of ferns in an angiosperm-dominated canopy. Proc. Nat. Acad. Sci. U.S.A. 106, 11200–11205.

Scott, R.J., Gastony, G.J., Weatherford, J.W., Nakazato, T., 2007. Characterization of four members of the alpha-tubulin gene family in *Ceratopteris richardii*. Am. Fern J. 97, 47–65.

Sessa, E.B., Zimmer, E.A., Givnish, T.J., 2012. Phylogeny, divergence times and historical biogeography of New World *Dryopteris* (Dryopteridaceae). Am. J. Bot. 99, 730–750.

Sessa, E.B., Banks, J.A., Barker, M.S., Der, J.P., Duffy, A.M., Graham, S.W., Hasebe, M., Langdale, J., Li, F.-W., Marchant, D.B., Pryer, K.M., Rothfels, C.J., Roux, S.J., Salmi, M.L., Soltis, D.E., Soltis, P.S., Stevenson, D.W., Wolf, P.G., 2014. Between two fern genomes. GigaScience 3, 15. http://dx.doi.org/doi:10.1186/2047-217X-3-15.

Shafer, A.B.A., Cullingham, C.I., Cote, S.D., Coltman, D.W., 2010. Of glaciers and refugia: a decade of study sheds new light on the phylogeography of northwestern North America. Mol. Ecol. 19, 4589–4621.

Shepherd, L.D., Perrie, L.R., Brownsey, P.J., 2007. Fire and ice: volcanic and glacial impacts on the phylogeography of the New Zealand forest fern *Asplenium hookerianum*. Mol. Ecol. 16, 4536–4549.

Shing, K.-H., 1990. *Cryptogramma*, in: Flora Reipublicae Sinicae. Beijing: Science Press 3, 98–103.

Sigel, E. M., Windham, M.D., Huiet, L., Yatskievych, G., Pryer, K.M., 2011. Species relationships and farina evolution in the cheilanthoid fern genus *Argyrochosma* (Pteridaceae). Syst. Bot. 36, 554–564.

Smith, A.R., Pryer, K.M., Schuettpelz, E., Korall, P., Schneider, H., Wolf, P.G., 2006. A classification for extant ferns. Taxon 55, 705–731.

Smith, S.A., Donoghue, M.J., 2010. Combining historical biogeography with niche modeling in the *Caprifolium* clade of *Lonicera* (Caprifoliaceae, Dipsacales). Syst. Biol. 59, 322–341.

Soltis, D.E., 1986. Genetic evidence for diploidy in *Equisetum*. Am. J. Bot.73, 908–913.

Soltis, D.E., Gitzendanner, M.A., Strenge, D.D., Soltis, P.S., 1997. Chloroplast DNA intraspecific phylogeography of plants from the Pacific Northwest of North America. Plant Syst. Evol. 206, 353–373.

Soltis, D.E., Soltis, P.S., 1999. Polyploidy: recurrent formation and genome evolution. Tr. Ecol. Evol. 14, 348–352.

Sundue, M.A., Rothfels, C.J., 2014. Stasis and convergence characterize morphological evolution in eupolypod II ferns. Ann. Bot. 113, 35–54.

Taberlet, P., Fumagelli, L., Wust-Saucy, A.-G., Cosson, J.F., 1998. Comparative phylogeography and postglacial colonization routes in Europe. Mol Ecol 7, 453–464.

Tidwell, W.D., Ash, S.R., 1994. A review of selected Triassic to early Cretaceous ferns. J. Plant Res. 107, 417–442.

Tiffney, B.H., 1985. The Eocene North Atlantic Land Bridge: Its importance in Tertiary and modern phytogeography of the northern hemisphere. J. Arnold Arbor. 66, 243–273.

Tremblay, N.O., D.J. Schoen. 1999. Molecular phylogeography of *Dryas integrifolia*: glacial refugia and postglacial recolonization. Mol. Ecol. 8, 1187–1198.

Trewick, S.A., Morgan-Richards, M., Russell, S.J., Henderson, S., Rumsey, F.J., Pintér, I., Barrett, J.A., Gibby, M., Vogel, J.C., 2002. Polyploidy, phylogeography and Pleistocene

refugia of the rockfern *Asplenium ceterach*: evidence from chloroplast DNA. Mol. Ecol. 11, 2003–2012.

Tryon, R.M., Tryon, A.F., 1990. *Pteridaceae, in* K. U. Kramer and P. S. Green [eds.], The families and genera of vascular plants, vol. I, Pteridophytes and gymnosperms. Springer-Verlag, Berlin, pp. 230–256.

Vaganov, A.V., Shmakov, A.I., Kuznetsov, A.A., Gureeva, I.I., 2010. Spore morphology of *Cryptogramma* R. Br. ex Richards species (Cryptogrammaceae). Turcz. 13, 50–58.

Vogel, J.C., Rumsey, F.J., Schneller, J.J., Barrett, J.A., Gibby, M. 1999. Where are the glacial refugia in Europe? Evidence from pteridophytes. Biol. J. Linn. Soc. 66, 23–37.

Wagner, W.H., 1954. Reticulate evolution in the Appalachian *Aspleniums*. Evol. 8, 103–118.

Waltari, E., Hijmans, R.J., Townsend Peterson, A., Nyari, A.S., Perkins, S.L., Guralnick, R.P., 2007. Locating Pleistocene refugia: comparing phylogeographic and ecological niche model predictions. PLOS One 7, e563. http://dx.doi.org/doi:10.1371/journal.pone.0000563.

Wang, L., Wu, Z-Q., Bystriakova, N., Ansell, S.W., Xiang, Q.-P., Heinrichs, J., Schneider, H., Zhang, X.-C., 2011. Phylogeography of the Sino-Himalayan fern *Lepisorus clathratus* on "The Roof of the World." PLOS One 6, e25896. http://dx.doi.org/doi:10.1371/journal.pone.0025896 .

Wang, B., J. Jiang, F. Xie and C. Li. 2012. Postglacial colonization of the Qinling Mountains: phylogeography of the swelled vent frog (*Feirana quadranus*). PLOS One 7, e41579. http://dx.doi.org/doi: 10.1371/journal.pone.0041579

Wen, J., 1999. Evolution of eastern Asian and eastern North American disjunct distributions in flowering plants. Ann. Rev. Ecol. Syst. 30, 421–455.

Wen, J., Zhang, J.-Q., Nie, Z.-L., Zhong, Y., Sun, H. 2014. Evolutionary diversifications of plants on the Qinghai-Tibet Plateau. Frontiers in Gen. 4, http://dx.doi.org/doi: 10.3389/fgene.2014.00004.

Werth, C.R., Guttman, S.I., Eshbaugh, W.H., 1985. Recurring origins of allopolyploid species in *Asplenium*. Science 228, 731–733.

Westergaard, K., Alsos, I.G., Popp, M., Engelskjon, T., Flatberg, K.I., Brochmann, C., 2011. Glacial survival may matter after all: nunatak signatures in the rare European populations of two west-arctic species. Mol. Ecol. 20, 376–393.

Wood, T.E., Takebayashi, N., Barker, M.S., Mayrose, I., Greenspoon, P.B., Rieseberg, L.H., 2009. The frequency of polyploid speciation in vascular plants. Proc. Nat. Acad. Sci. U.S.A. 106, 13875–13879.

Zhang, G-M., Zhang, X-C., 2003. Taxonomic revision of the genus *Cryptogramma* R.Br. from China. Acta Phyto. Sin. 41, 475–482.

Zhang, G., Zhang, X., Chen, Z., 2005. Phylogeny of cryptogrammoid ferns and related taxa based on *rbcL* sequences. Nord. J. Bot. 23, 485–493.